Quantification and Modeling of the Air Entrainment in the Stern Flow Region

ONR N00014-03-1-0825

PI: Juan C. Lasheras. (lasheras@ucsd.edu)
Javier Rodriguez (fjrodrigez@ucsd.edu) , Alberto Aliseda (aaliseda@u.washington.edu) University of California, San Diego
La Jolla, CA 92093-0411

Ship Wavebreaking Workshop
March 28-29, 2007

Motivation for studying the air entrainment by stationary 2-D and 3-D turbulent breakers formed at the stern of a surface ship

- There are no detailed studies of three-dimensional stern breakers including the effect of the corner flow (stern geometry)

Our study:
- Two-dimensional deep-water breaker
  - -air entrainment and bubble formation
- Three-dimensional deep-water breaker
  - -Effect of the corner flow

Steady –unsteady measurements

Two-dimensional deep-water breaker

- Effect of the Fr number on the air entrainment

Three-dimensional deep-water breaker

- Mechanisms of air entrainment
- Effect of the corner flow

<u>Fresh and Sea Water</u>

Experimental Setup

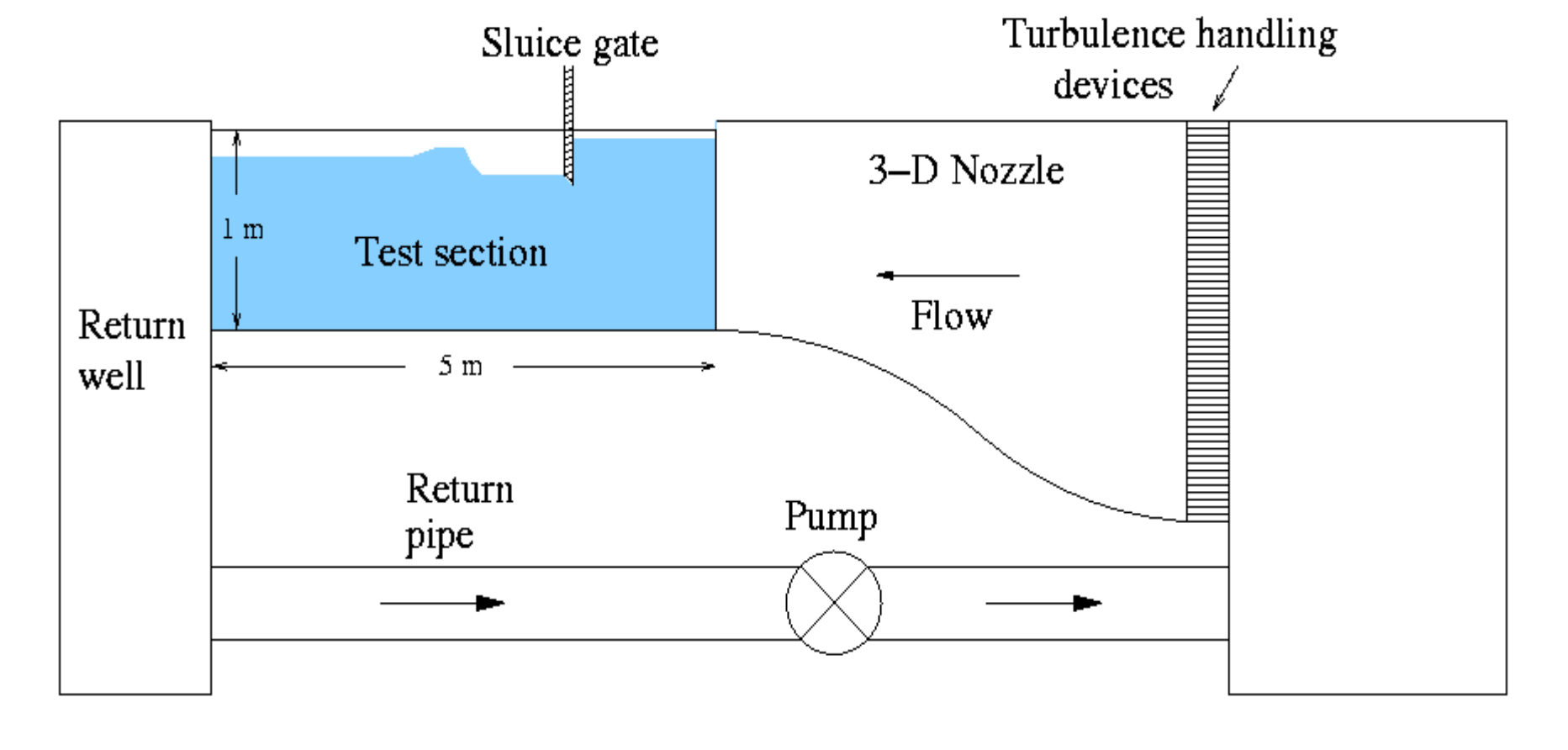

Experiments include using sluice gates as well as three-dimensional bodies resembling the stern of a surface ship

Effect of the Boundary Layer on the Hull

Laminar/Turbulent

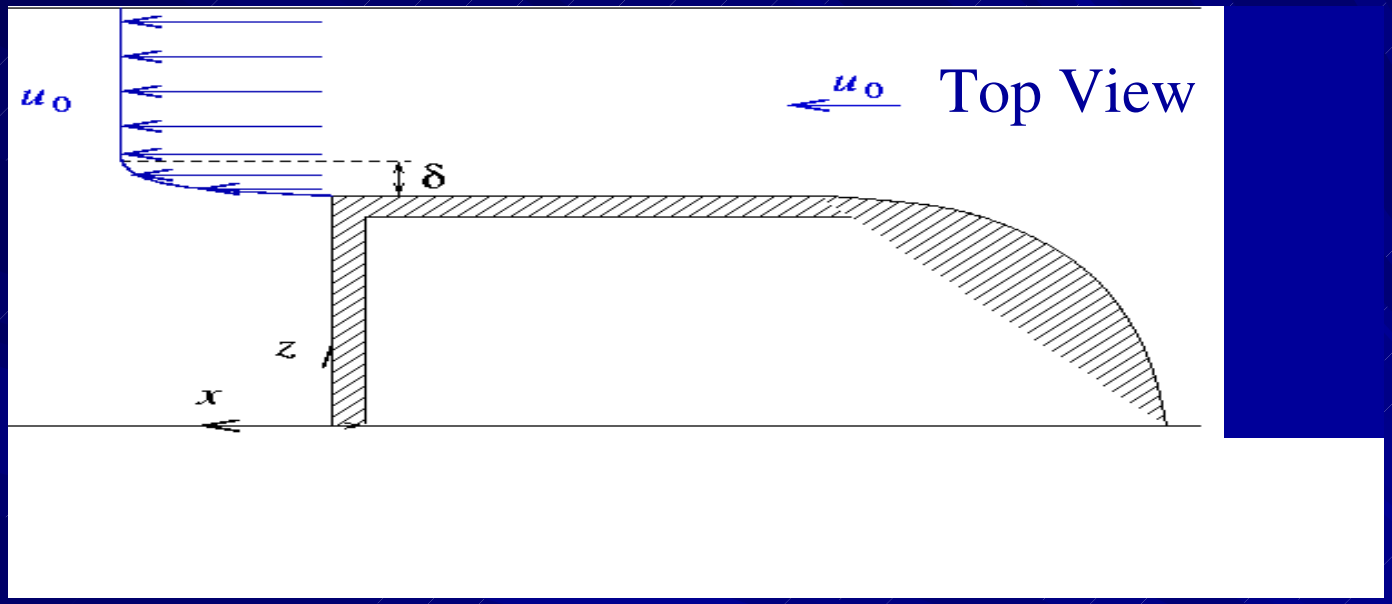

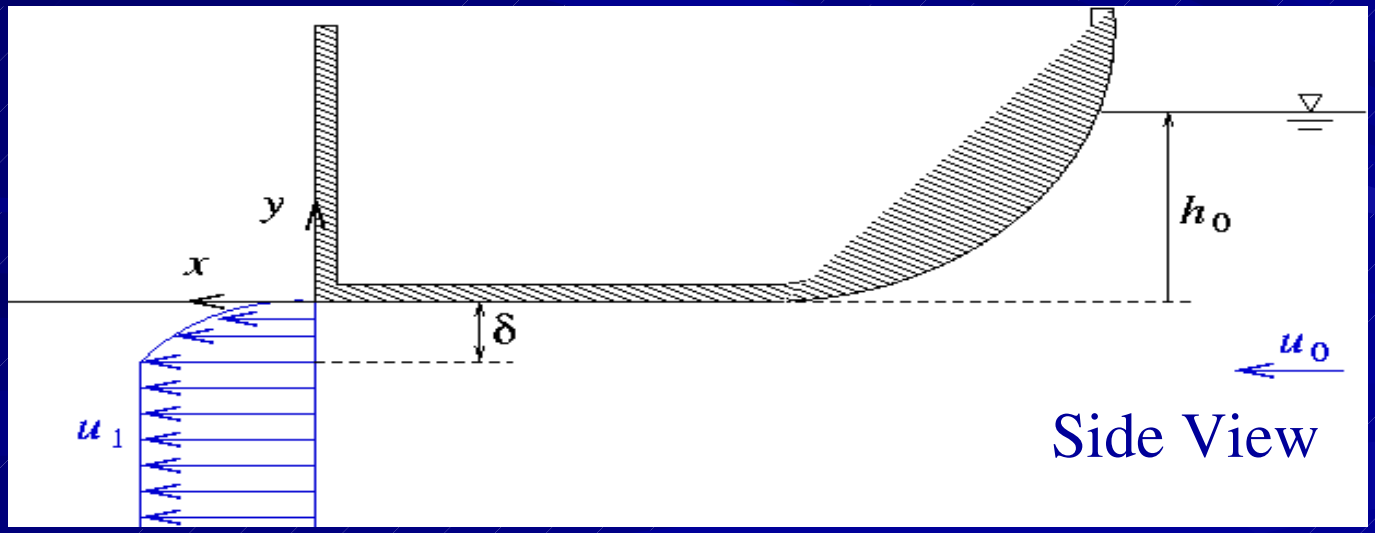

Mechanism of Air entrainment and Bubble Formation by a Two-Dimensional Deep-Water Stern Breaker

Unsteady Bubbly Flow Modeling

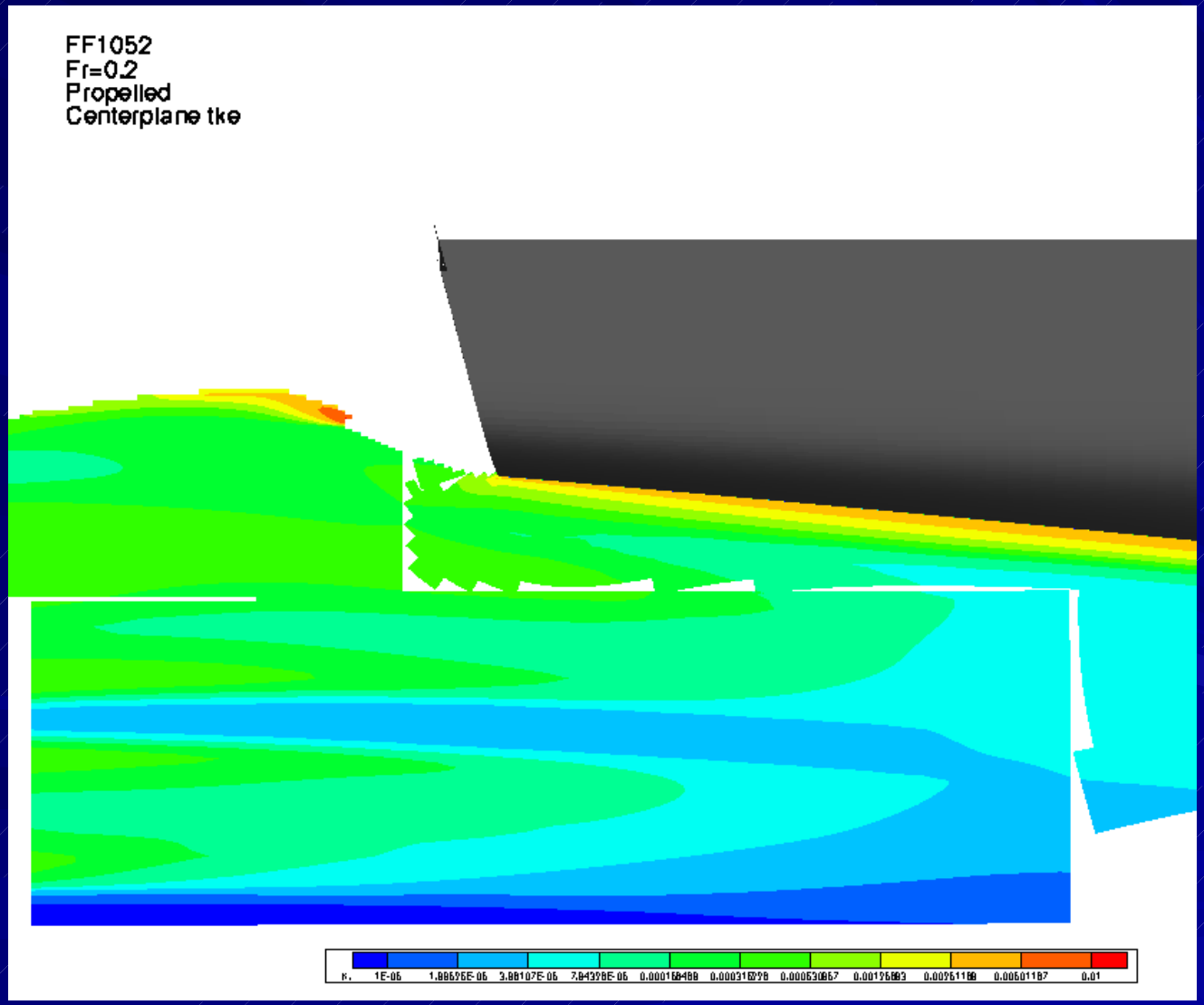

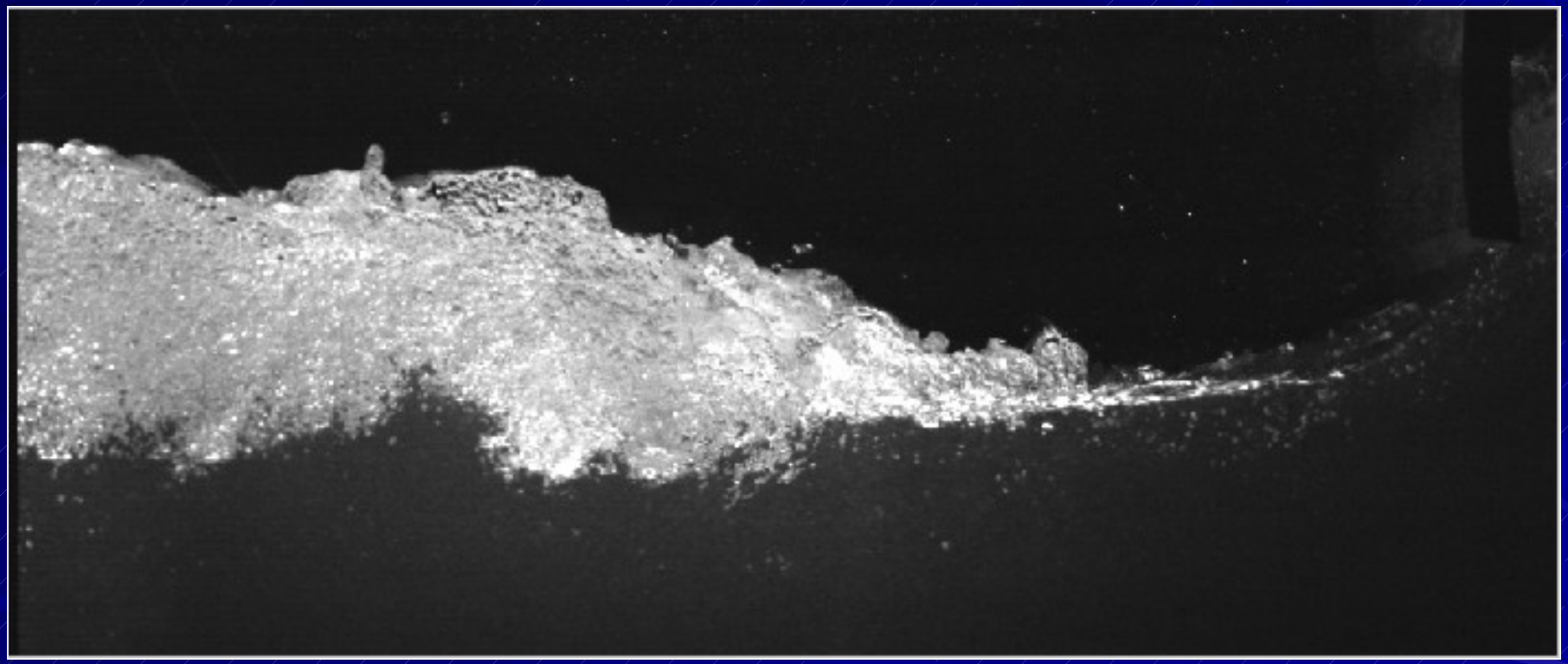

quasi-stationary toe

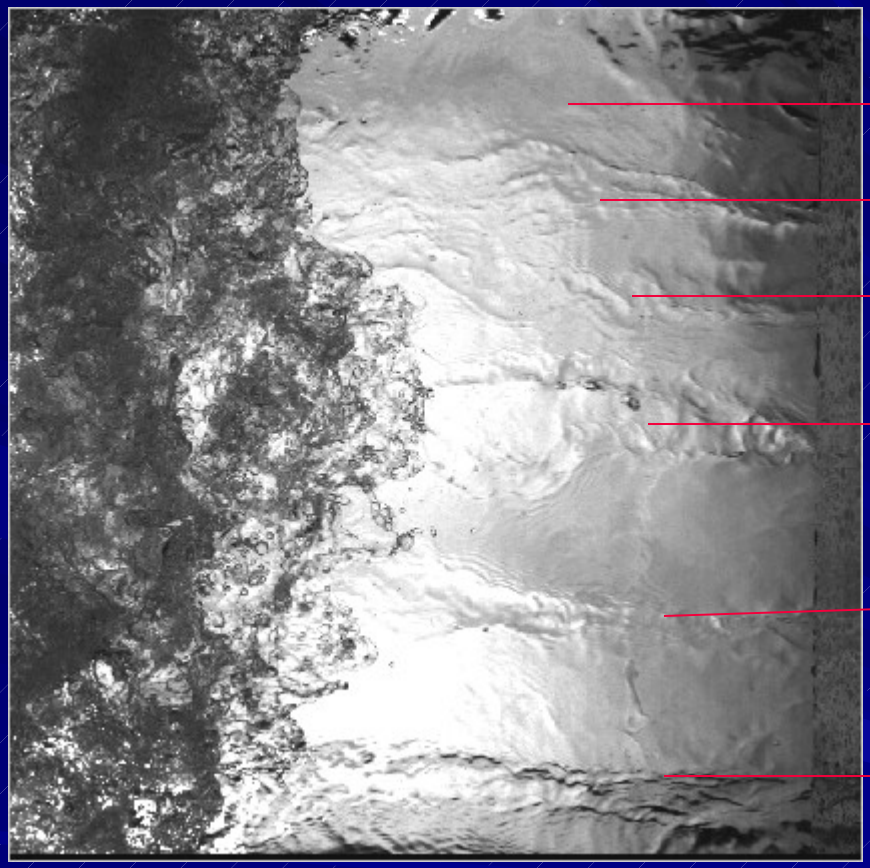

Top View. Stationary 2-D Stern Breaker

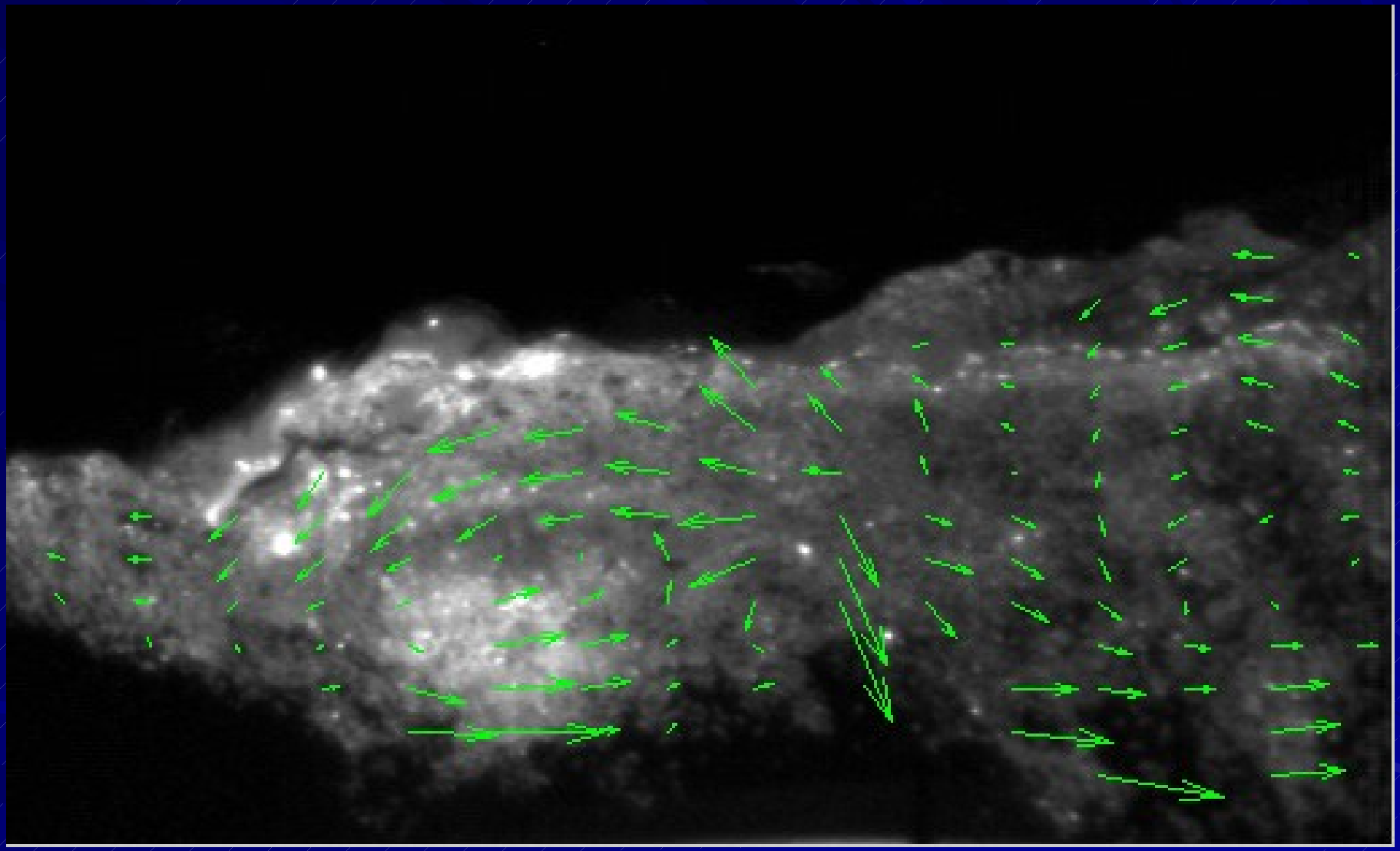

Passage time of the LS's

- The passage time of the LS's at a given location can be also measured.

$$I(x_{fix},t)=\int_y \text{image}(x_{fix},t)\,dy$$

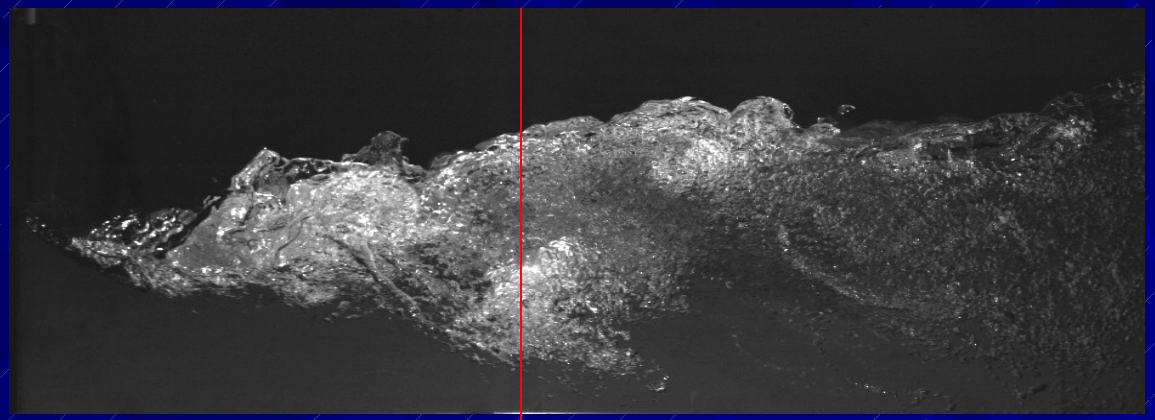

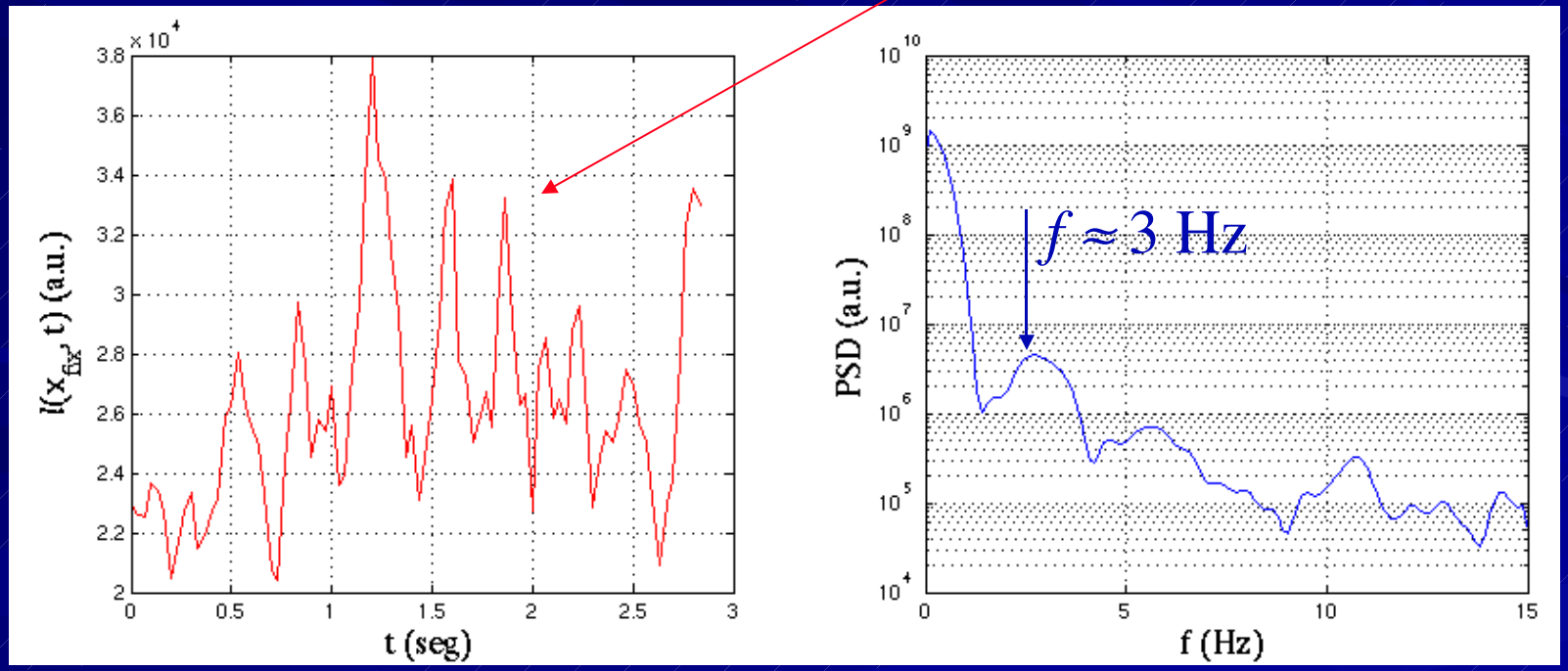

Velocity and size of the LS's

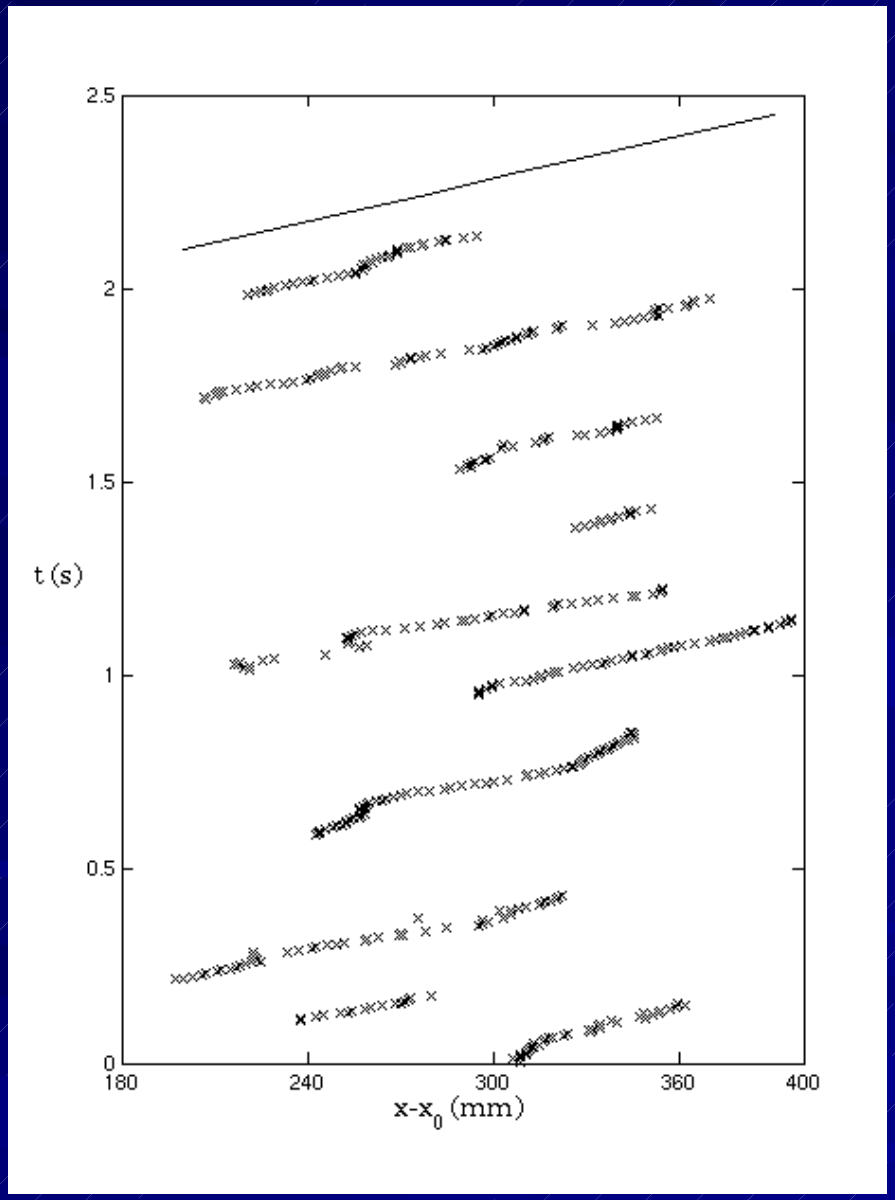

- Experimental conditions:
  U_0 = 2.25 m/s; Δh = 8 cm

- The LS's move with a mean velocity U_{mean} = 0.45 m/s.

- The size $l(x)$ of the LS's growths almost linearly:

$$l(x) = \delta\,(x - x_0)$$

$$\delta = 0.4\ (\approx 20^{o})$$

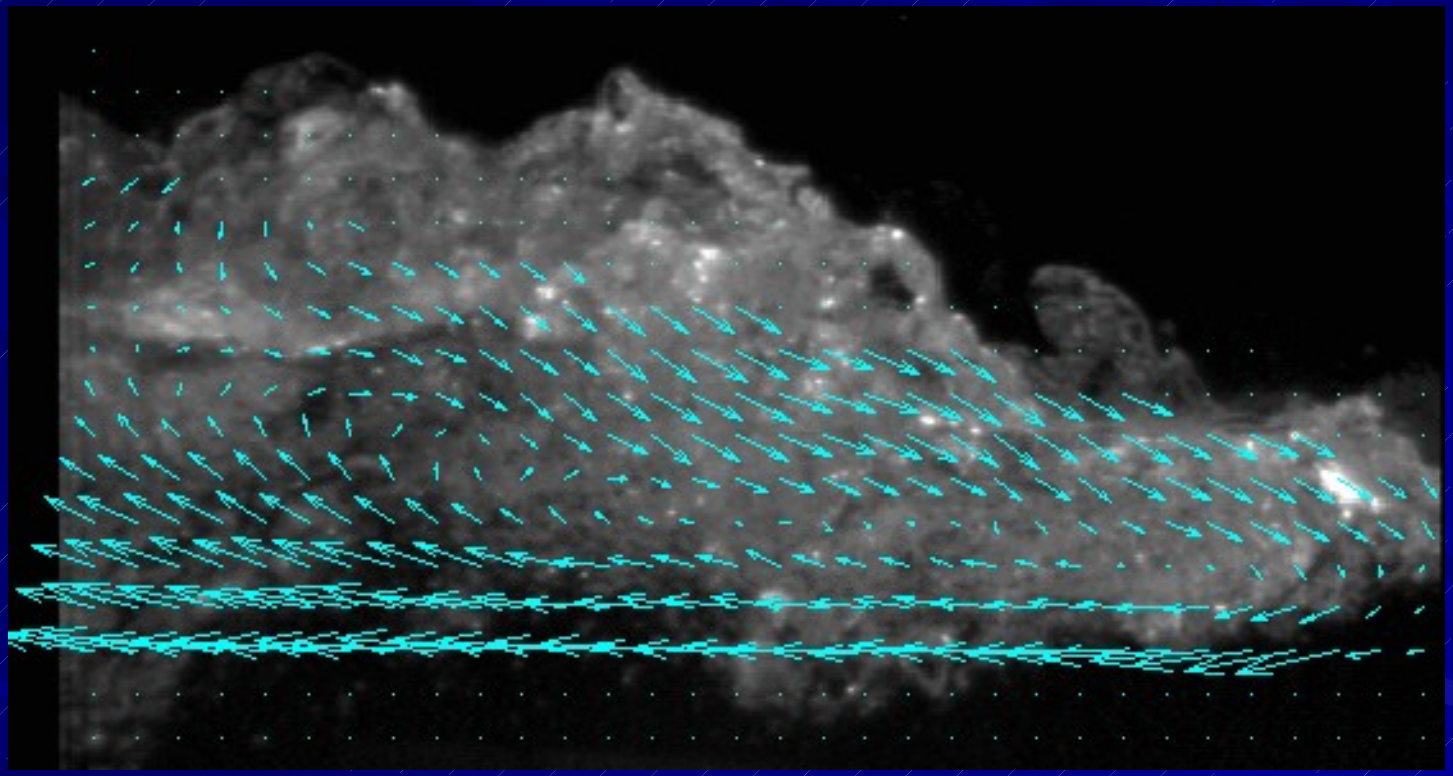

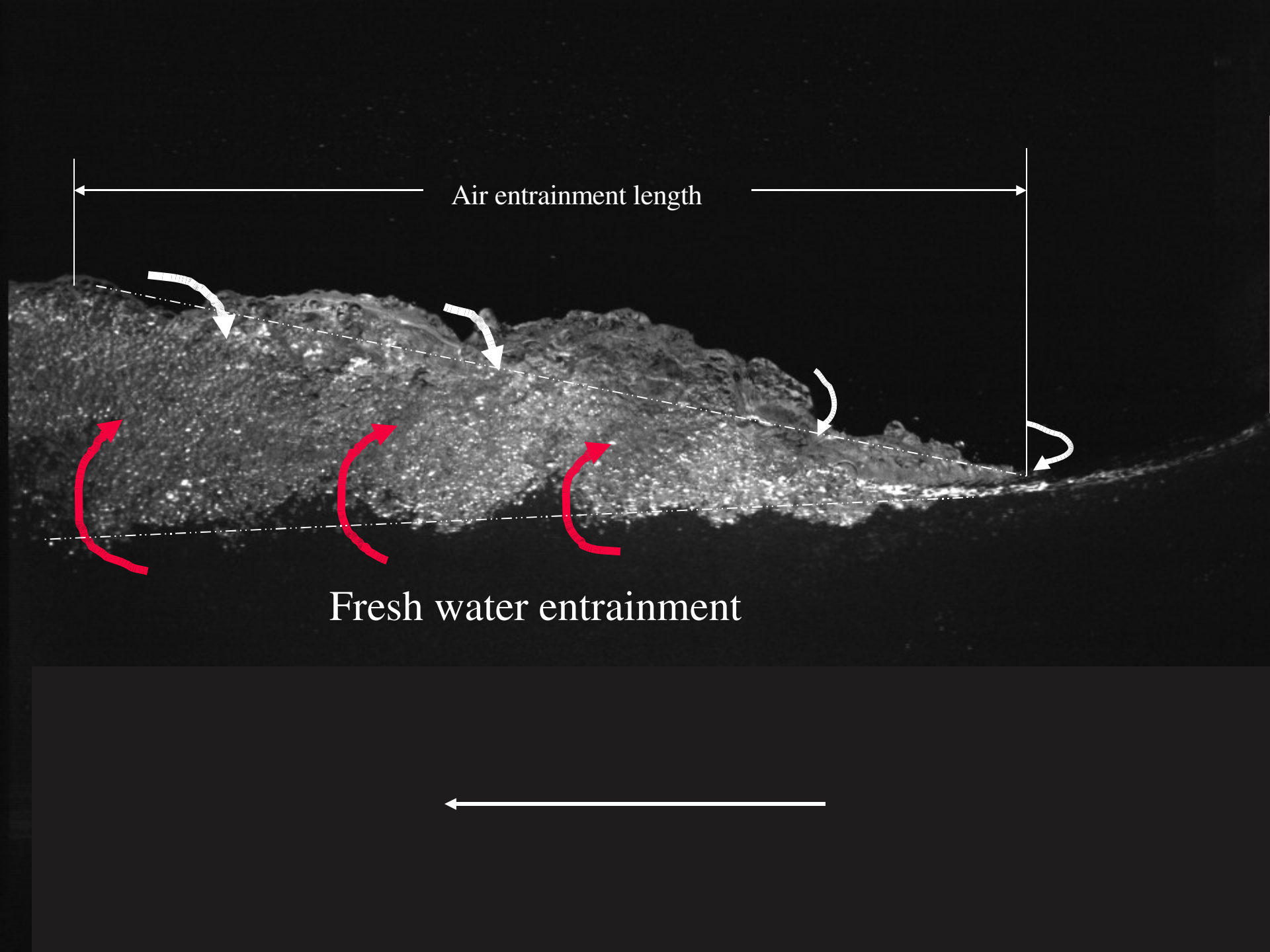
Air entrainment length
Fresh water entrainment

Air entrainment model

$l = l(x)$

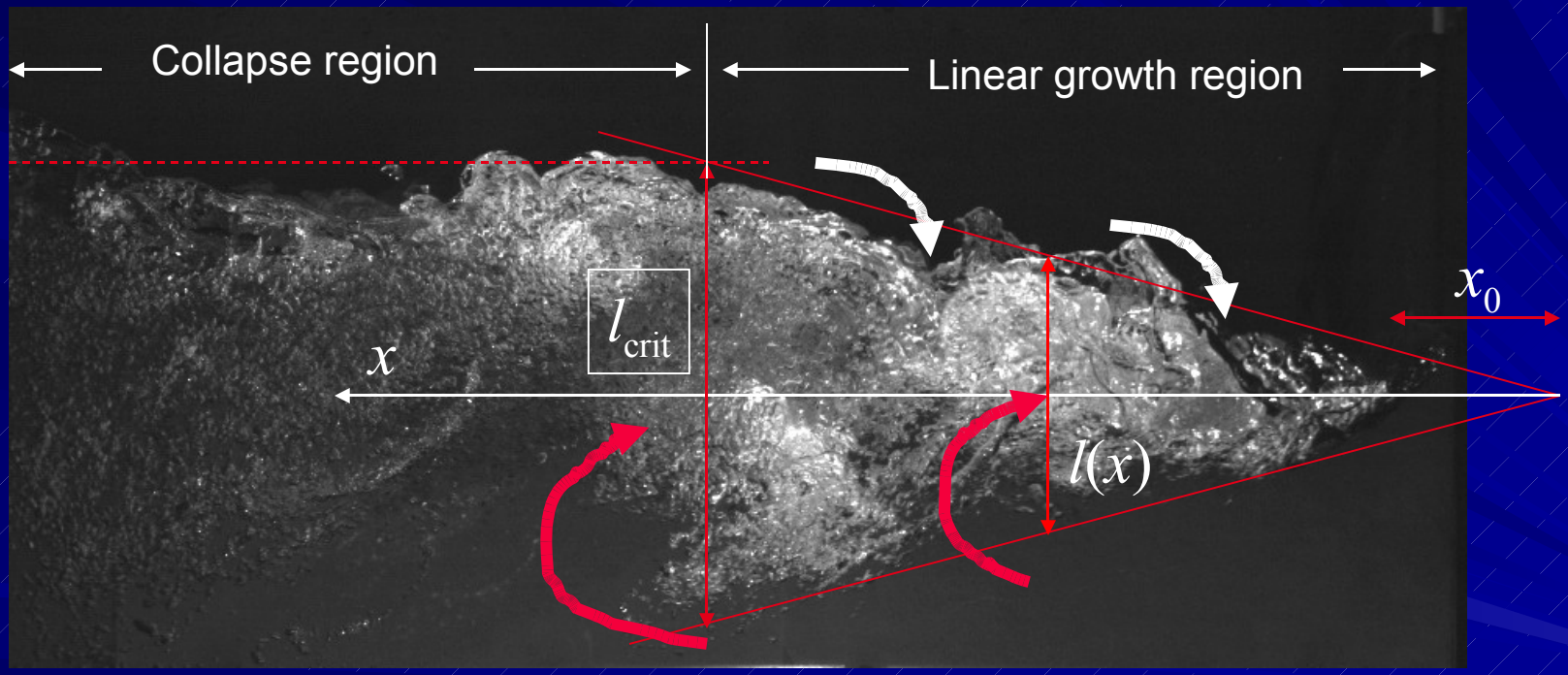

Results

Analysis of the mean velocity profiles. Self-similar horizontal velocity profiles.

- If the adimensional velocity profiles are plotted against $\eta = (y - y_{0.1})/(y_{0.35} - y_{0.1})$ they exhibit self-similarity

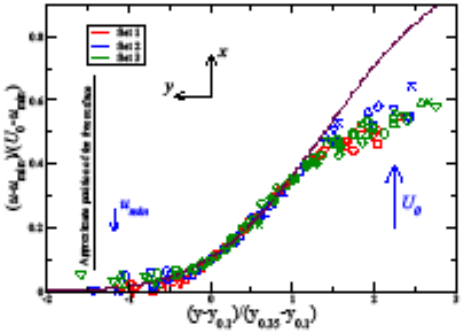

- Close to the interface with the potential-flow region, the profiles departure from the profile proposed by Townsend (1976), $U = (1 + \mathrm{erf}((\eta - \eta_0)/C))/2$.

Discussion

Growth rate of the mixing layer (I/II)

- In the classical mixing layer, the growth rate $\mathrm{d}\ell/\mathrm{d}x$ is given by:

$$\frac{U_0 + u_{\min}}{U_0 - u_{\min}} \frac{\mathrm{d}\ell}{\mathrm{d}x} = 2\beta = 0.028$$

being β the entrainment parameter (Townsend, 1976).

- In the present flow, assuming a velocity profile $U = (1 + \mathrm{erf}((\eta - \eta_0)/C))/2$, the growth rate is given by:

$$\frac{\mathrm{d}\ell}{\mathrm{d}x} = 1.11 \frac{\mathrm{d}(y_{0.1} - y_{0.35})}{\mathrm{d}x}$$

- The growth rates calculated for the three sets are:

Set	1	2	3
Growth rate, $\mathrm{d}\ell/\mathrm{d}x$	0.11	0.14	0.12
$(U_0 + u_{\min})/(U_0 - u_{\min})$	0.852	0.824	0.965
$(U_0 + u_{\min})/(U_0 - u_{\min})\,\mathrm{d}\ell/\mathrm{d}x$	0.095	0.113	0.118

- **Air entrainment and bubble formation by a three-dimensional deep-water stern breaker**
  - Effect of the corner flow

Air Entrainment Mechanism
Steady 3-D Breaker

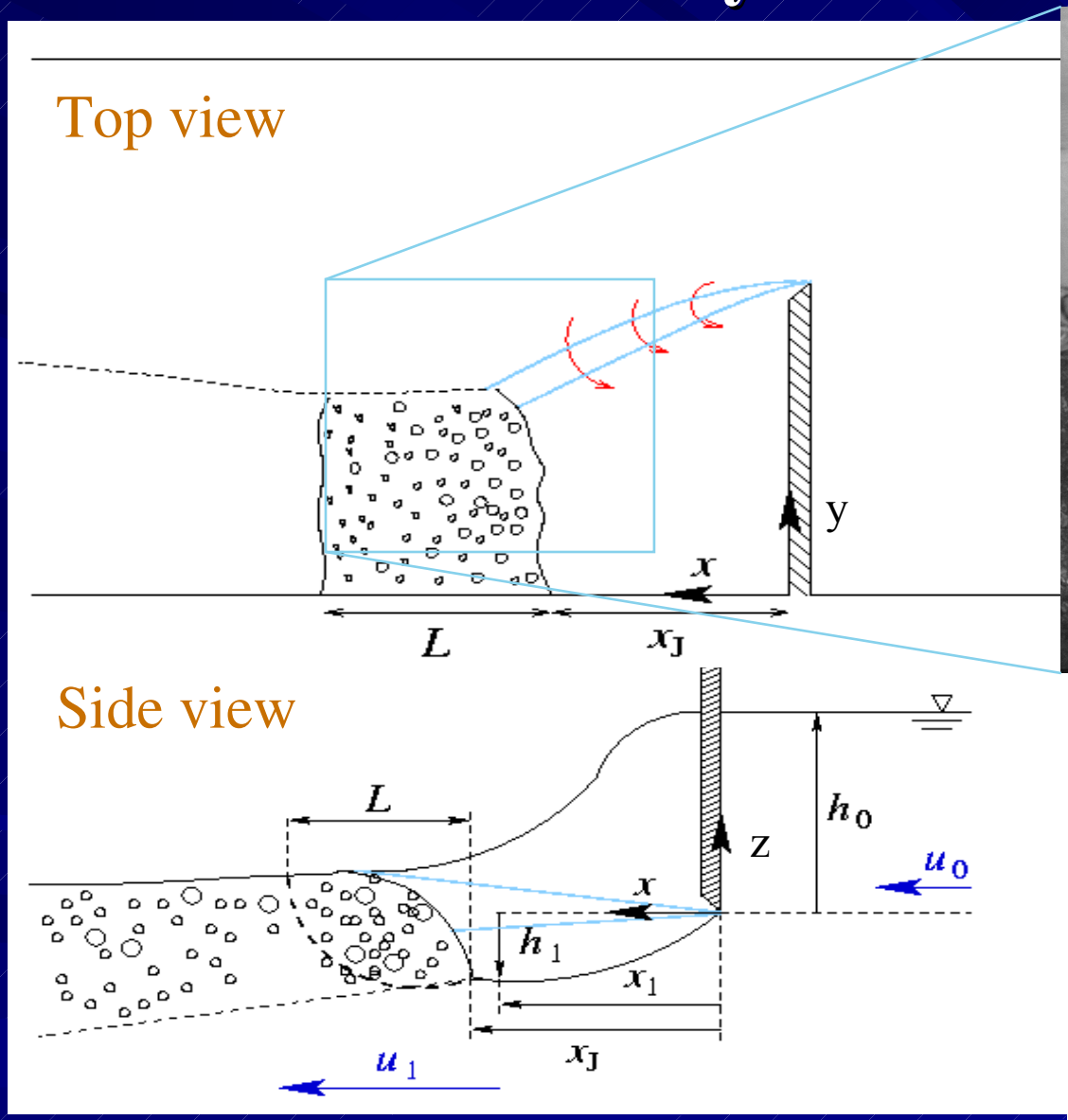

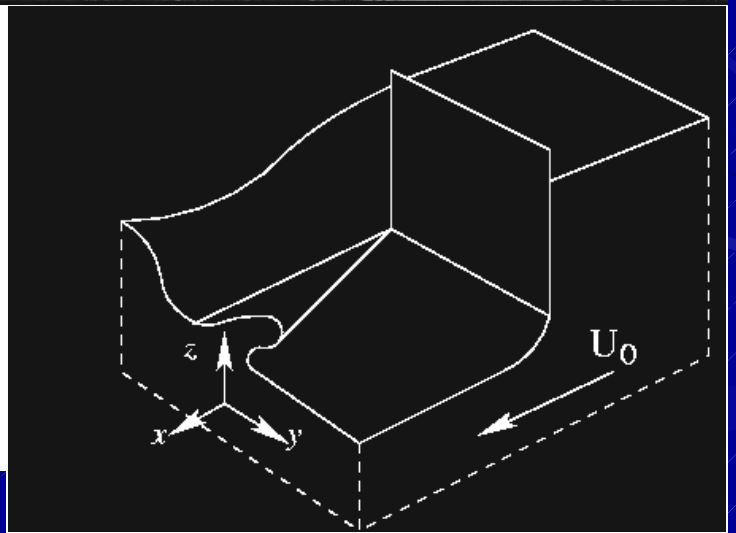


10:42:40:04

Unsteady Bubbly Flow Modeling

FF1052 stern wave

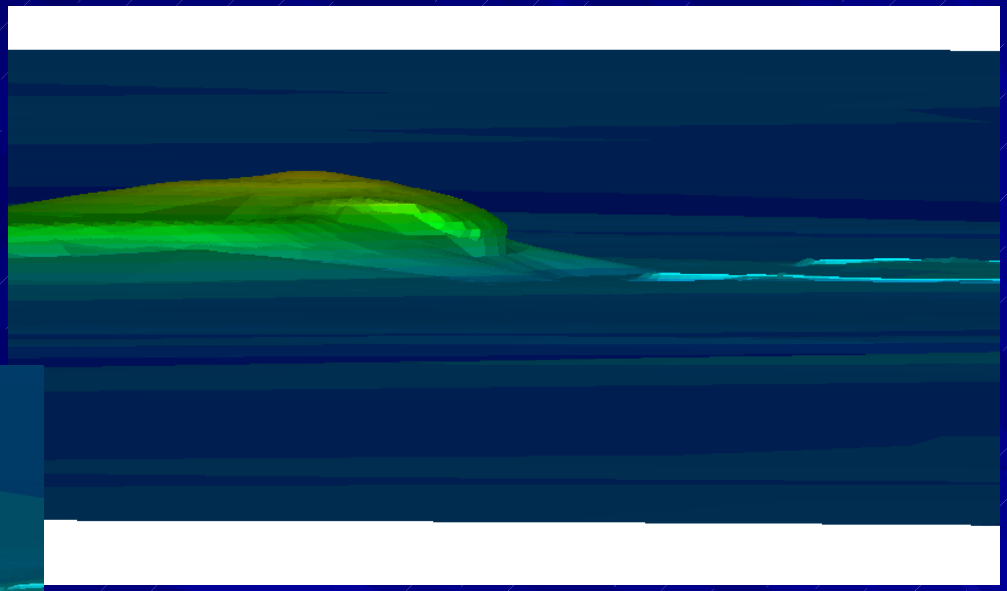

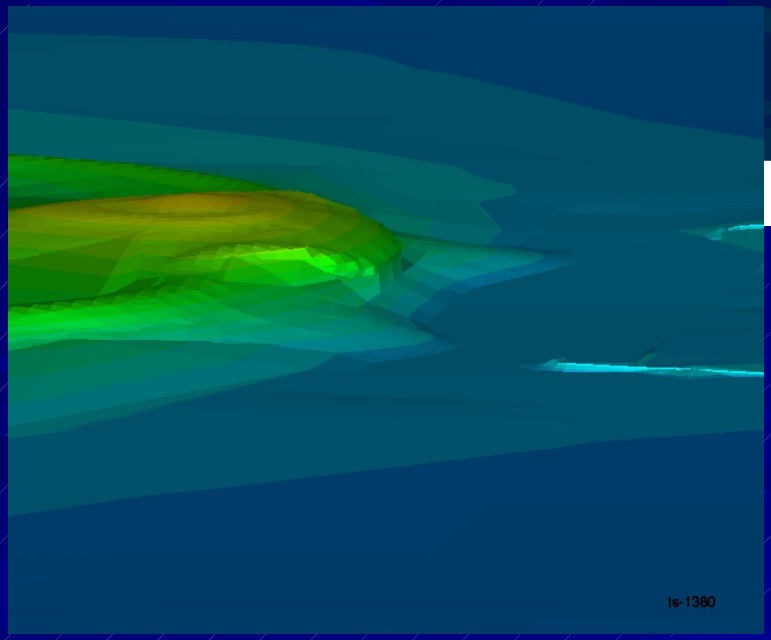

Bibliographical review

HYDRAULIC FLOWS IN SUDDEN EXPANSIONS:

• Unconfined Expansion of supercritical water flows. Hager and Yasuda, Journal of Engineering Mechanics,123 (5). 1997.

• Supercritical flow at abrupt expansions. Hager and Mazunder, Proc. Instn Civ. Engrs. Wat., Marit. & Energy, 96. 1992

EVOLUTION OF NONLINEAR WAVES ON A STEEP SLOPE:

• Nonlinearity of the Three-dimensional Flow Past a Blunt Ship. Fernandez, Journal of Fluid Mechanics, 108. 1981.

• Nonlinear Evolution of Small Disturbances into Roll Waves in an Inclined Open channel. Yu and Kevorkian, Journal of Fluid Mechanics, 243. 1992.

• Potential Energy in Steep and Breaking Waves. Schultz, Huh and Griffin, Journal of Fluid Mechanics, 278. 1994.

CRITERIA BETWEEN SPILLING AND PLUNGING:

• Experimental Investigation of Wave Breaking Criteria Based on Wave Phase Speeds. Stansell and MacFarlane, Journal of Physical Oceanography, 32 . 2002.

• Wave breaking in deep water. Banner and Peregrine. Annual Review of Fluid Mechanics, 25. 1993.

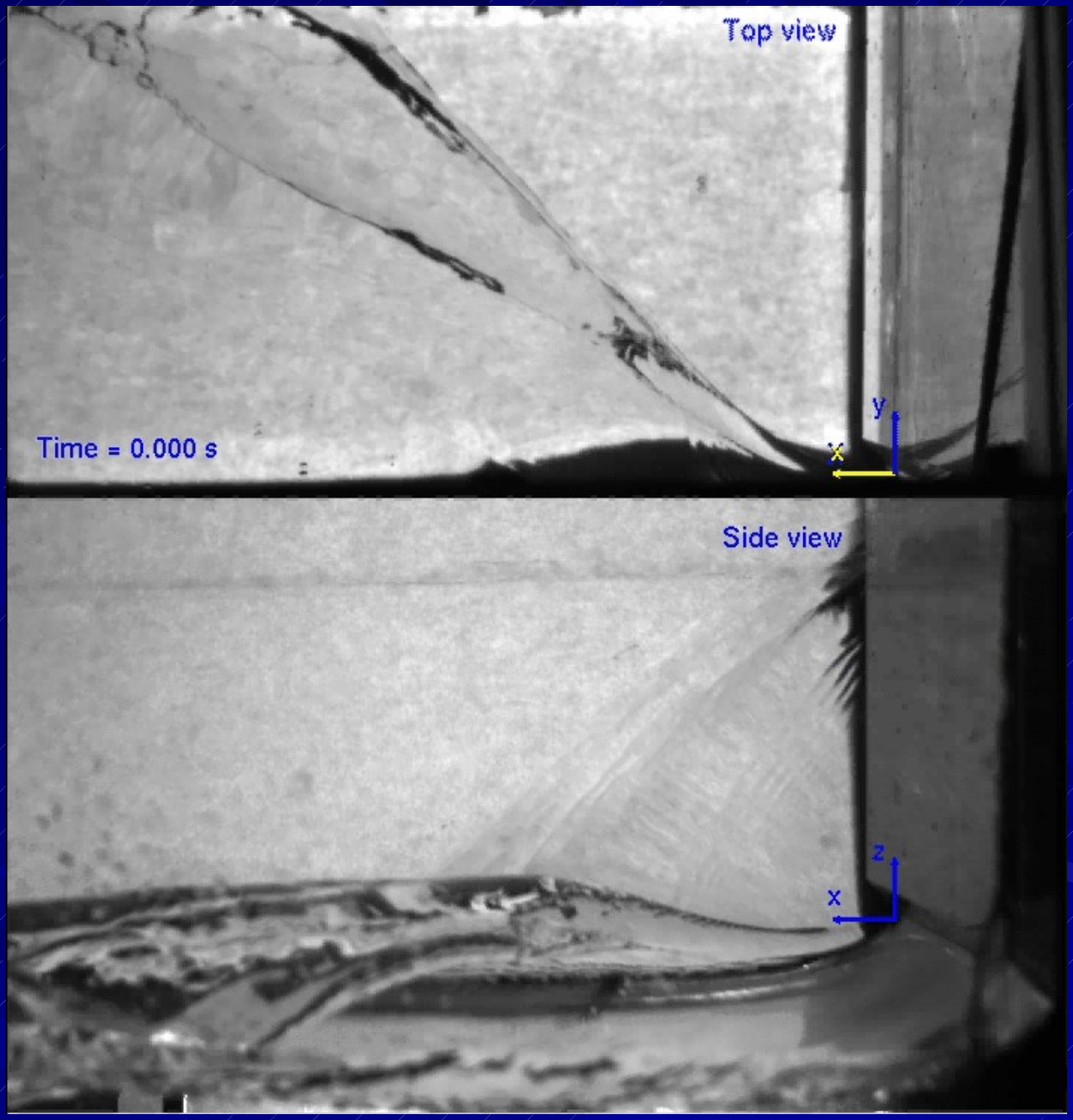

U

U

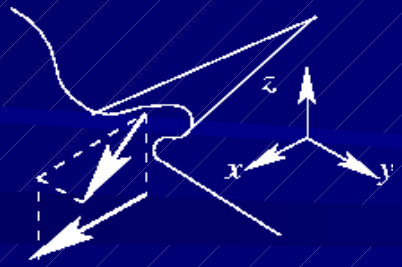

Experimental results

Different wave breaking regimes

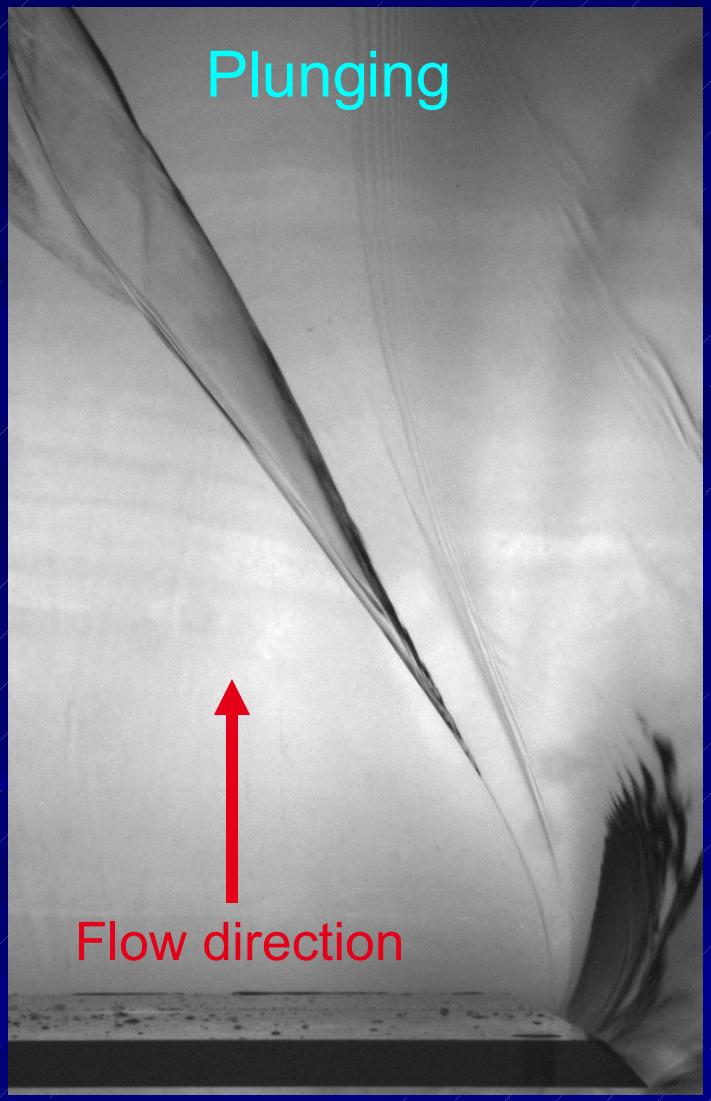

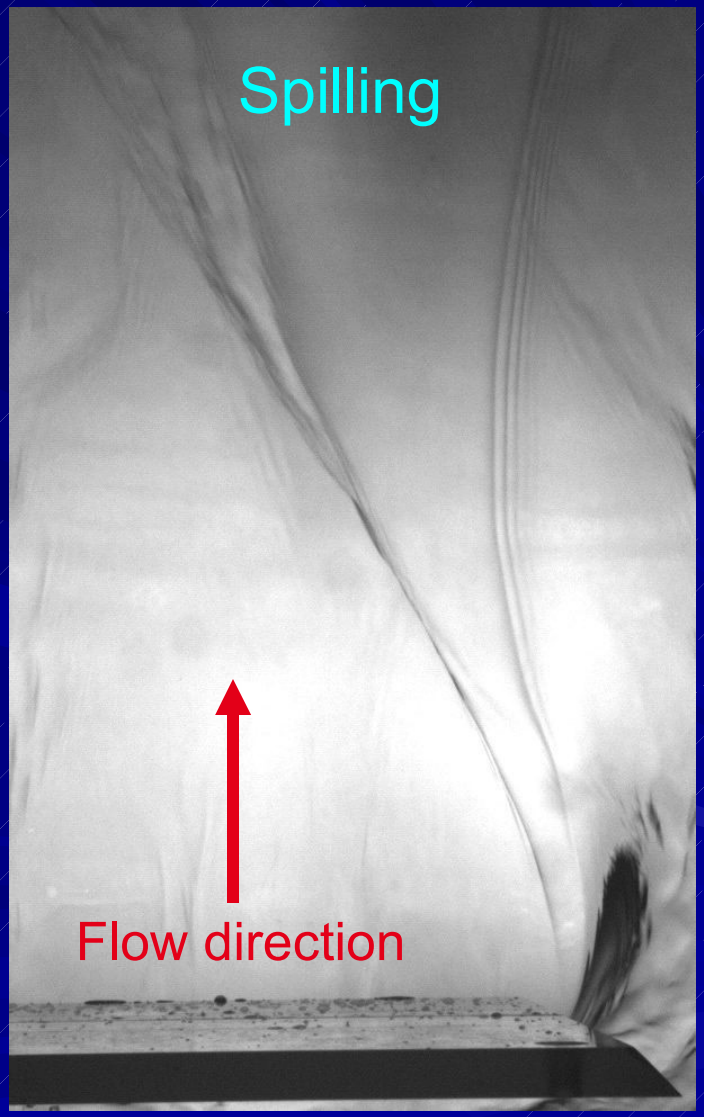

Experimental results

Different wave breaking regimes

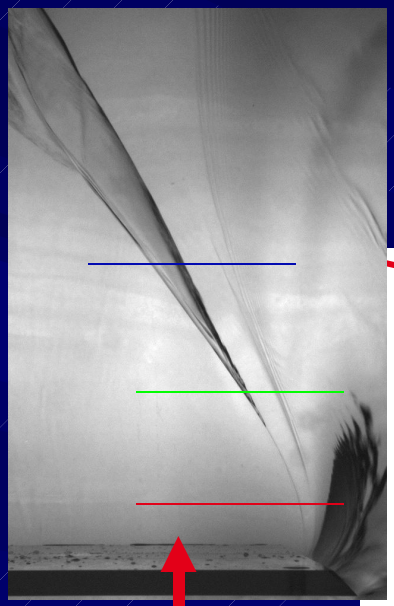

Flow direction

Plunging

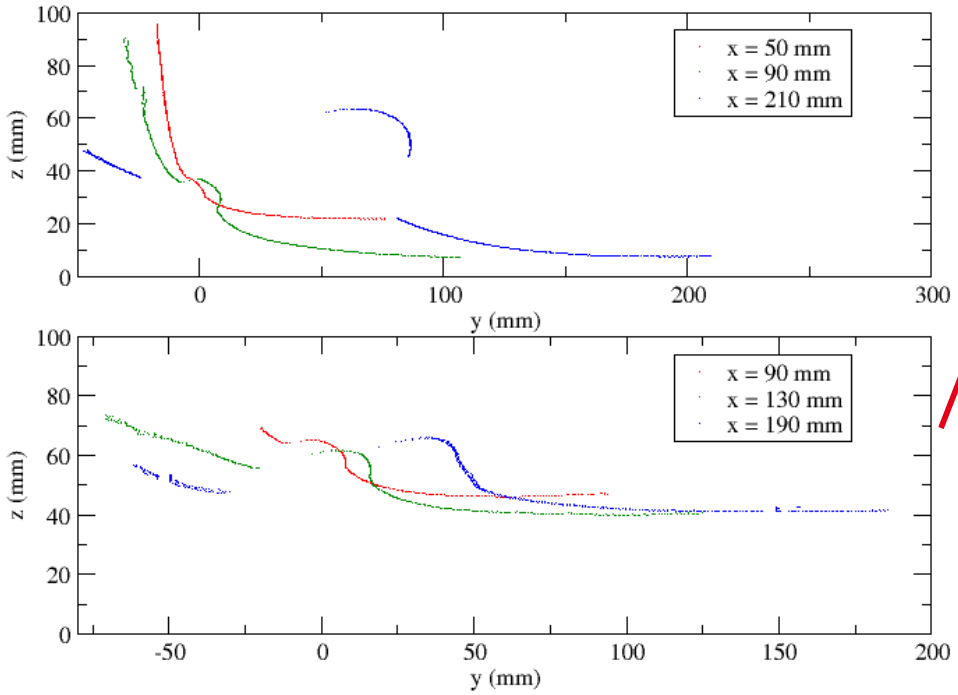

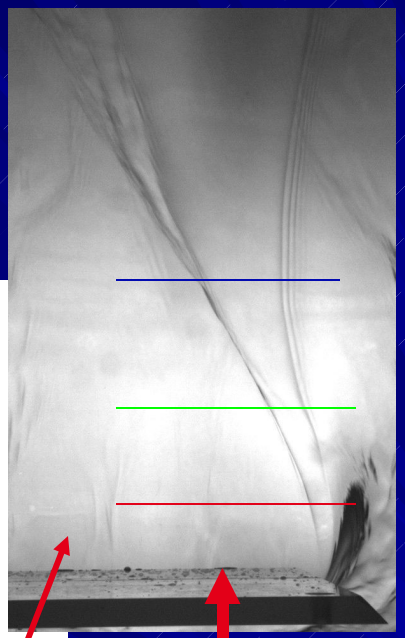

Flow direction

Spilling

Flow configuration

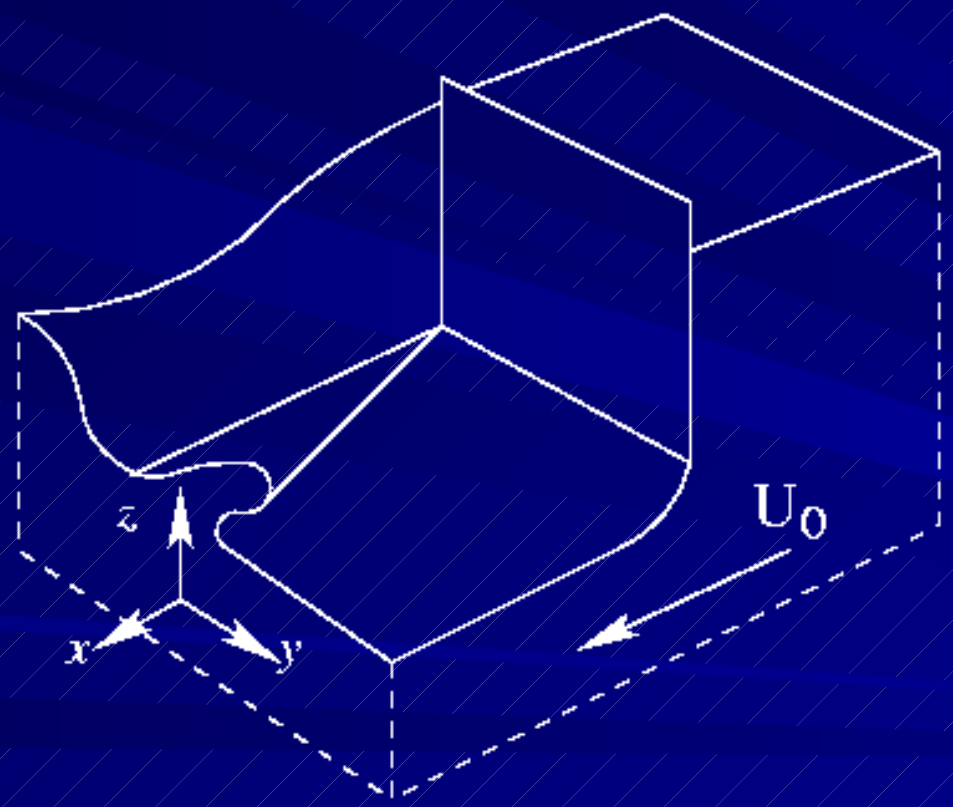

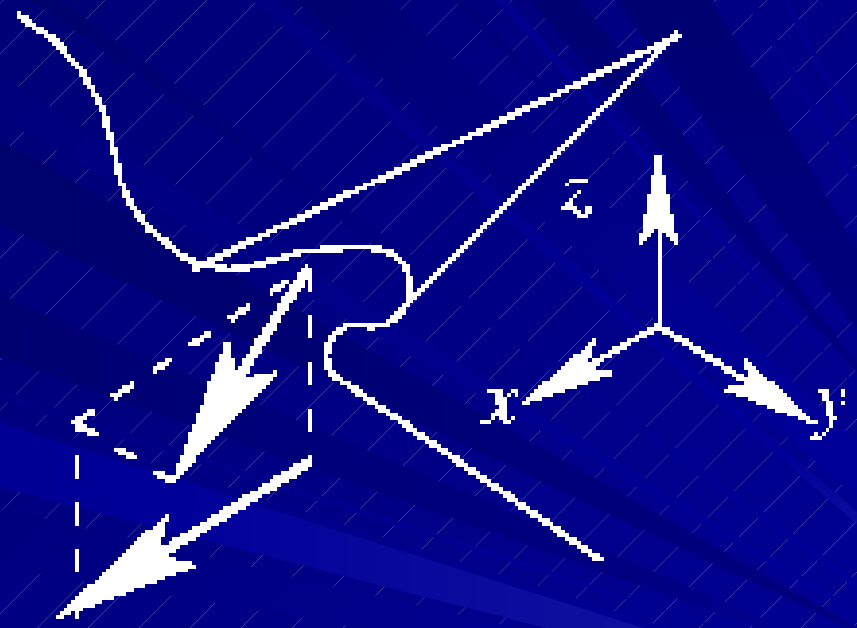

Vertex wave. Two configurations

- Measurements of the free surface for two representative sets:

Plunging breaker

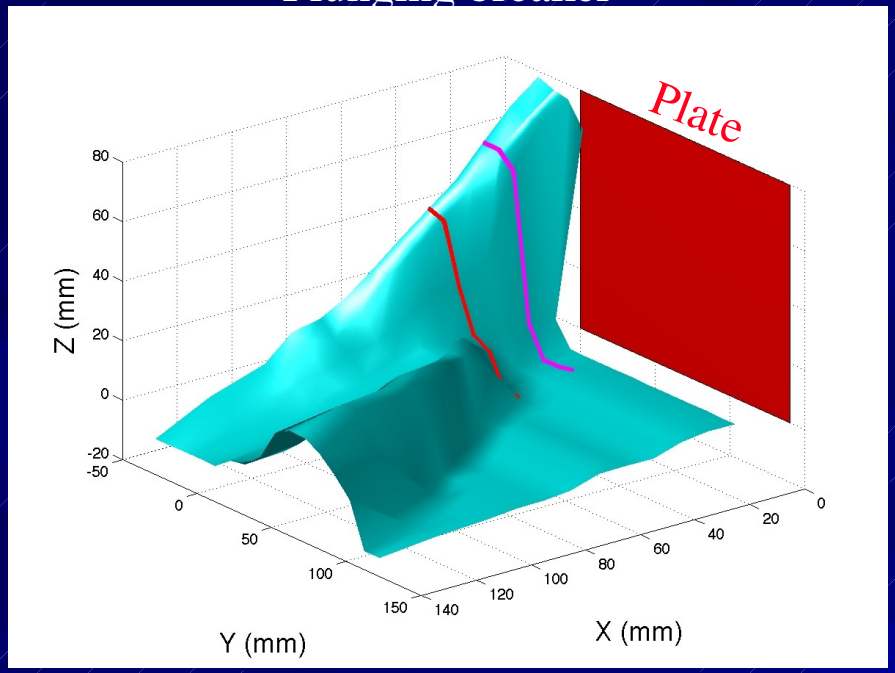

In this experiment, the crest separates at the red line

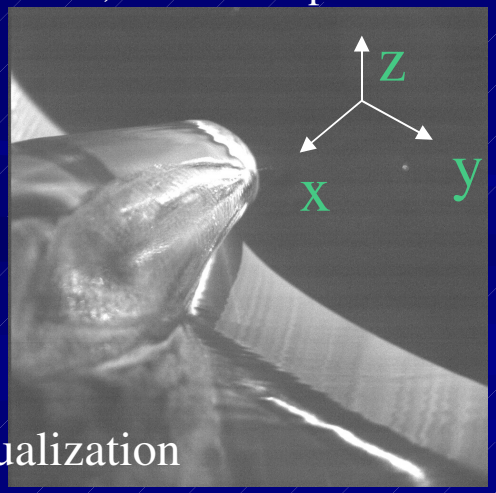

LIF visualization

Spilling breaker

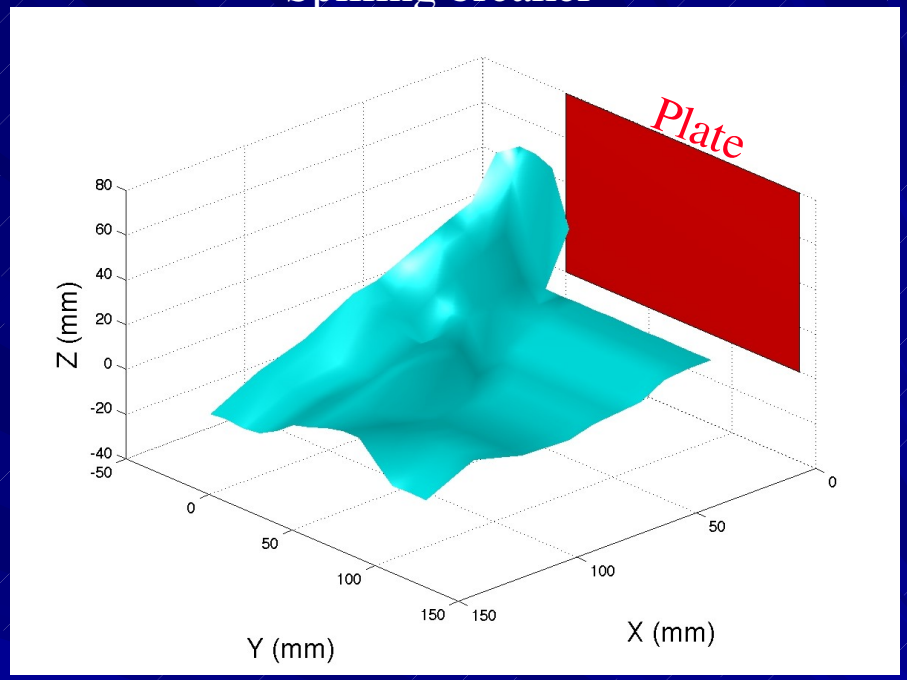

No separation of the wave crest

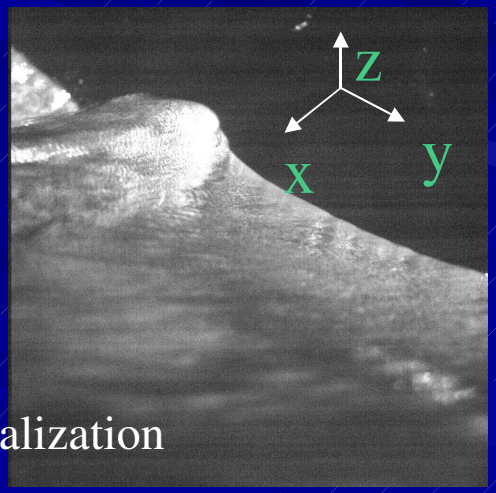

LIF visualization

Which mechanism generates the wave?

- To investigate the formation of the wave, LDA measurements have been performed.

- Only two components (X and Z) could be measured. The third one was calculated by integration of the continuity equation:

measured

computed

$$\nabla \cdot \vec{v} = 0 \Rightarrow \frac{\partial u}{\partial x} + \frac{\partial v}{\partial y} + \frac{\partial w}{\partial z} = 0$$

- With the computed Y-component of the velocity, streamwise vorticity has been calculated for two cross-sectional sections: x=16 mm (the closest to the plate that could be measured, magenta line in the figure) and x=40 (where separation of the wave

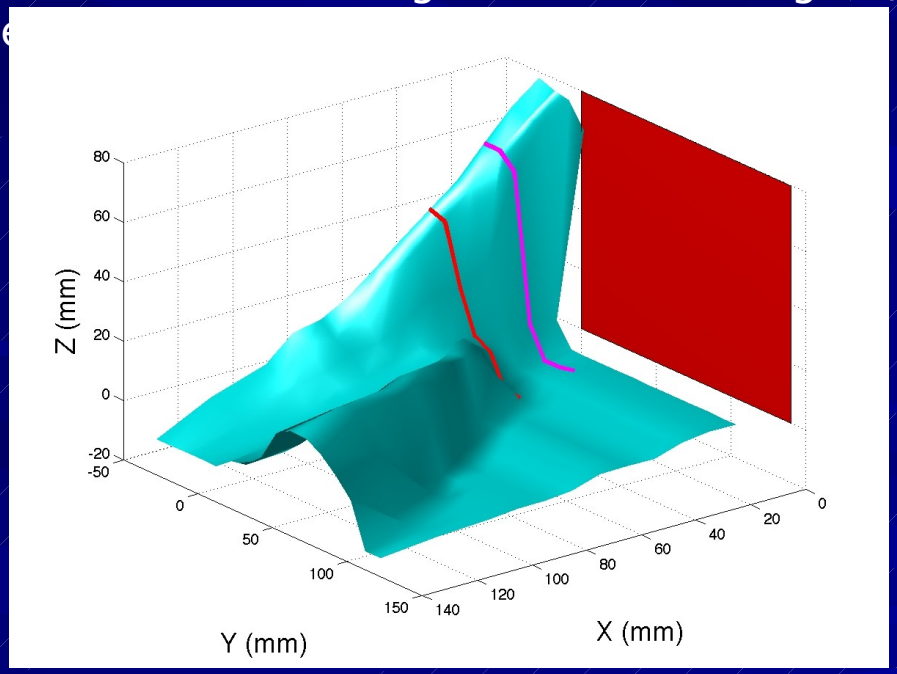

Which mechanism generates the wave?

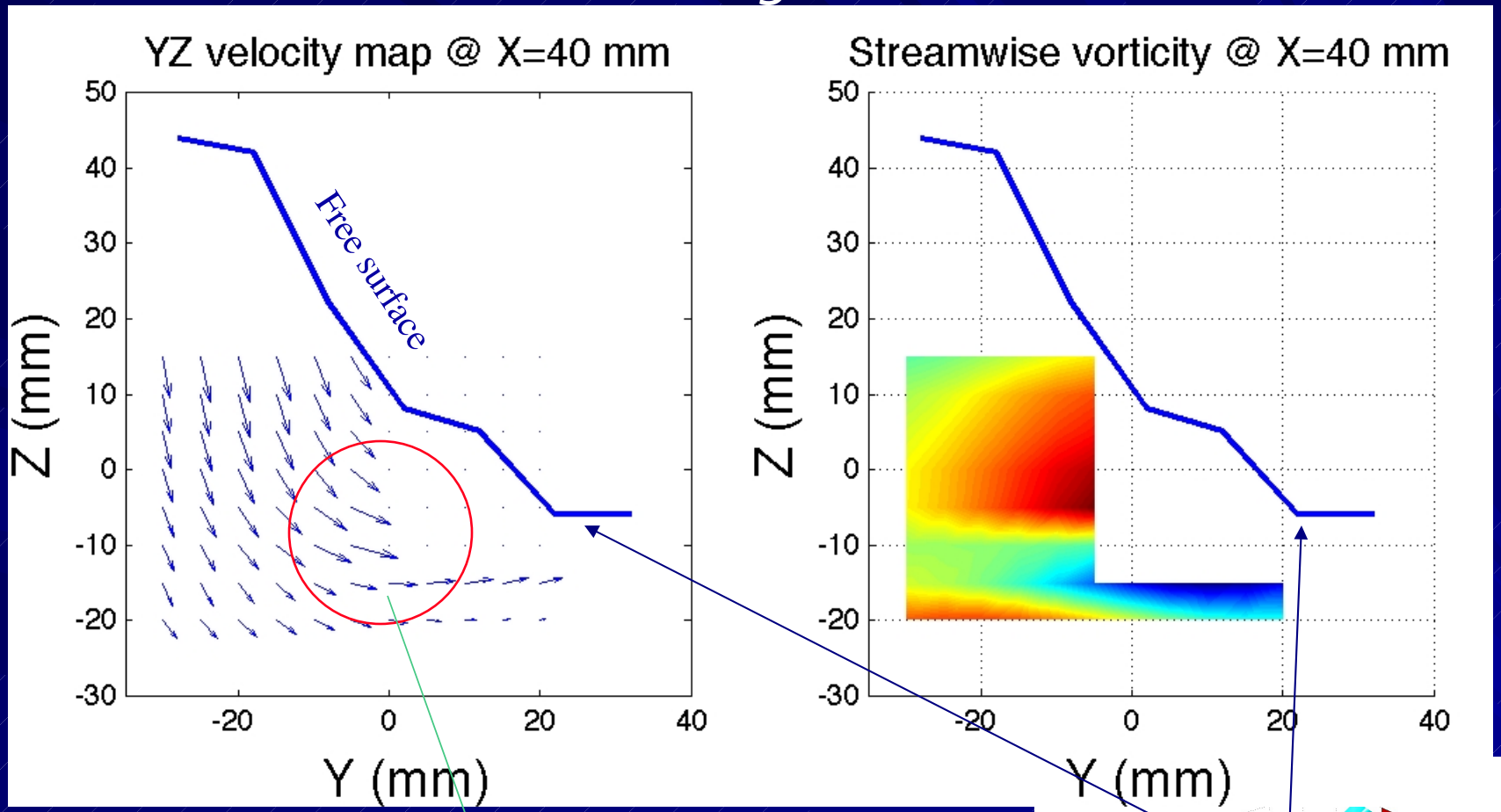

There is a transversal "jet" approximately at the depth of the edge of the plate.

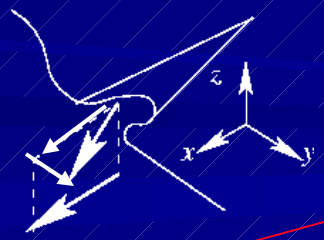

section where the wave crest separates

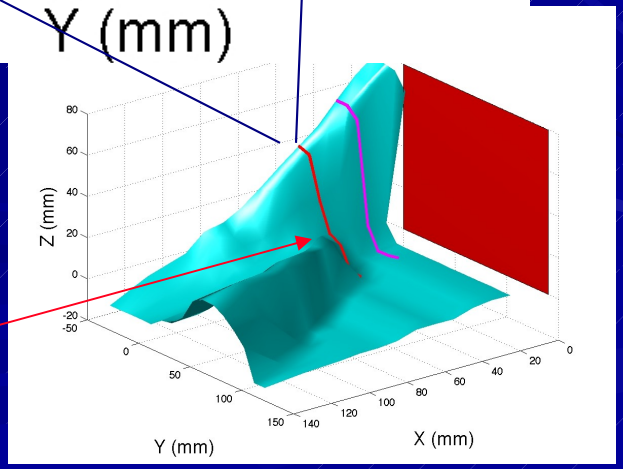

mechanism of wave generation

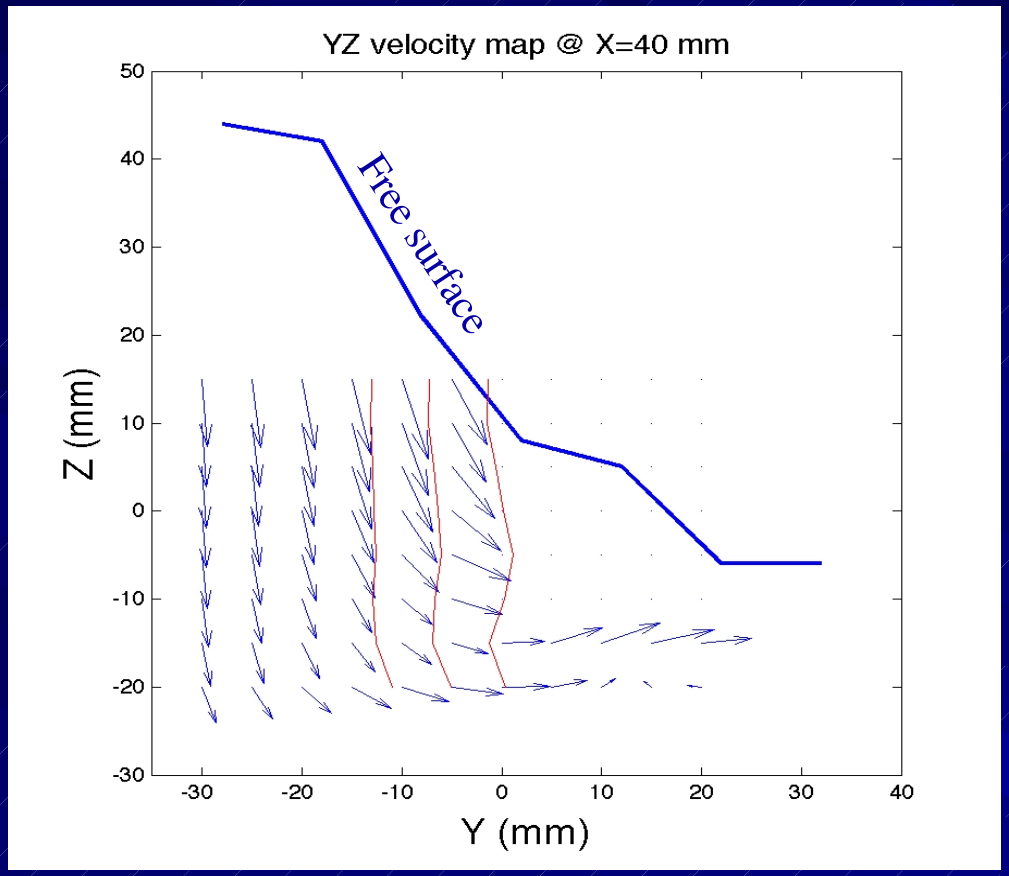

Y-velocity profiles (red lines) show the existence of the "jet".

- Assuming gravity is the driving mechanism, the transversal velocity, $v(z)$, would be of the order:

$$v \sim \sqrt{2\,g\,(h_0 - h)}$$

for $h > h_1$. In other words, the hydrostatic pressure driving the spilling is $\Delta p \sim \rho\, g\,(h_0 - h)$

- For $z < h_1$, on the other hand, this hydrostatic pressure is opposed by another one of the order:

$$\Delta p \sim \rho\, g\,(h_1 - h)$$

- Therefore, the maximum v should be at $z \approx h_1$, as observed

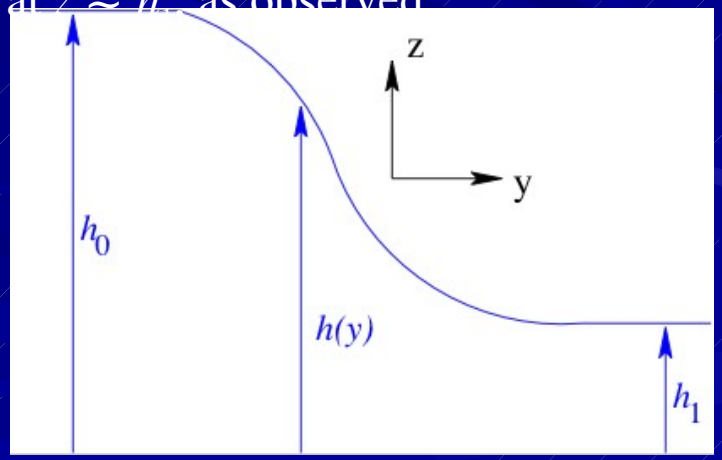

ansversal velocity/vorticity & free surface

Vorticity measured at X=16 mm (plunging wave)

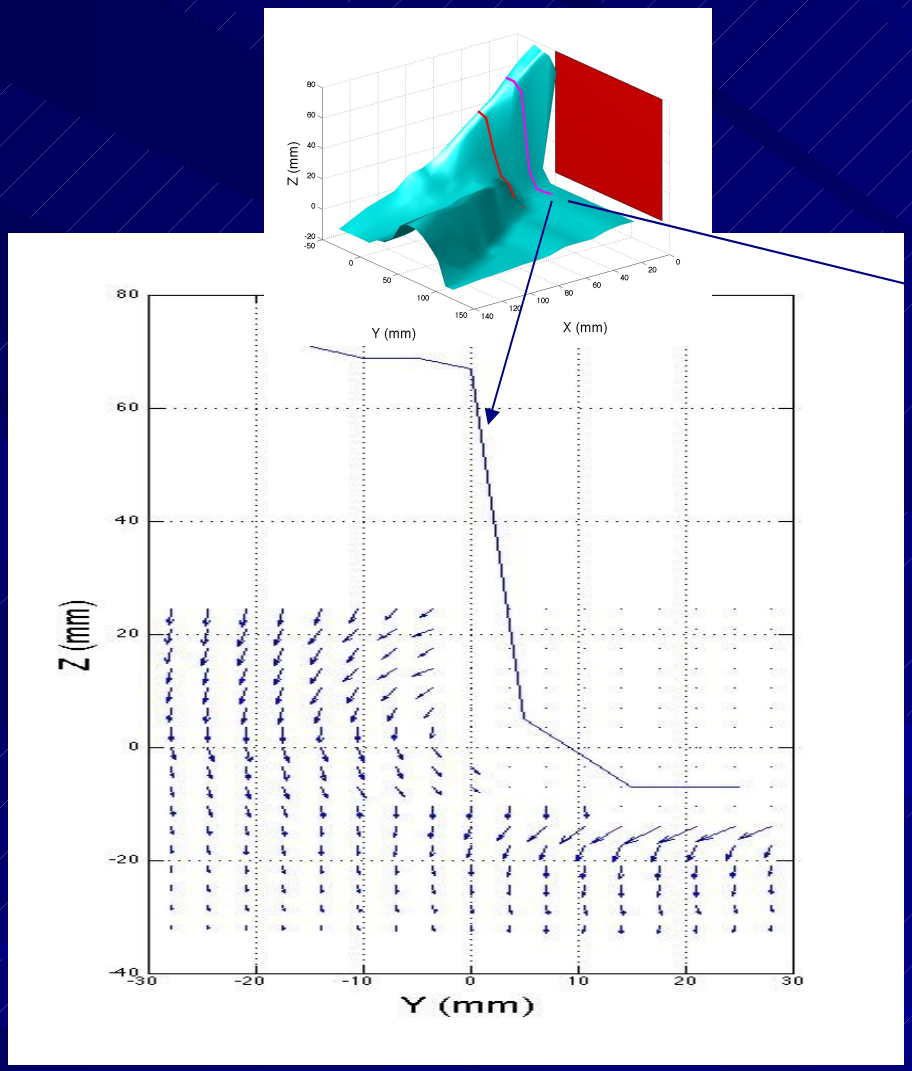

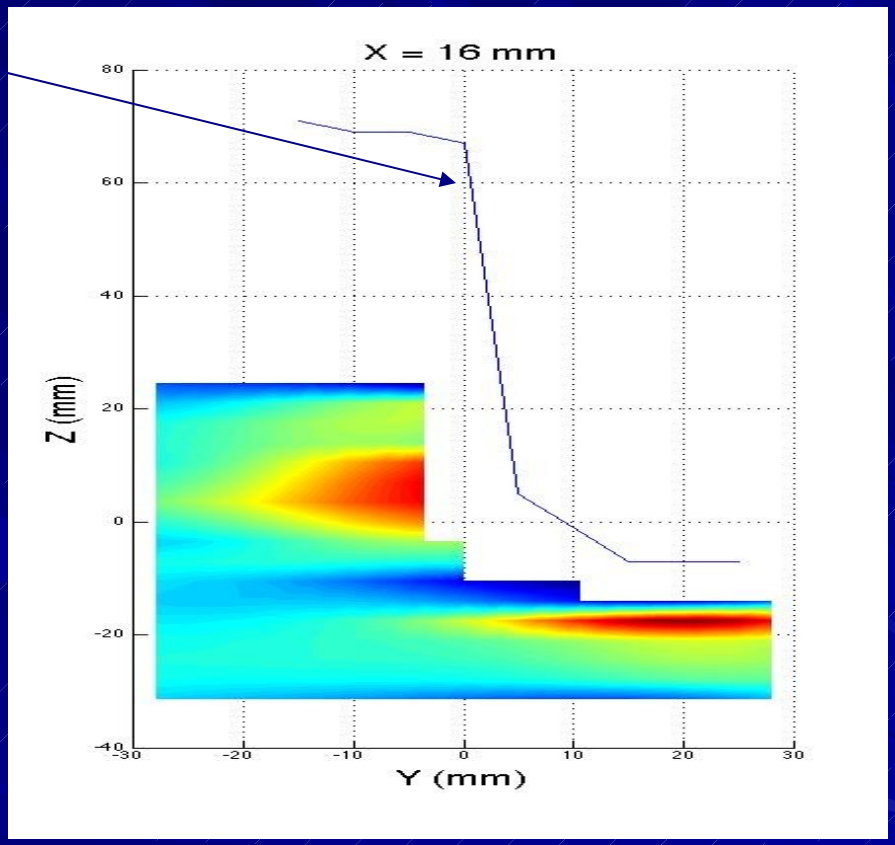

Vy-Vz vector map @ X=16 mm

Streamwise vorticity @ X=16 mm

Modellig the wave formation

The streamwise velocity is uniform within ±20% in the region where the wave d

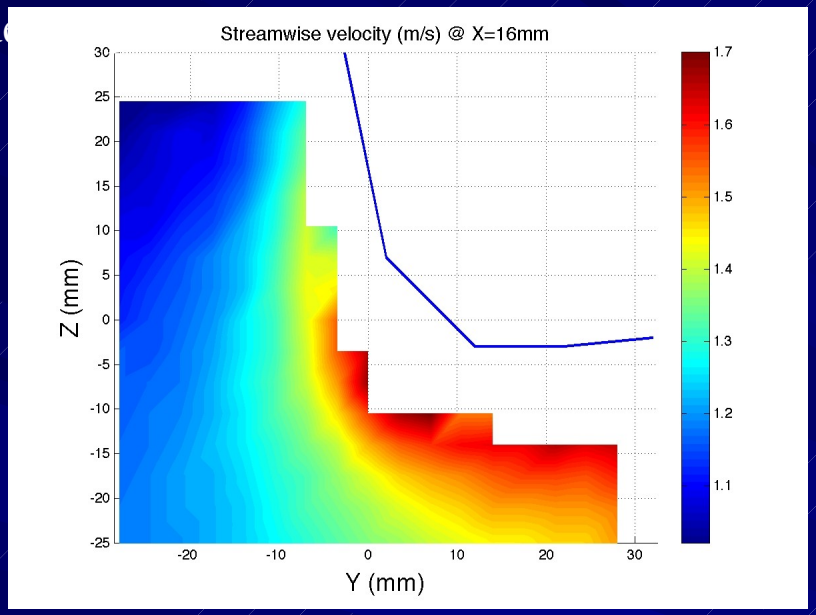

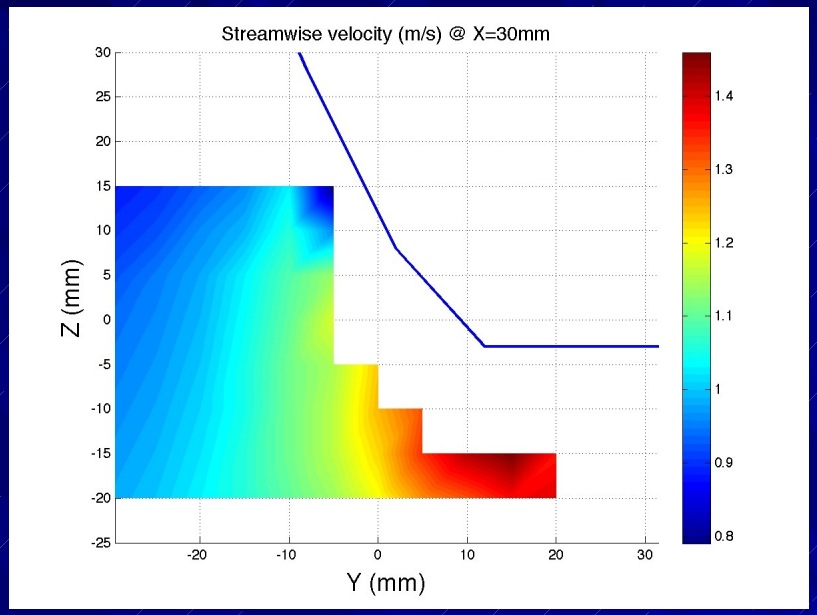

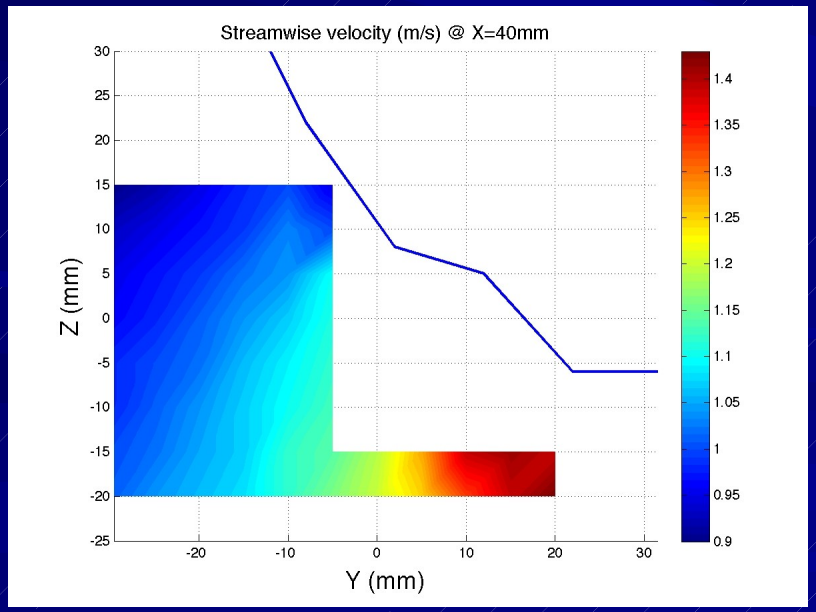

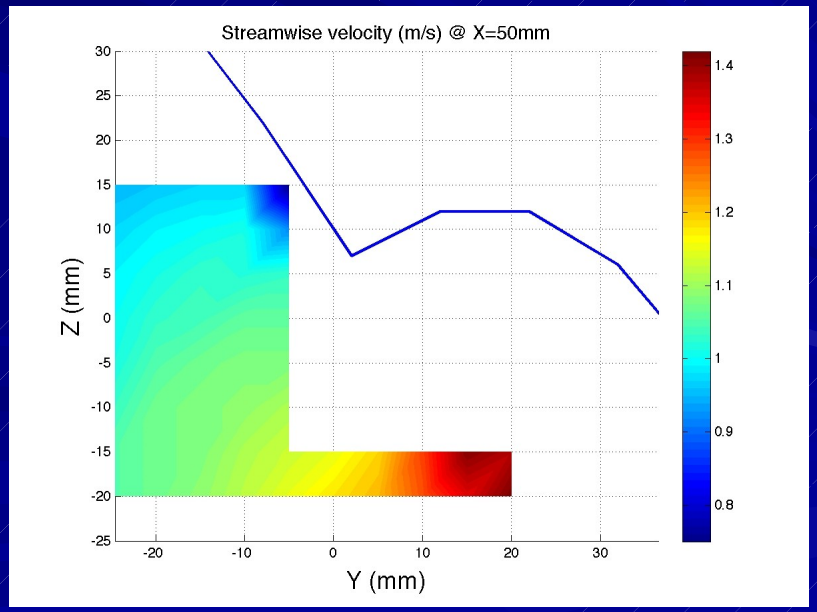

Modellig the wave formation

• Since the formation mechanism seems to be gravity driven, can it be described by some modification of the shallow water equations?

• Hager & Yasuda (1997) proposed a simplified model based on the shallow water equations to study a similar problem. The model assumes a velocity field (u, v, w) = (U + u', v, w) with U >> u', v, w: <u>2D+Time approach.</u>

• In our problem, the large aspect ratio of the wave guarantees (u >> v, w) (in fact, this has beencorroborated experimentally), and one can we assume U >> u'

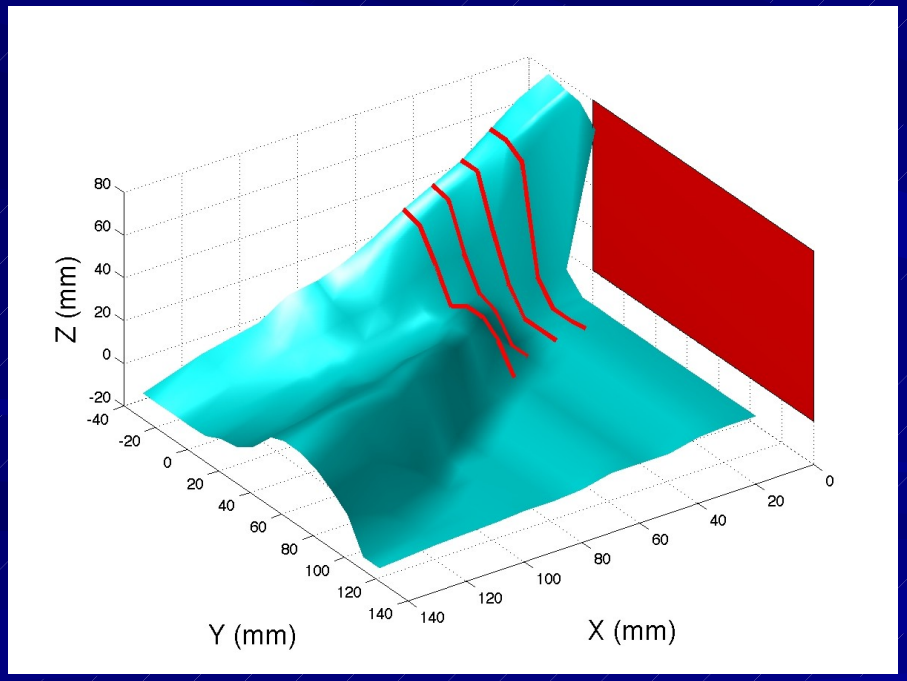

• Streamwise velocity contours have been measured at the sections indicated by red lines in the figure.

Wave generation mechanisms (I)

- Steady flow
- Velocity field can be written:

$$\vec{u} = \left(U_0 + u_x, u_y, u_z\right)$$

with $U_0 >> (u_x, u_y, u_z)$

- Gradients in the x coordinate are much smaller than in the y,z

$$\frac{\partial}{\partial x} << \frac{\partial}{\partial y}, \frac{\partial}{\partial z}$$

- Under these assumptions, there is an analogy between the evolution along the x axis of the wave profile in the y,z plane and the time evolution of a 2D wave: x/U_0 emerges as a time-like variable

$$U_0 \frac{\partial}{\partial x} \hat{U} \frac{\partial}{\partial t}$$

Wave generation mechanisms

- Assuming that the potential flow approximation is valid, the velocity field can be written as

$$\vec{u} = \tilde{\mathrm{N}} f$$

- The velocity potential and the pressure are given by the following equations

$$\frac{\partial^2 f}{\partial y^2} + \frac{\partial^2 f}{\partial z^2} = 0$$

$$U_0 \frac{\partial f}{\partial x} + \frac{1}{2}\left(\left(\frac{\partial f}{\partial y}\right)^2 + \left(\frac{\partial f}{\partial z}\right)^2\right) + \frac{p}{\rho} + gz = 0$$

- That must be completed with the boundary conditions

$$U_0 \frac{\partial f}{\partial x} + \frac{\partial f}{\partial y}\frac{\partial f}{\partial y} - \frac{\partial f}{\partial z} = 0 \quad \text{and} \quad p = 0$$ at the free surface, $z = f(x, y)$

$$f \to 0 \quad \text{as} \quad z \to -\infty \quad y \to \pm\infty \quad \text{and} \quad f(x=0, y) = f_0(y) \quad \text{at } x = 0.$$

Modellig the wave formation

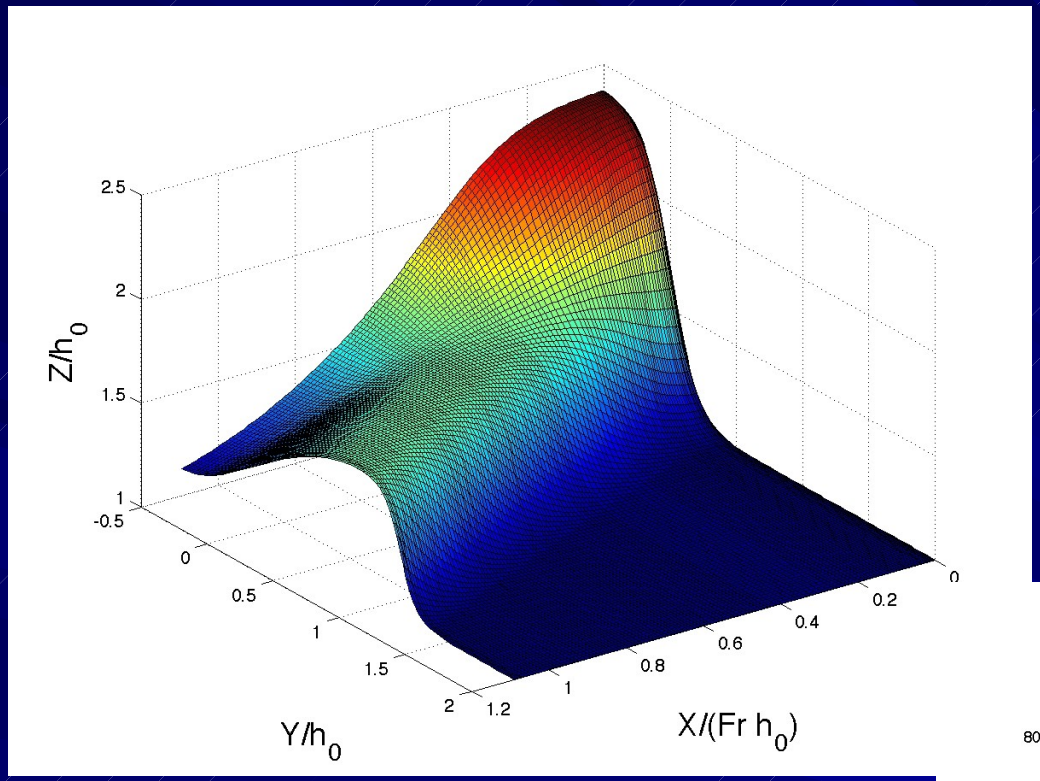

The model is clearly able to capture the mechanism of wave formation.

Experimental measurements

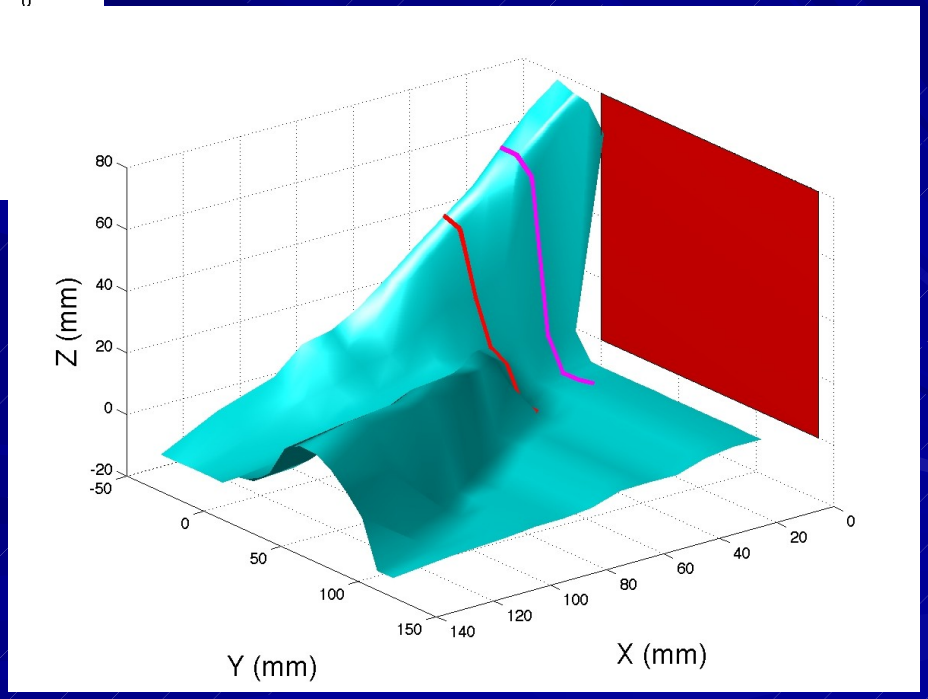

Numerical simulation. The purple line in the experimental measurements was used as initial condition.

Plunging-Spilling transition

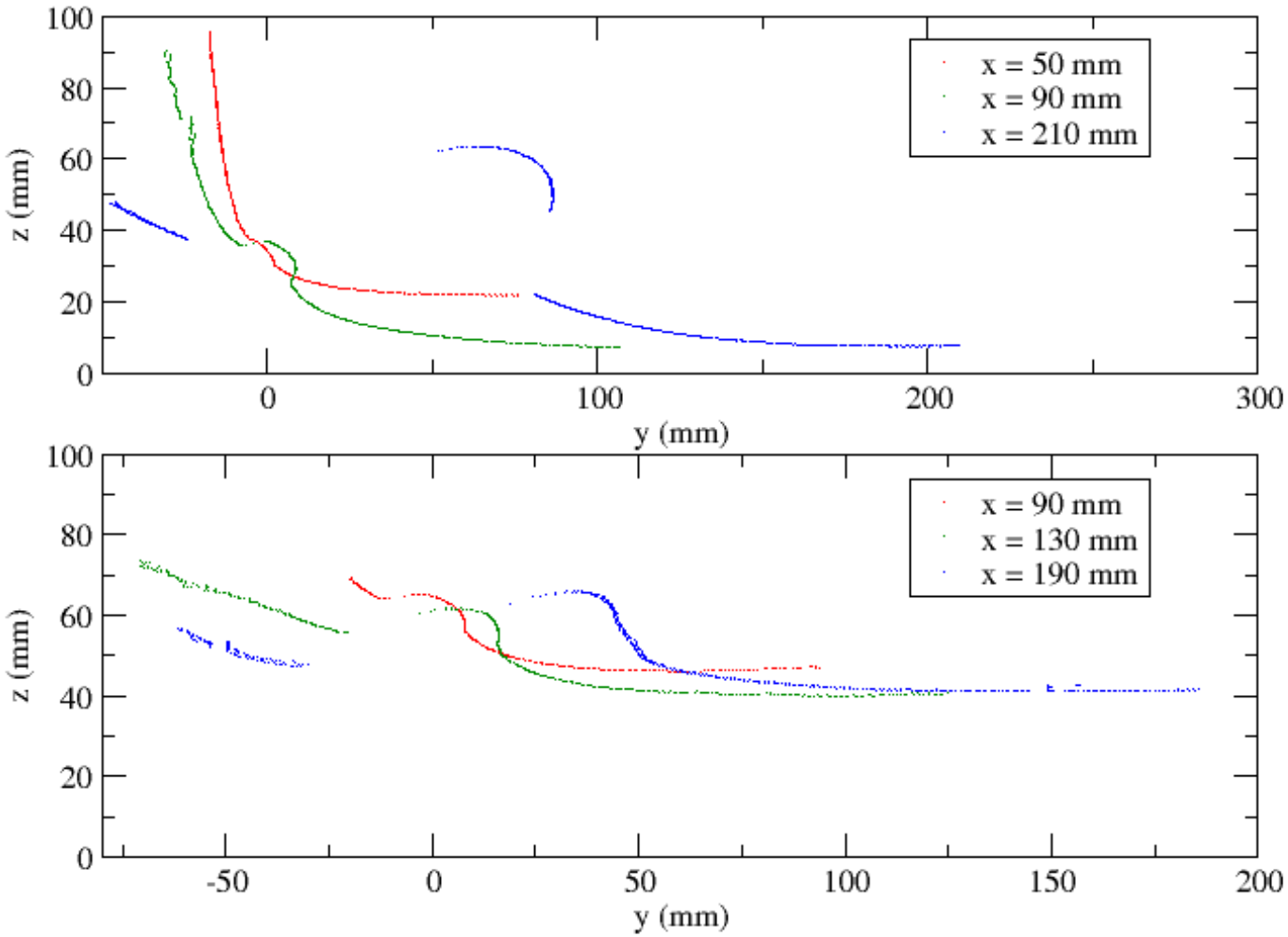

Plunging-Spilling transition

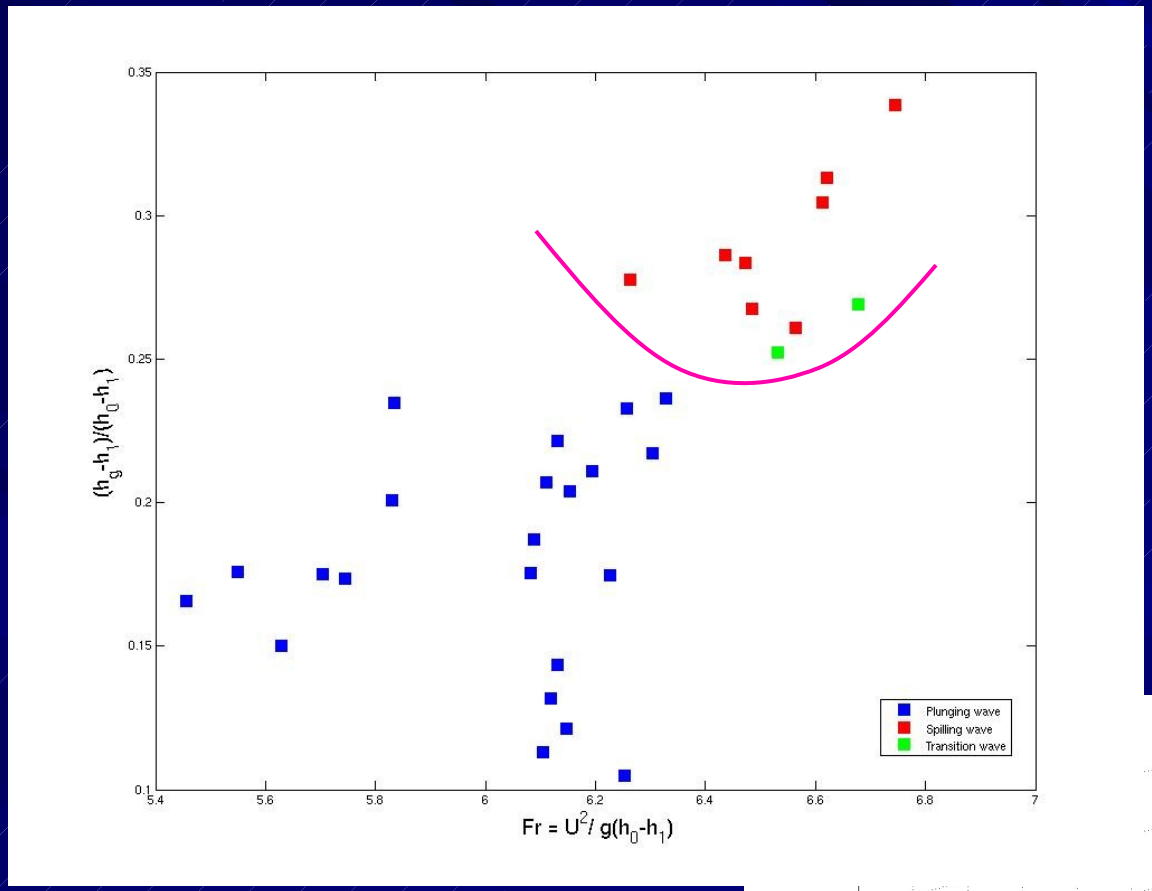

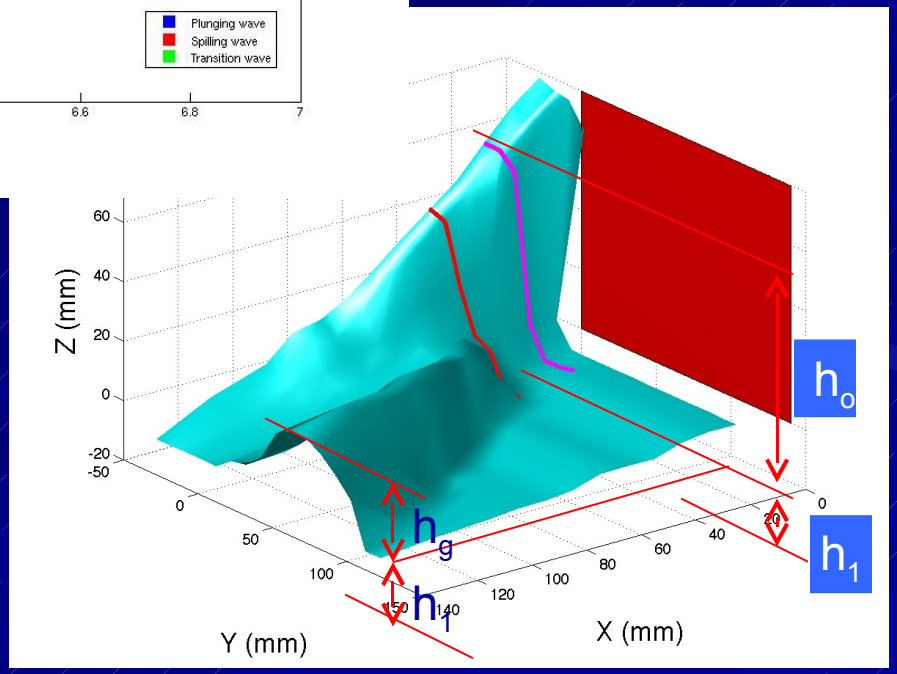

h_o-h_1

h_g-h_1

Plunging-Spilling transition

• Once the phenomenon is know to be gravity-driven, a criterion is proposed to determine whether the wave will break in a plunging or spilling way.

• Since the maximum Y-velocity was found at the same depth as the vertex of the plate, the farther this point is from the minimum height of the free surface (h_1), the easier should be for the "jet" to separate and therefore, to form a plunging wave.

• On the other hand, the energy of the "jet" is given by the Froude number. So both parameters should be the relevant ones to characterize the wave.

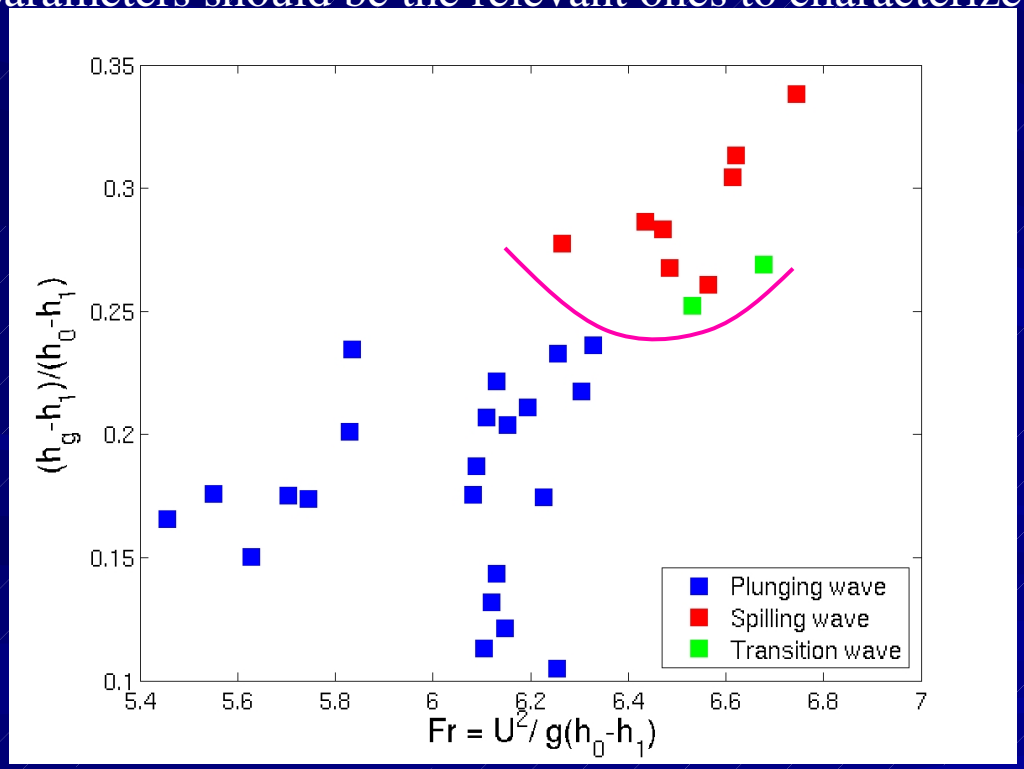

• In fact, there exists a single curve in the space defined by both parameters that separates plunging from spilling waves.

• More measurements will extend this curve to the region of larger heights and lower Fr numbers, where currently there are no measurements.

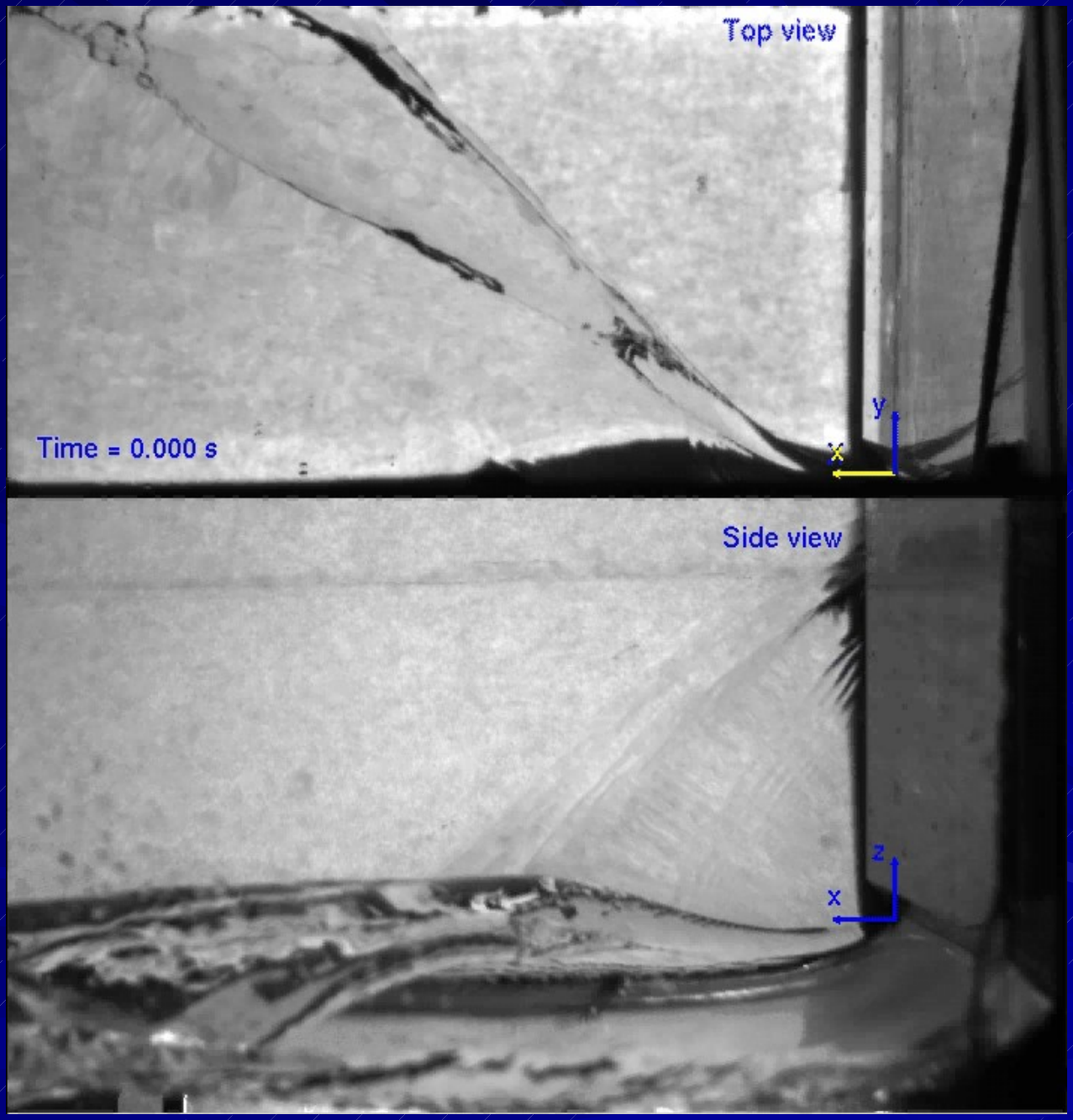

U

U

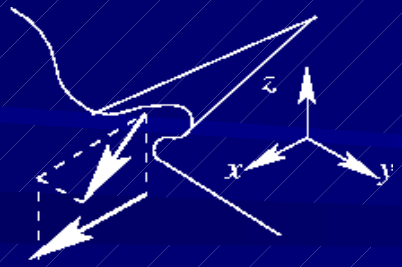

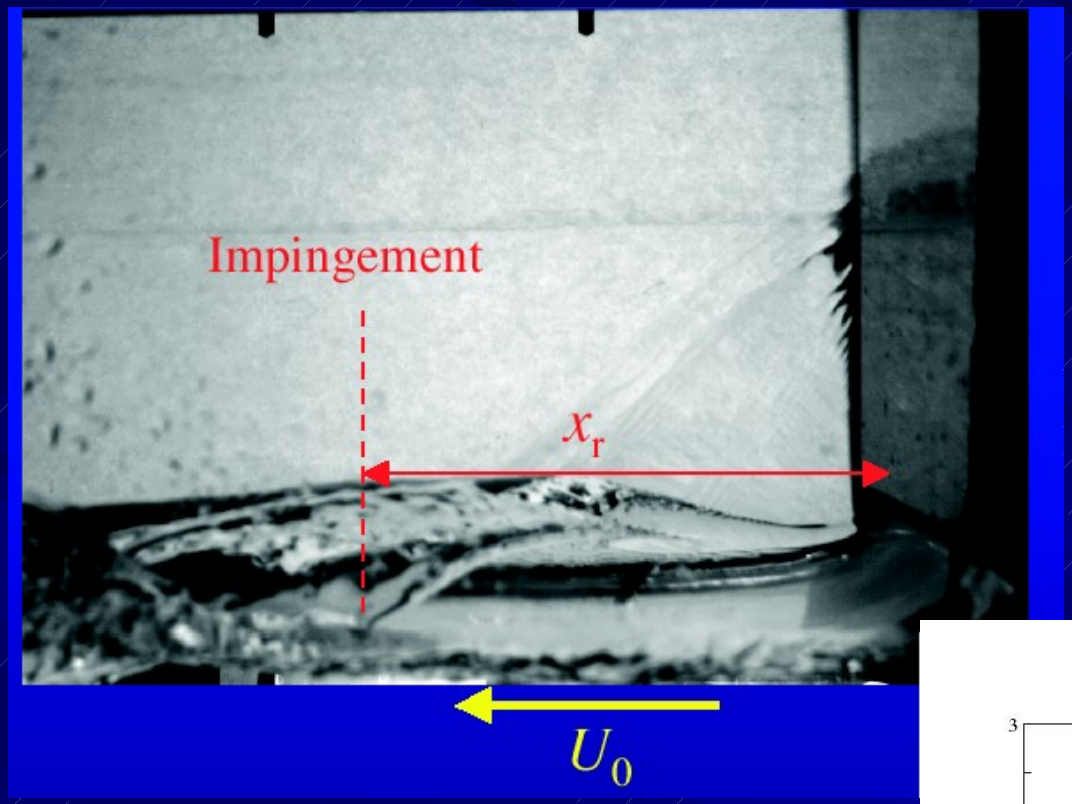

If the height of the gate h_o is kept constant, then

$$x_r = C\,U_0\,\sqrt{2\,\Delta h/g}$$

$\Delta h = h_0 - h_1$

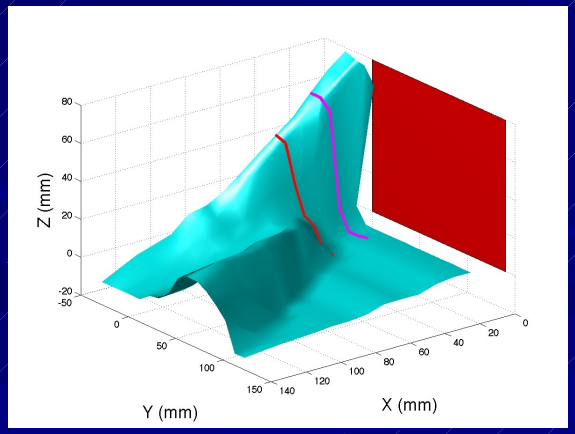

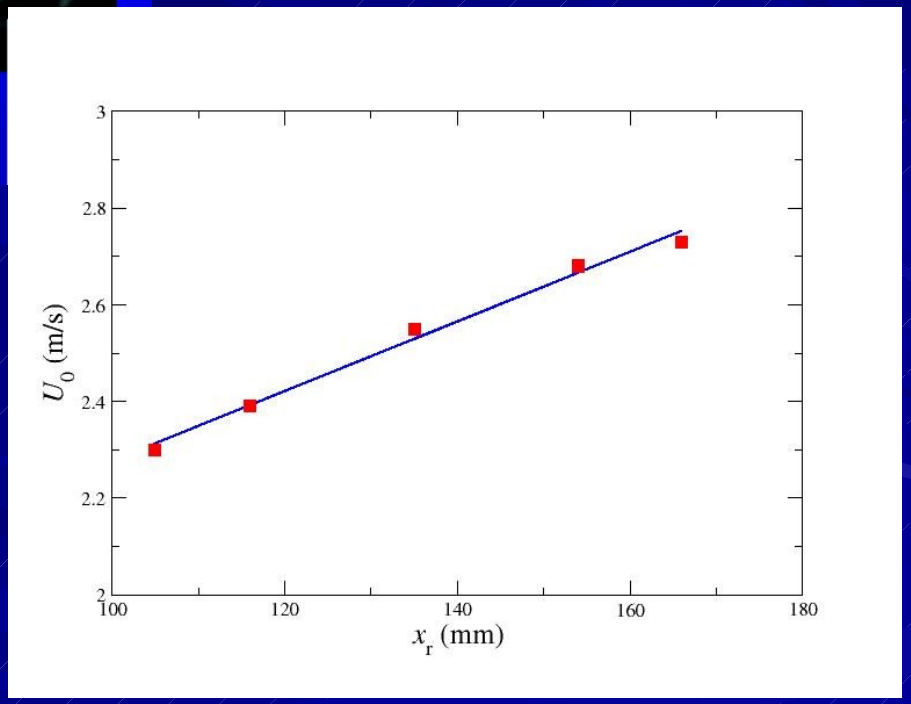

Impingement velocity

• The position of the impingement point ("range" of the ballistic trajectory of the wave crest) has been measured for different sets, with velocities ranging from U = 1 to 3 m/s and gate heights h_o = 20 to 80 mm.

• A new Froude number may be defined based on the height difference: $Fr_g = U^2/g(h_g-h_1)$. Guided by the idea of a ballistic trajectory, we seek a relation of the form:

$$\left(\frac{x_r}{(h_g - h_1)}\right)^2 \sim Fr_g$$

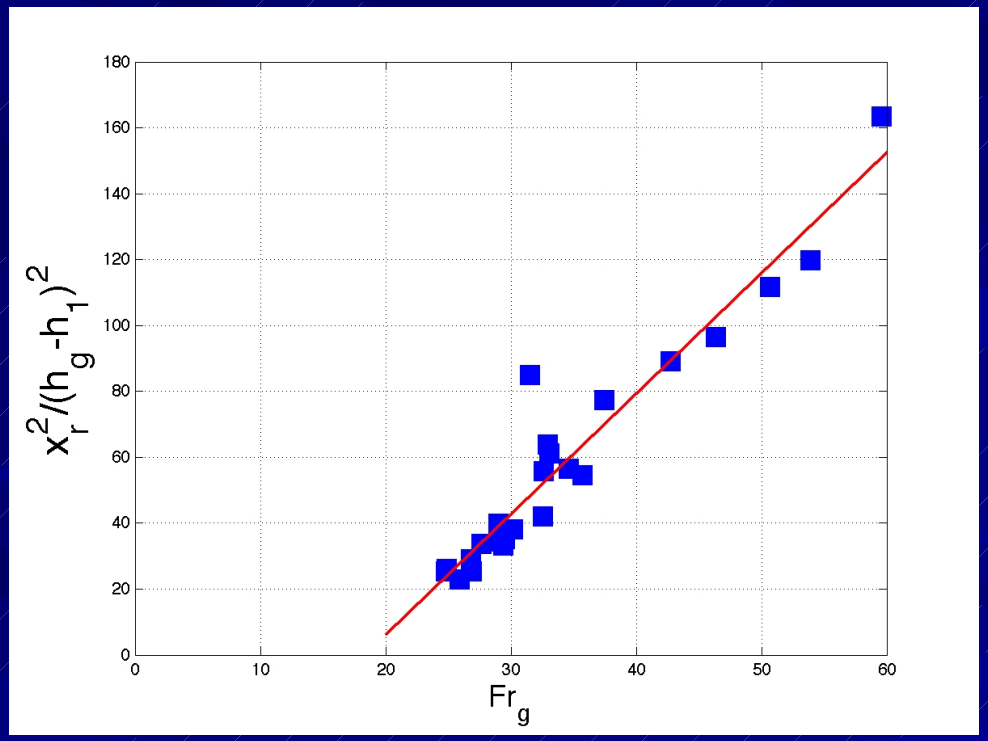

• Indeed such a relation exists (red line), but it seems that the speed of the ballistic trajectory depends on an "excess" Froude number:

$$\Delta Fr = Fr_g - Fr_{g,\mathrm{crit}}$$

with $Fr_{crit} \approx 20$.

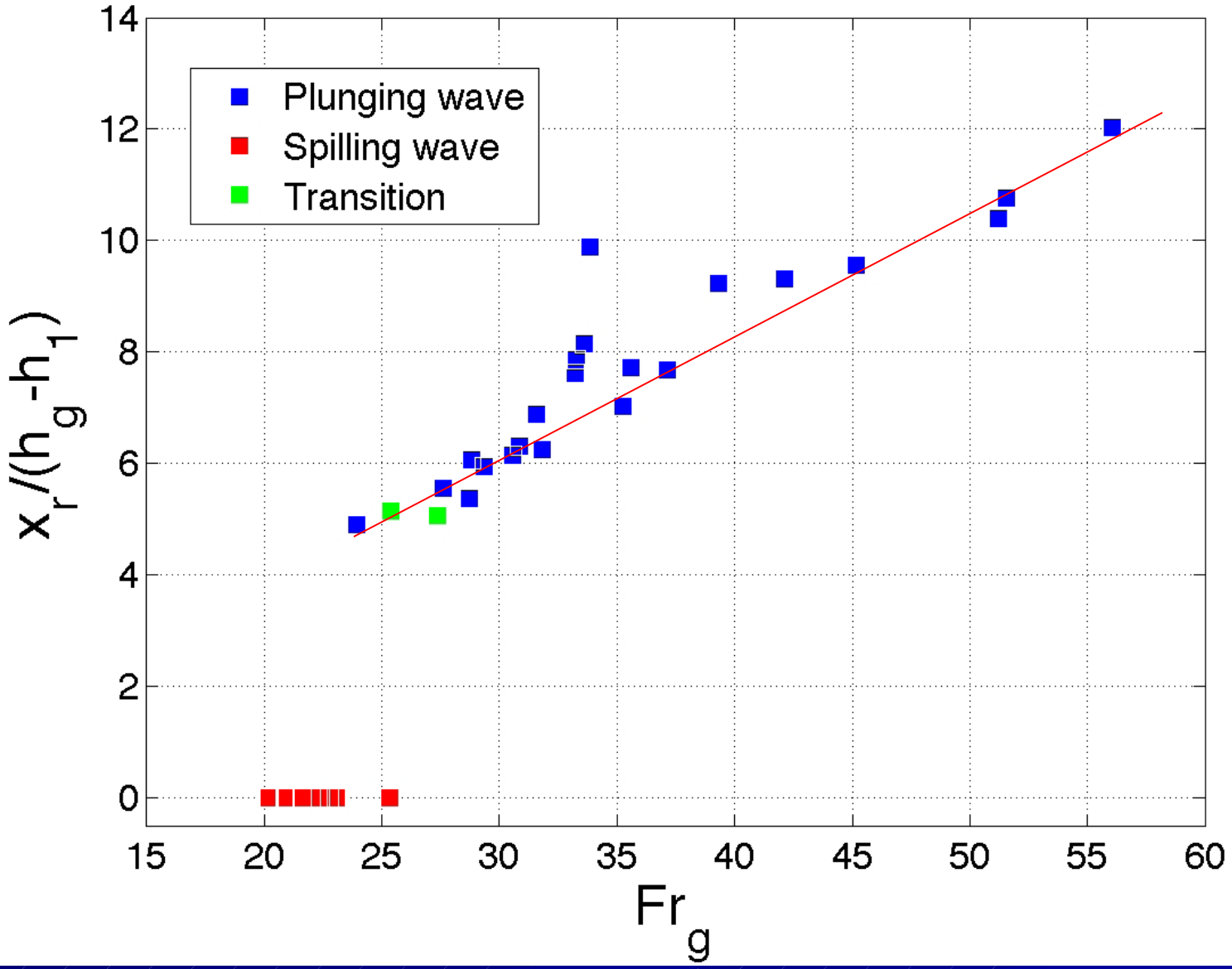
Plunging wave
Spilling wave
Transition
$x_r/(h_g-h_1)$
Fr_g
0
2
4
6
8
10
12
14
15
20
25
30
35
40
45
50
55
60

Experimental results

Breaking wave does not depend on the channel depth

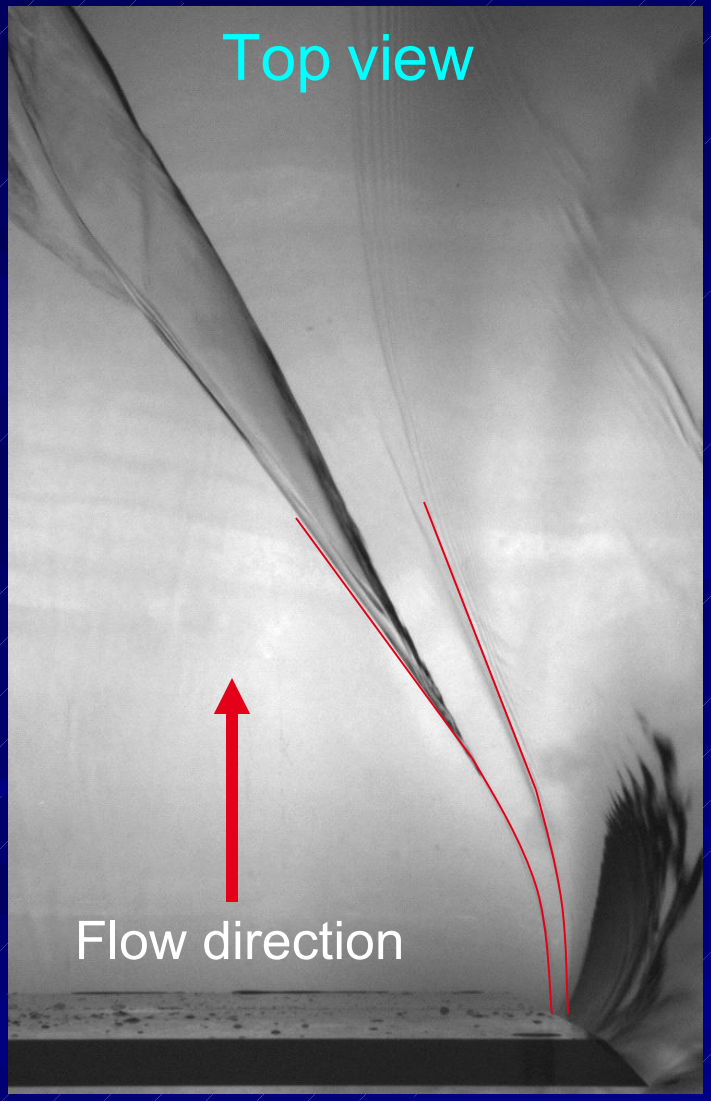

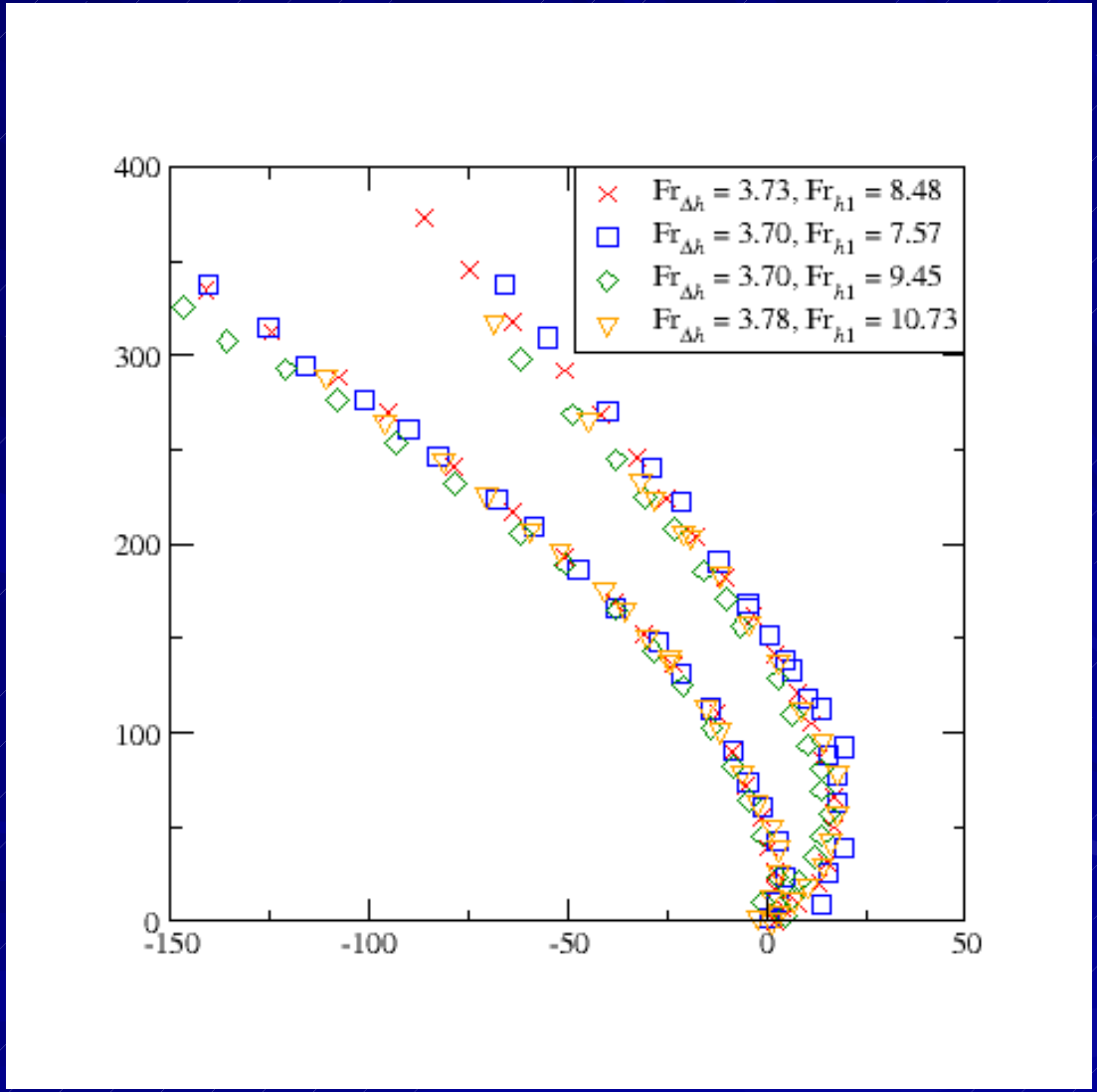

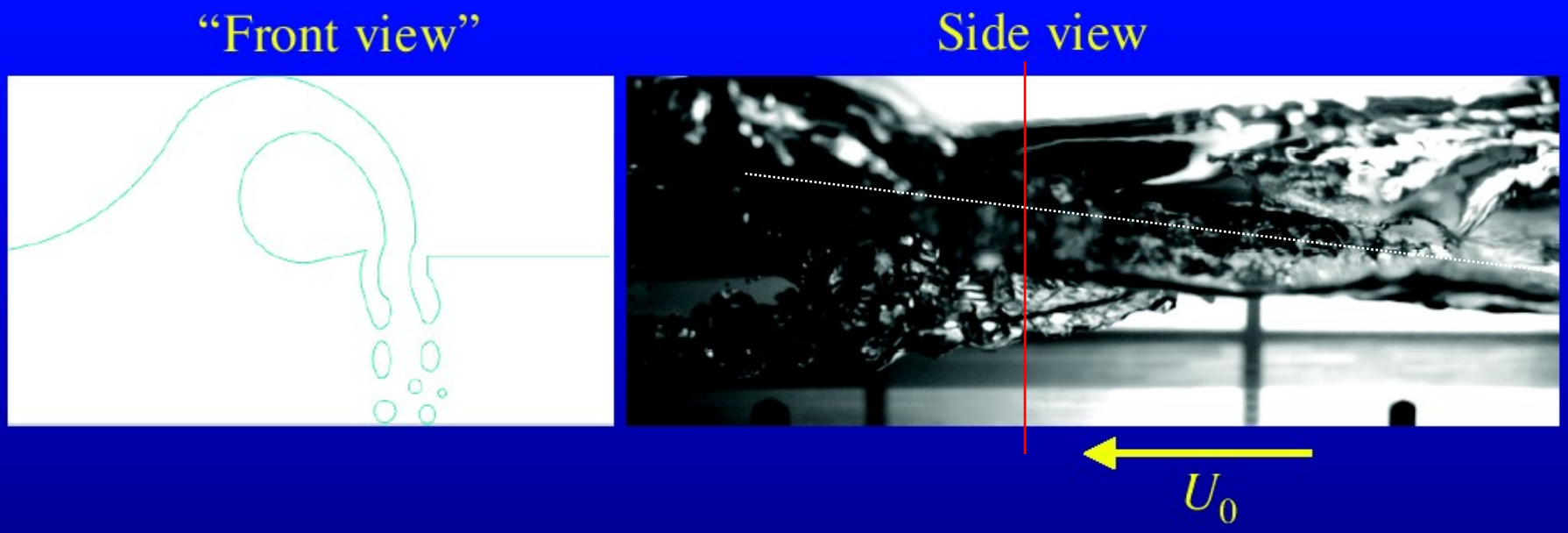

Air Entrainment and Depth of Penetration

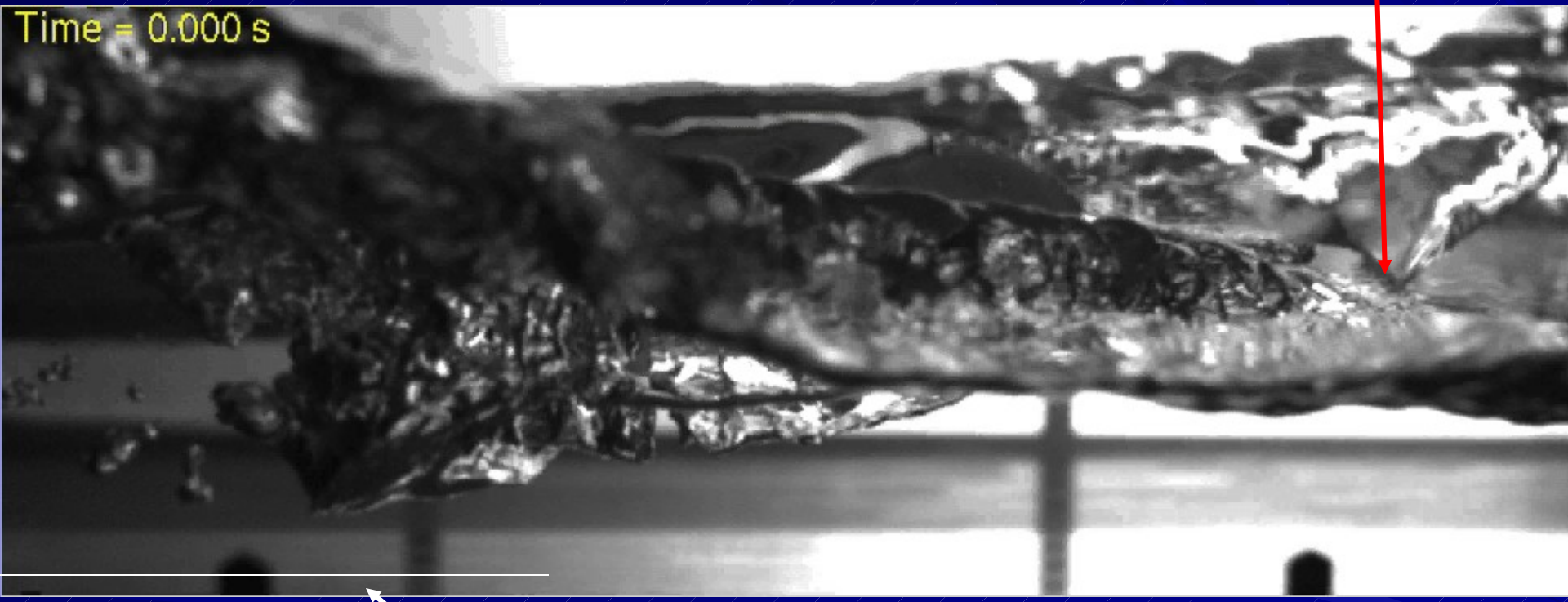

Penetration depth

Detail of the entrainment region

- The plunging wave impinges on the free surface, leading to the entrainment of large amounts of air at this point.

- The depth at which air bubbles are transported depends mainly on the velocity of the wave crest at the impingement position (Clanet & Lasheras, 1999).

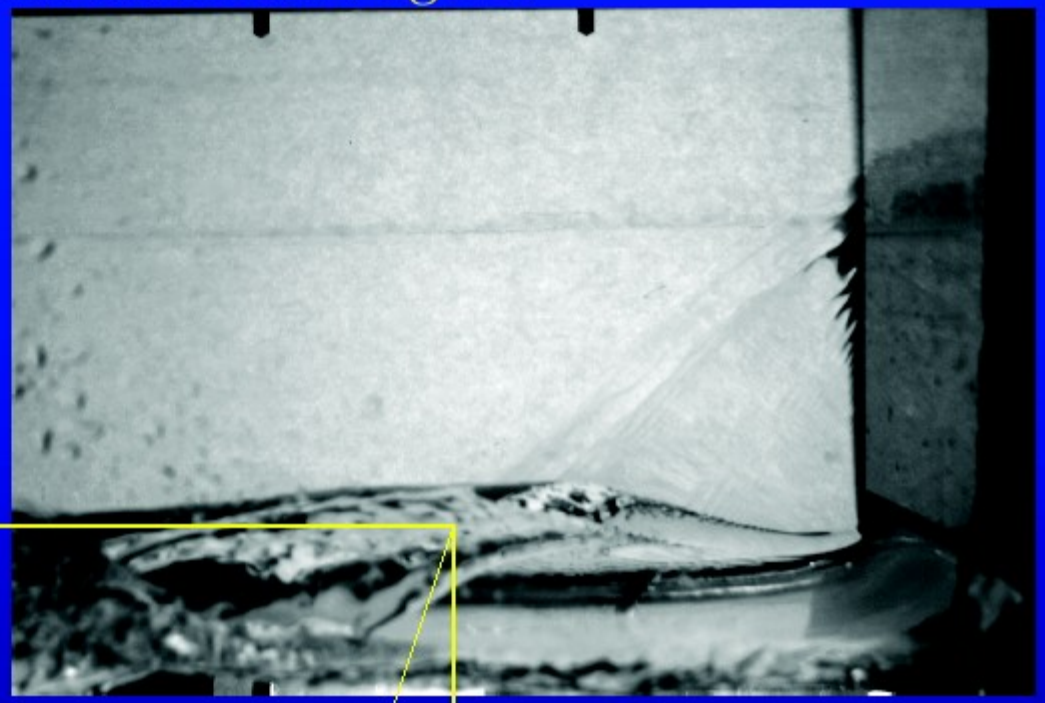

U

Free surface

U

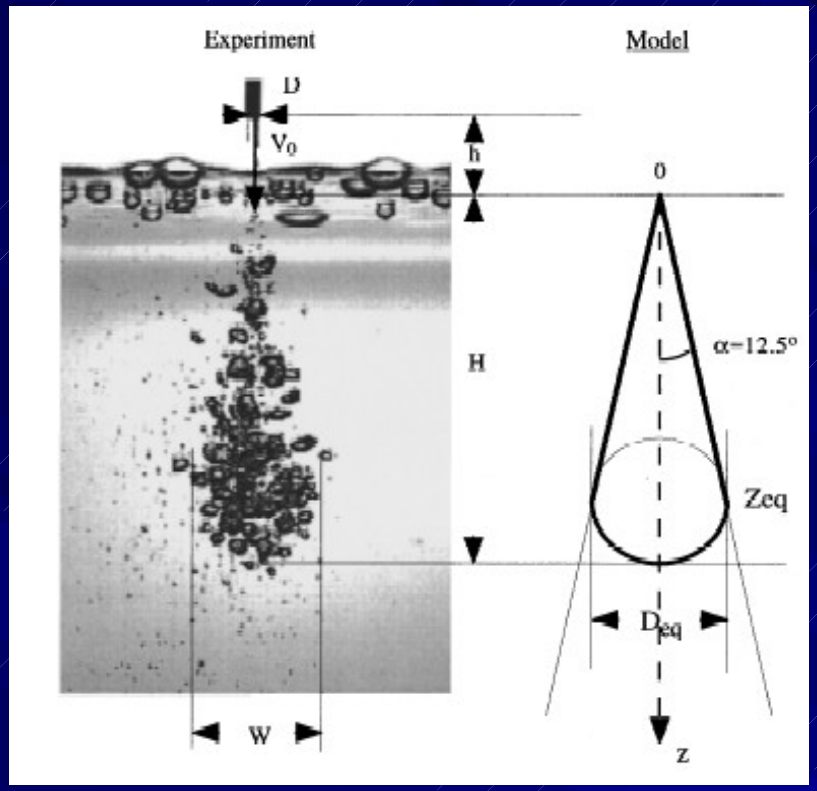

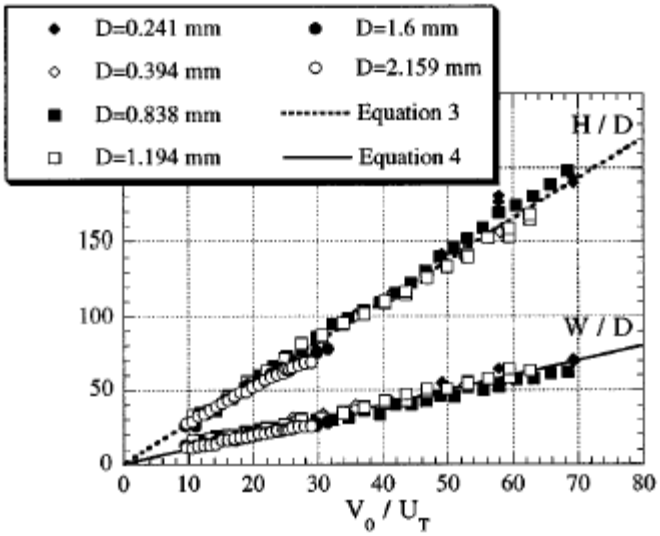

FIG. 3. Penetration depth H/D and width W/D as a function of V_0/U_T for different diameters.

$$\frac{H}{D} = \frac{1}{2\tan\alpha}\frac{V_0}{U_T}.$$

To estimate the mean velocity of the submerged jet as a function of the downstream location, we model the jet as an equivalent water jet with an initial momentum flux given by $\pi\rho V_{j0}^2 D_{j0}^2/4$, where V_{j0} and D_{j0} are the diameter and velocity of the jet at the point of impact with the flat interface.

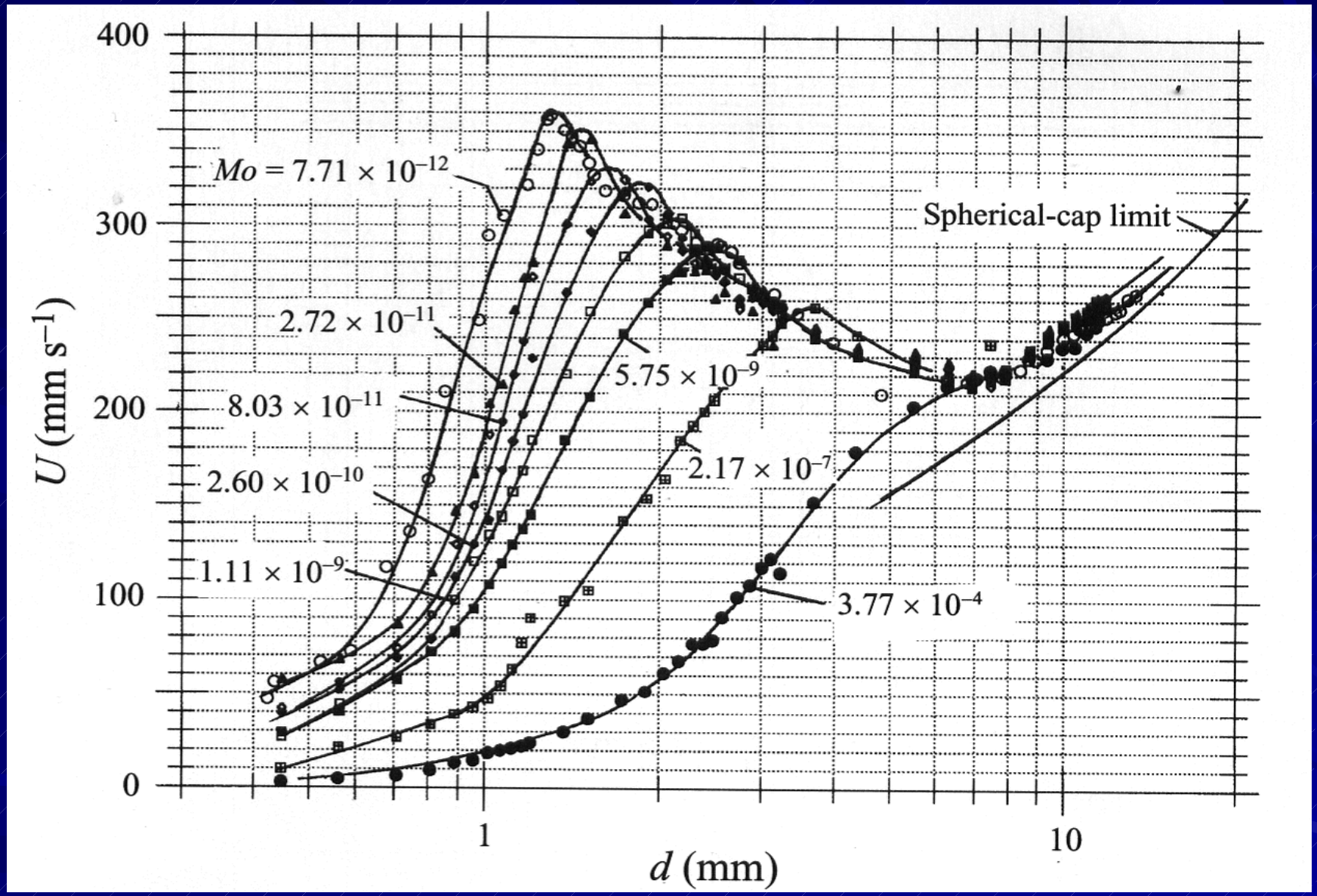

$$Mo = \frac{g\mu_L^4}{\rho_L \sigma^3},$$

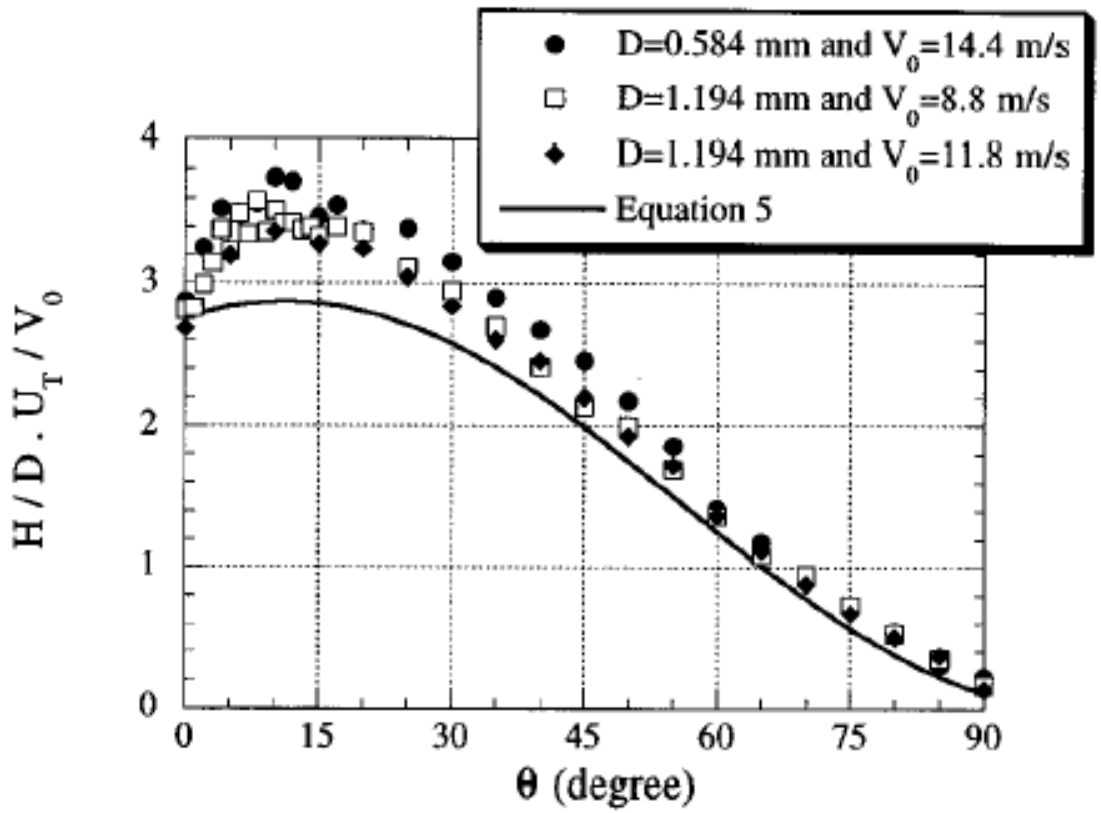

FIG. 4. Non dimensional penetration depth H/D. U_T/V_0 as a function of the penetration angle θ, for different diameters and velocities.

$$\frac{H}{D}=\frac{(1+\tan\alpha)\cos\theta+\tan\alpha\,\sin\theta}{2\tan\alpha}\,\frac{\cos(\theta-\alpha)}{\cos\alpha}\,\frac{V_0}{U_T}. \quad (5)$$

Air Entrainment Mechanism
Steady 3-D Breaker

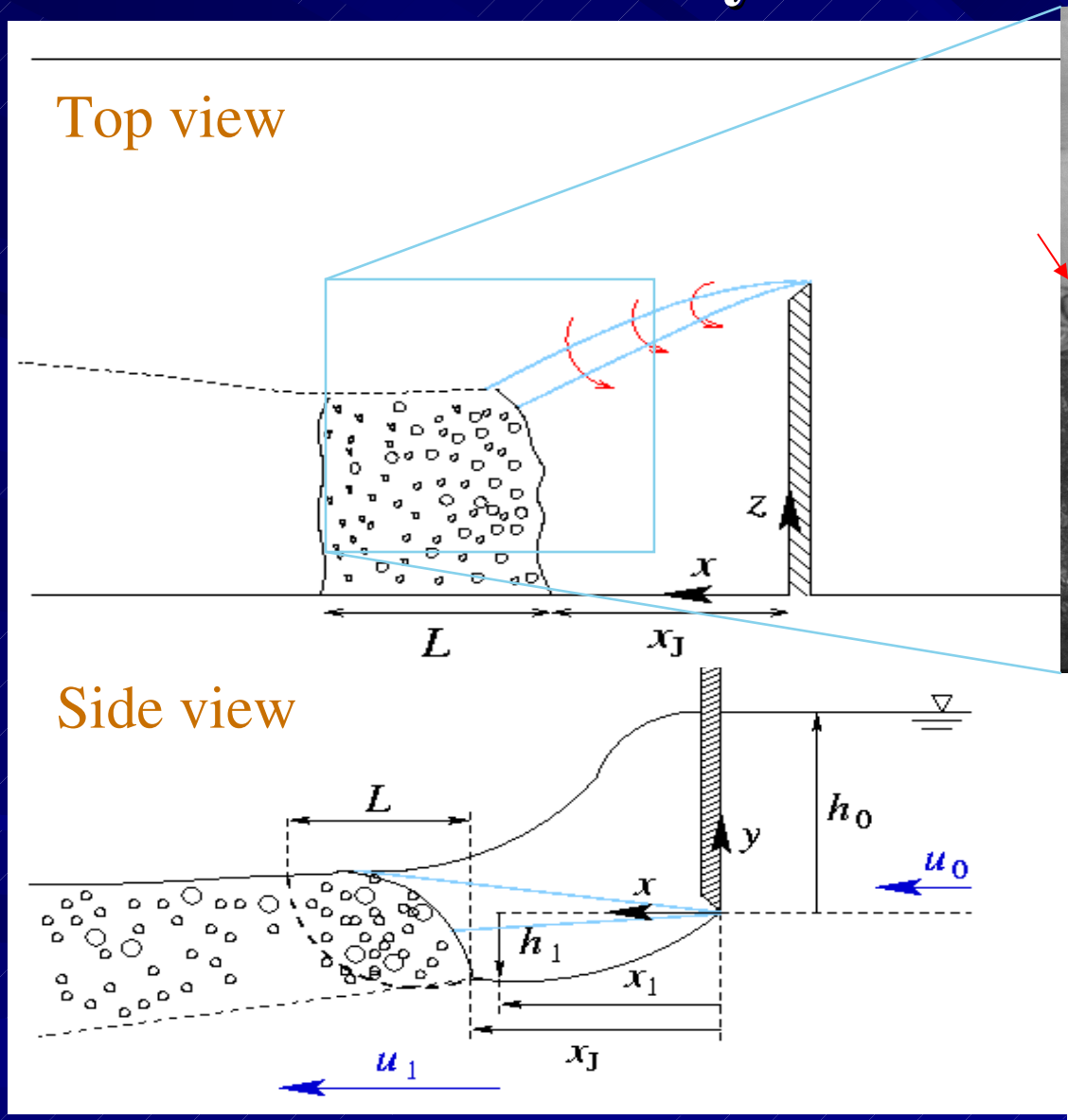

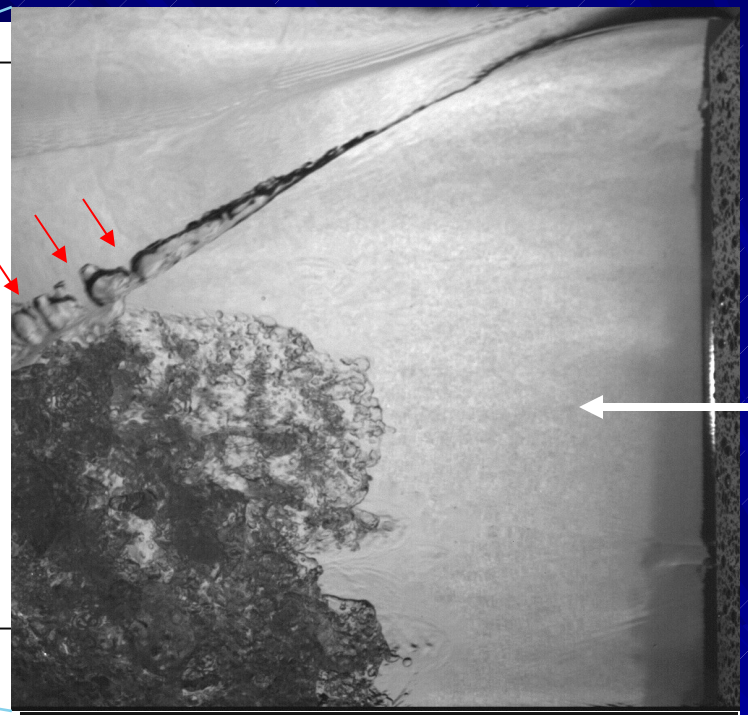

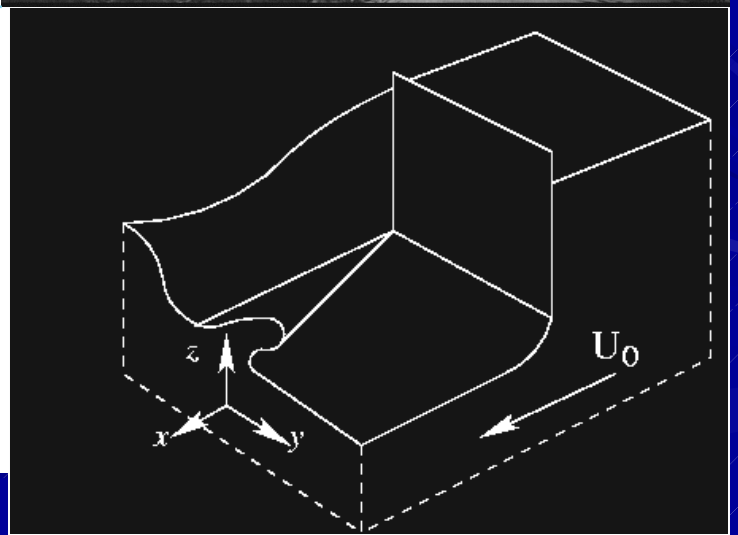

Enhanced air entrainment mechanism (3-D)

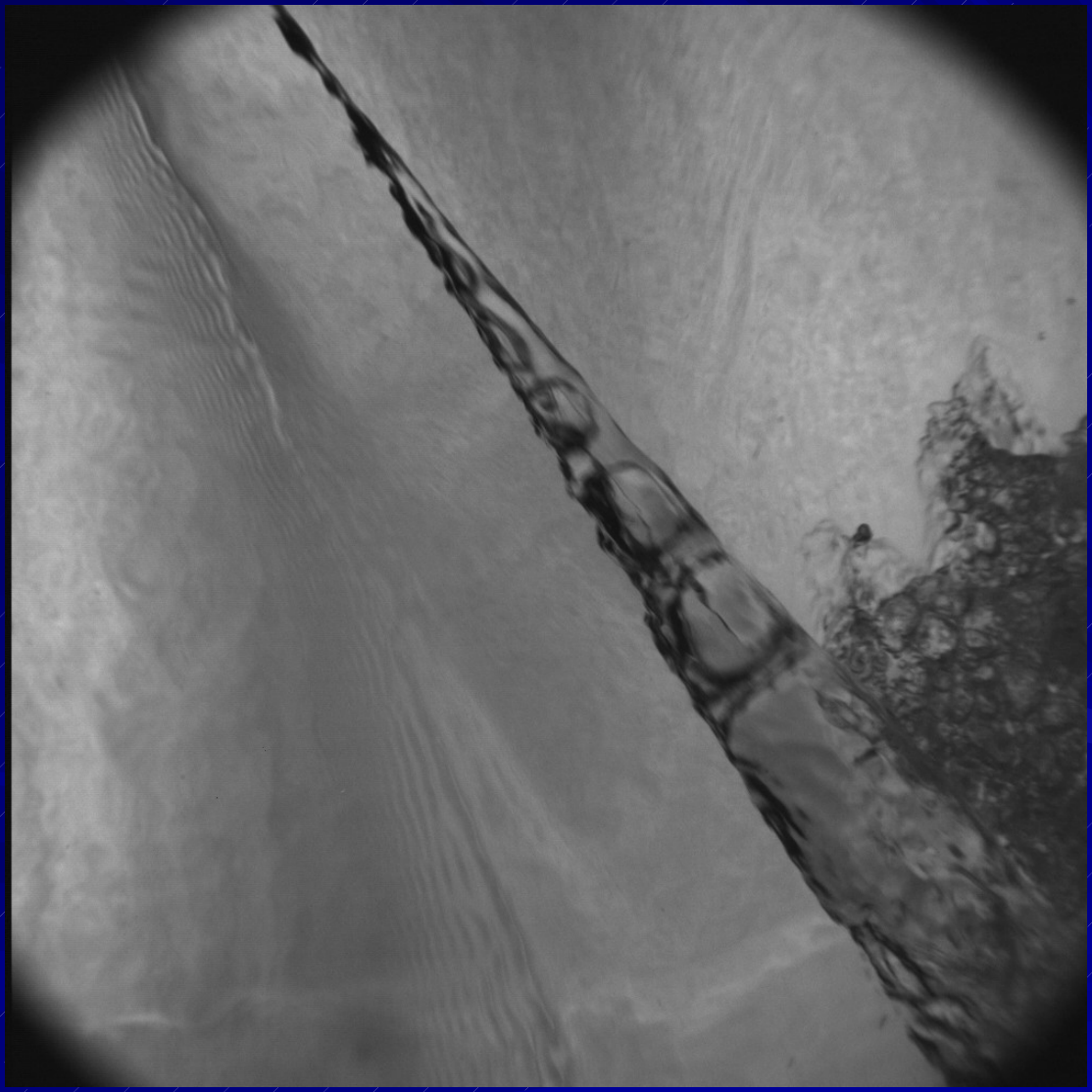

Air entrainment mechanism due to the instability of the core of the corner vortex (3-D)

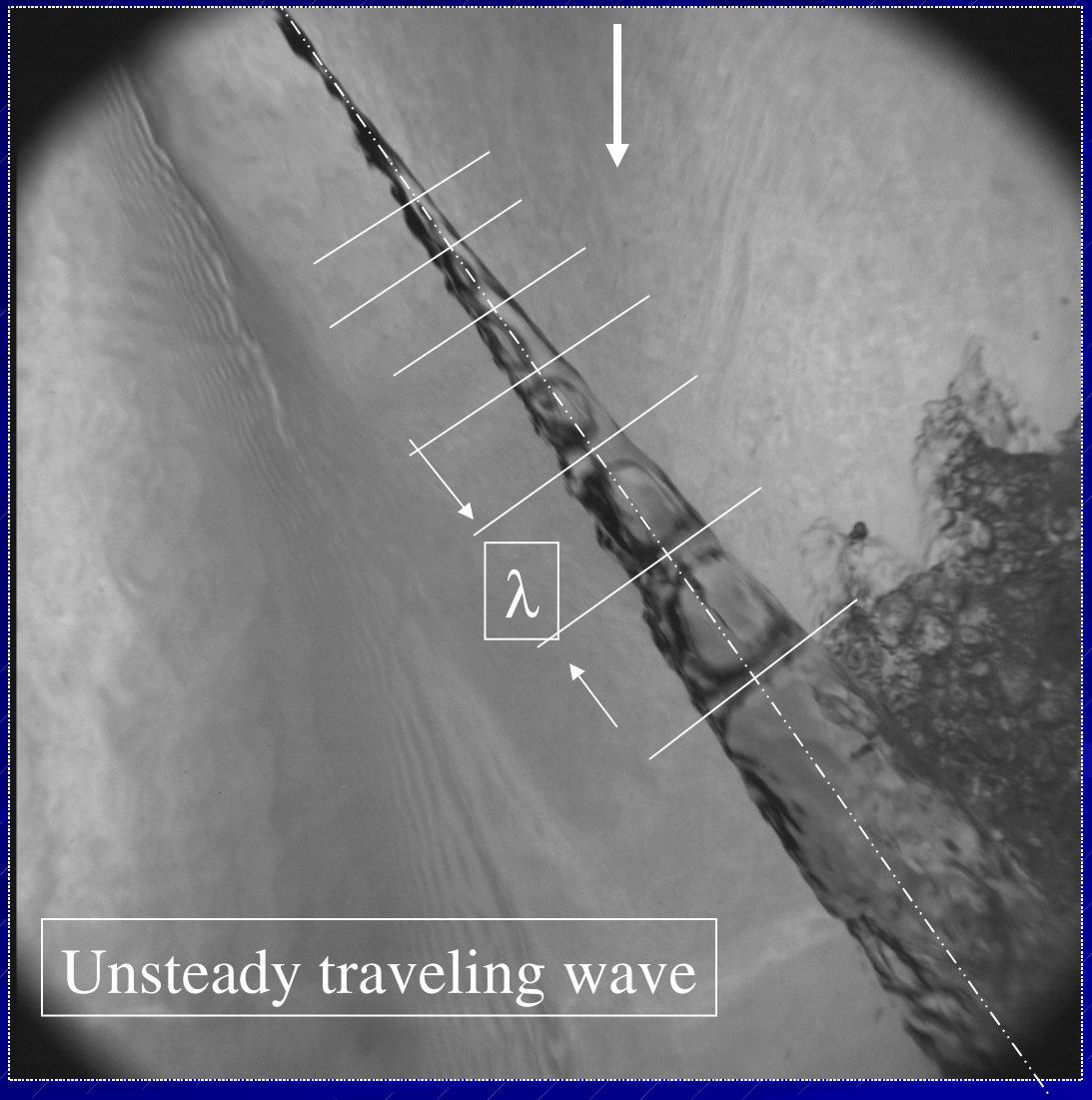

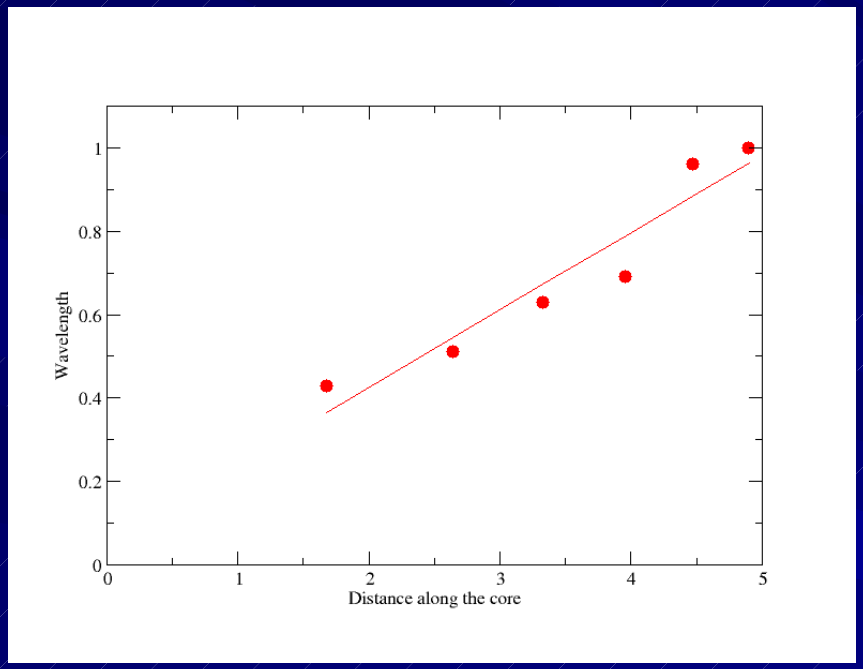

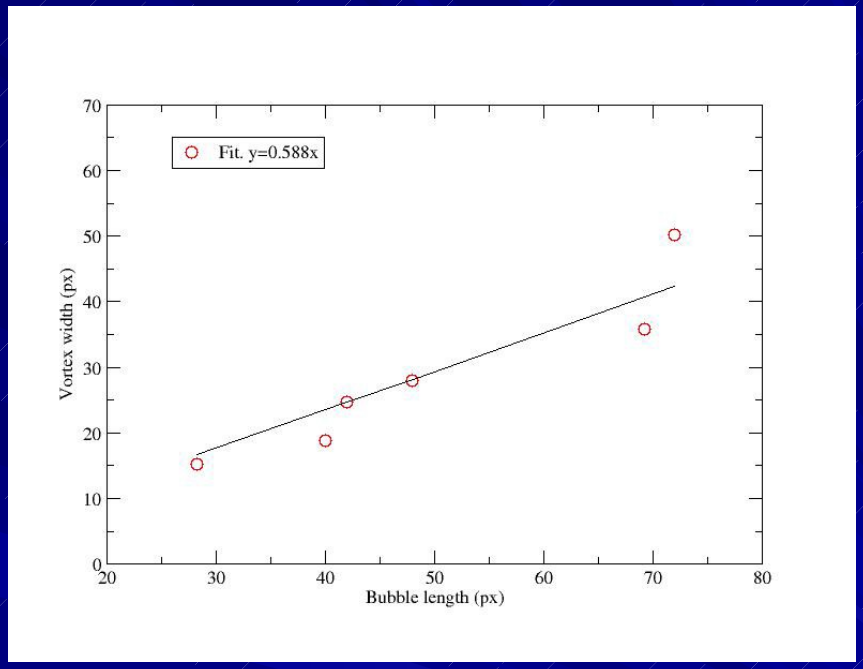

Wavelength of the core instability of the “corner vortex”

Two-dimensional flow

- The region close to the toe of a bore has been studied experimentally using statistical correlation techniques.
- Accurate measurements of the advection velocities of the large scale eddies observed in the flow have shown that they move significantly slower than what would be expected in a single-phase mixing layer.
- The roller described in the literature emerges as an structure in the mean velocity field even though no recirculating motion exists at any particular time. The air entrainment at the toe is not the dominant mechanism.
- The shear layer grows linearly in a region that coincides fairly well with that occupied by the roller.
- Velocity profiles within this region exhibit a self-similar behavior. However, the self-similar velocity profile does not follow the one proposed by Townsend.
- The growth rate of the shear layer is about 3.5 larger than that expected for a classical mixing layer. This is consistent with the slower advection velocity of the large scale features.

Conclusions & Work in progress
3-D Corner Flow

- Entrainment due to the three-dimensional corner flow
  - Criterion for the transition

    spilling breaker

    plunging breaker

Air entrainment

Entrainment depth

Bubble size distribution

Future work:

Extension to sea water

11.2 kts Elevation (Lidar sweeping away from transom)

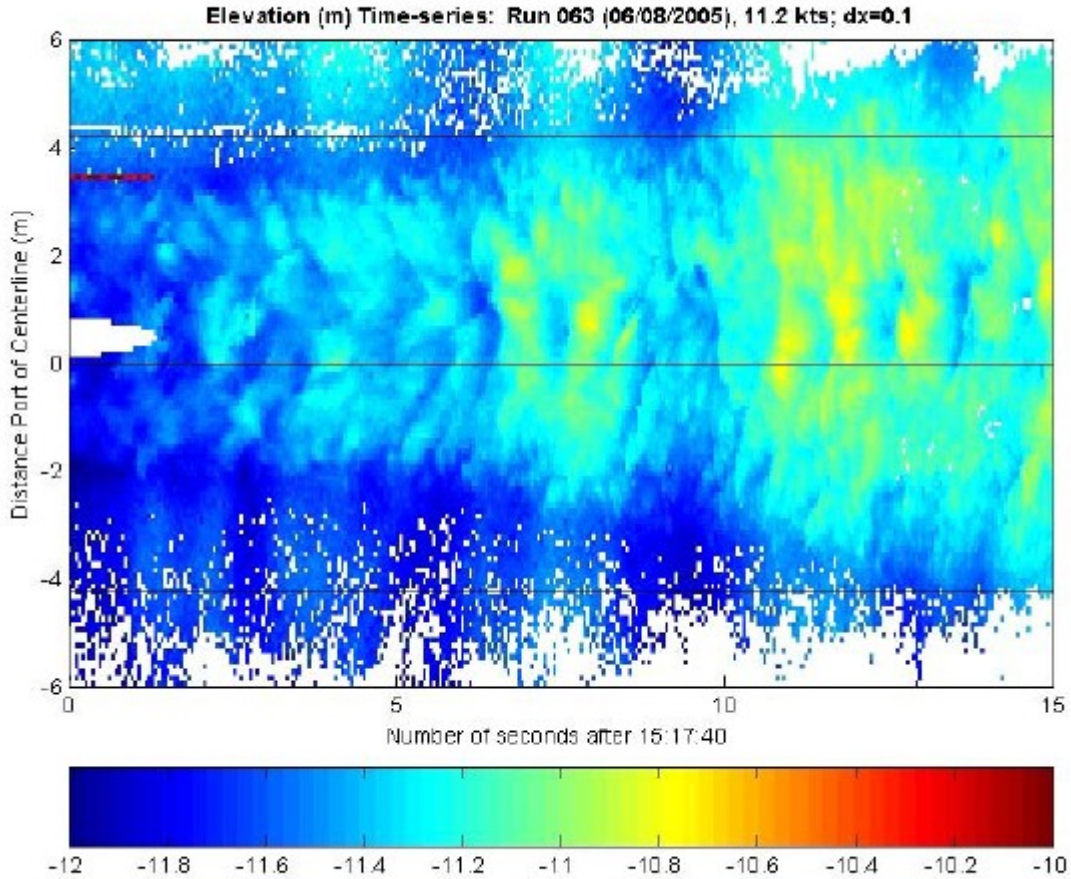

Boat -----data shown is sweeping aft….

Air entrainment and bubble formation by a two-dimensional deep-water stern breaker

- Effect of the Fr number on the air entrainment

- **Air entrainment and bubble formation by a three-dimensional deep-water stern breaker**
  - Mechanisms of air entrainment
  - Effect of the corner flow

Experimental results
Plunging-Spilling Criterion

- Transition between both regimes seems to be determined by the flow steepness.
- Further experiments are needed

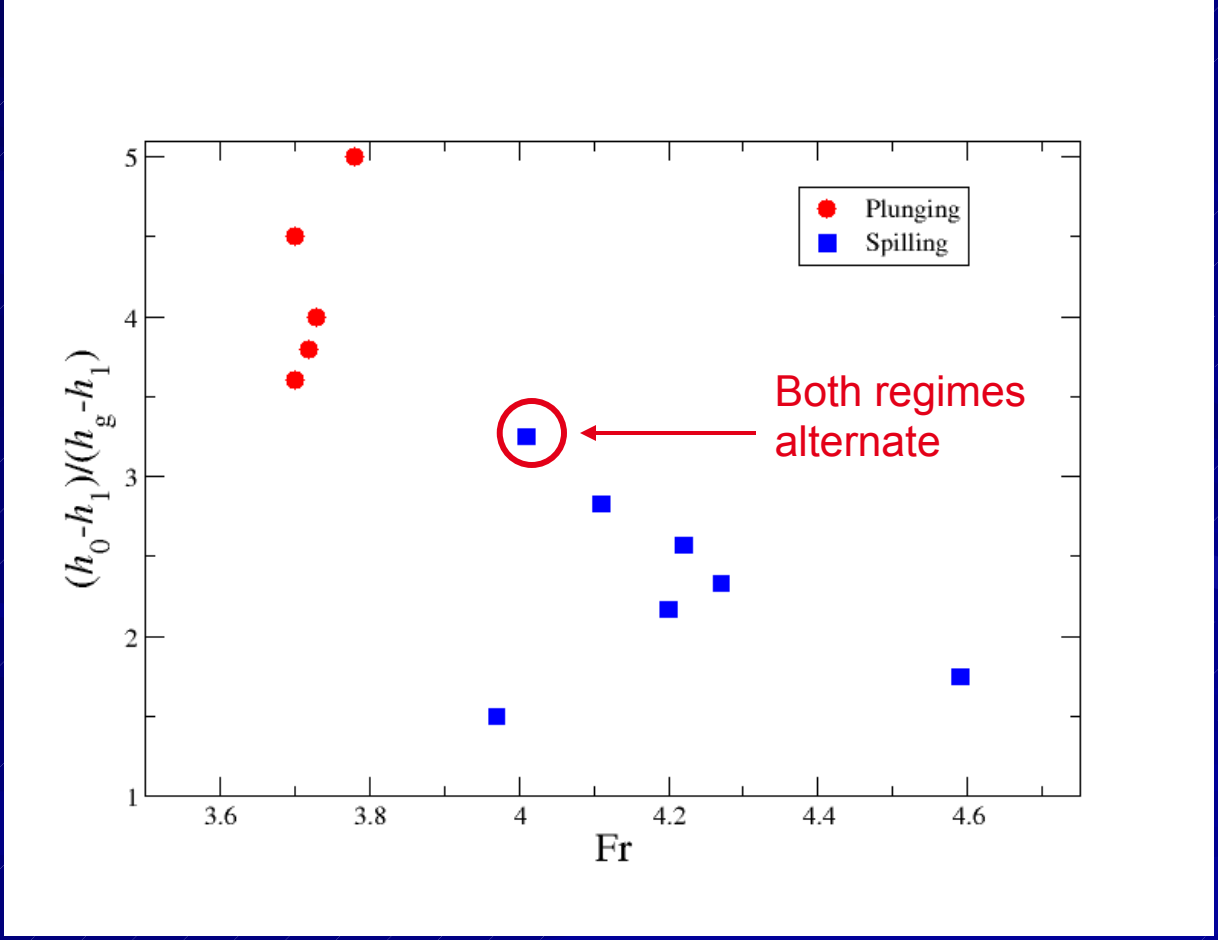

Implementation of the model in URANS simulations

Since the LTF entrainment model is based on the behavior of the large flow structures, which can not be simulated with URANS, the relevant information must be related to the mean value of the turbulent magnitudes of the flow.

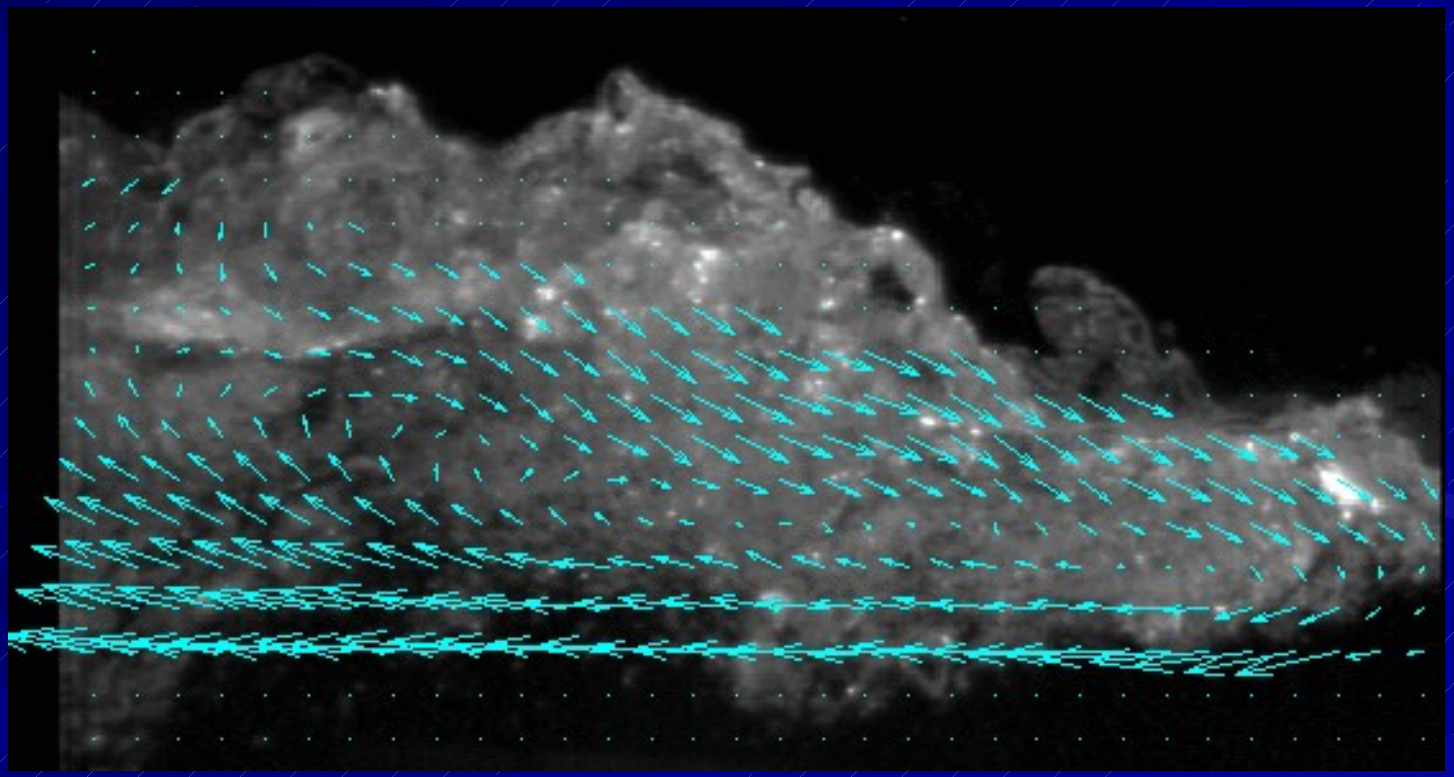

Air entrainment model: entrainment length and turnover velocity

B) Entrainment length w
C) Turnover velocity u_l

Computed from PIV measurements for a large number of eddies

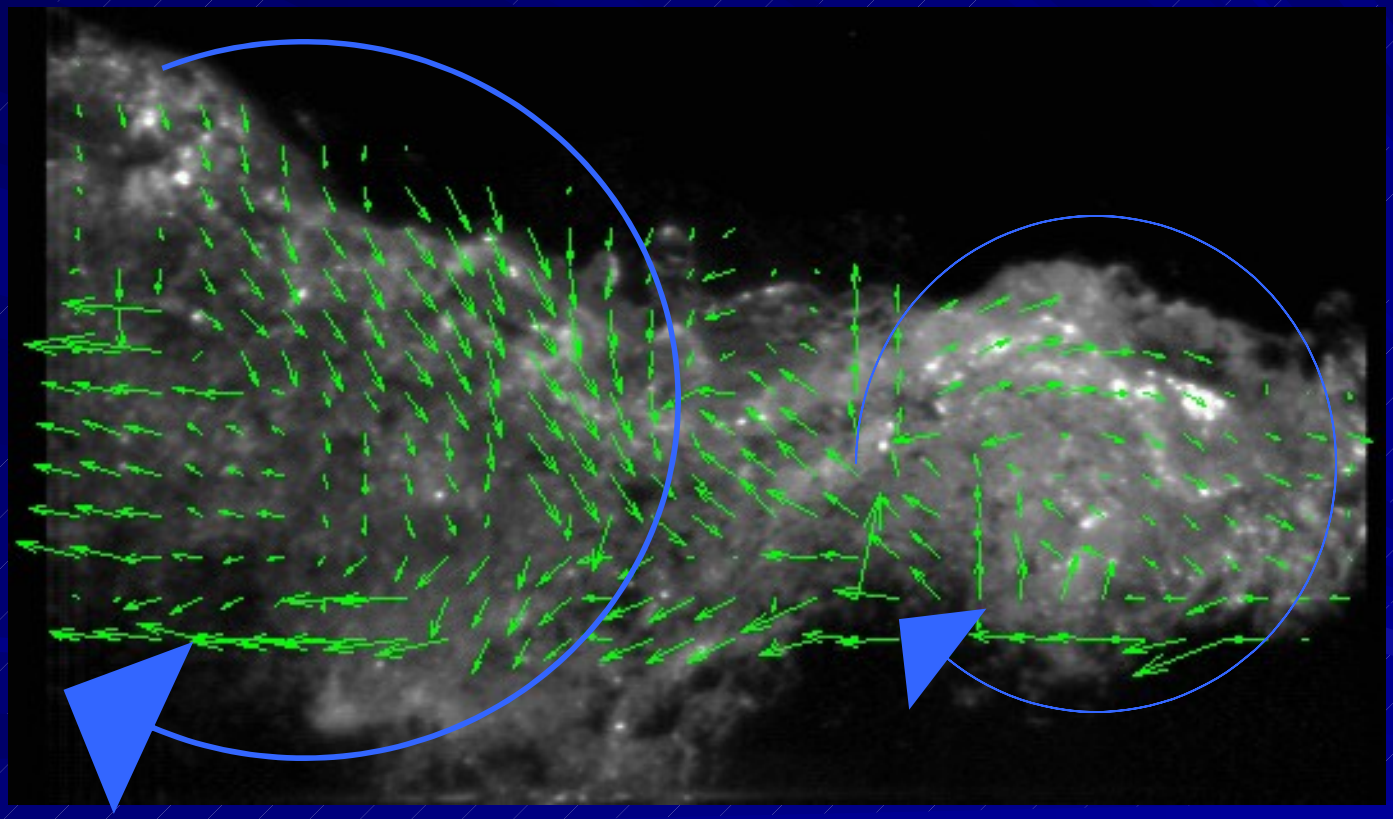

Self similar mean velocity profiles

- Mean velocity profiles collapse when properly dimensionalized.

$$\frac{u(x,y)-u_{\min}(x)}{U_0-u_{\min}(x)}=f\left(\frac{y}{d(x-x_0)}\right)$$

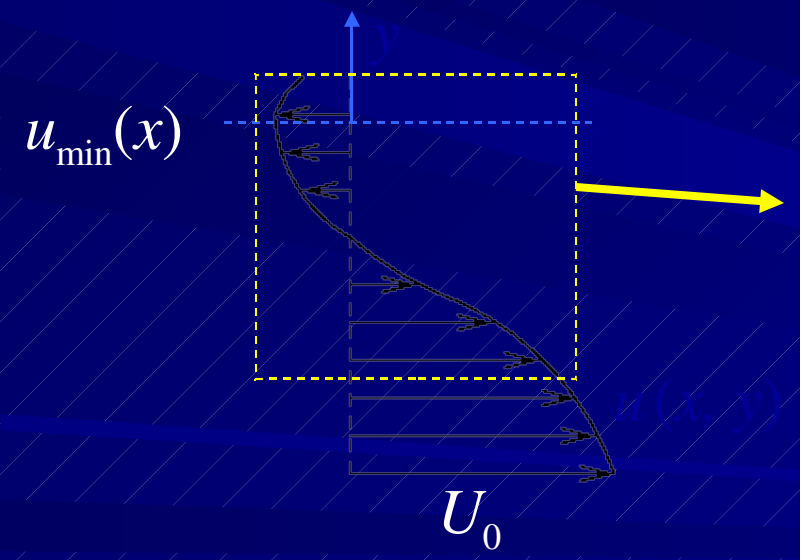

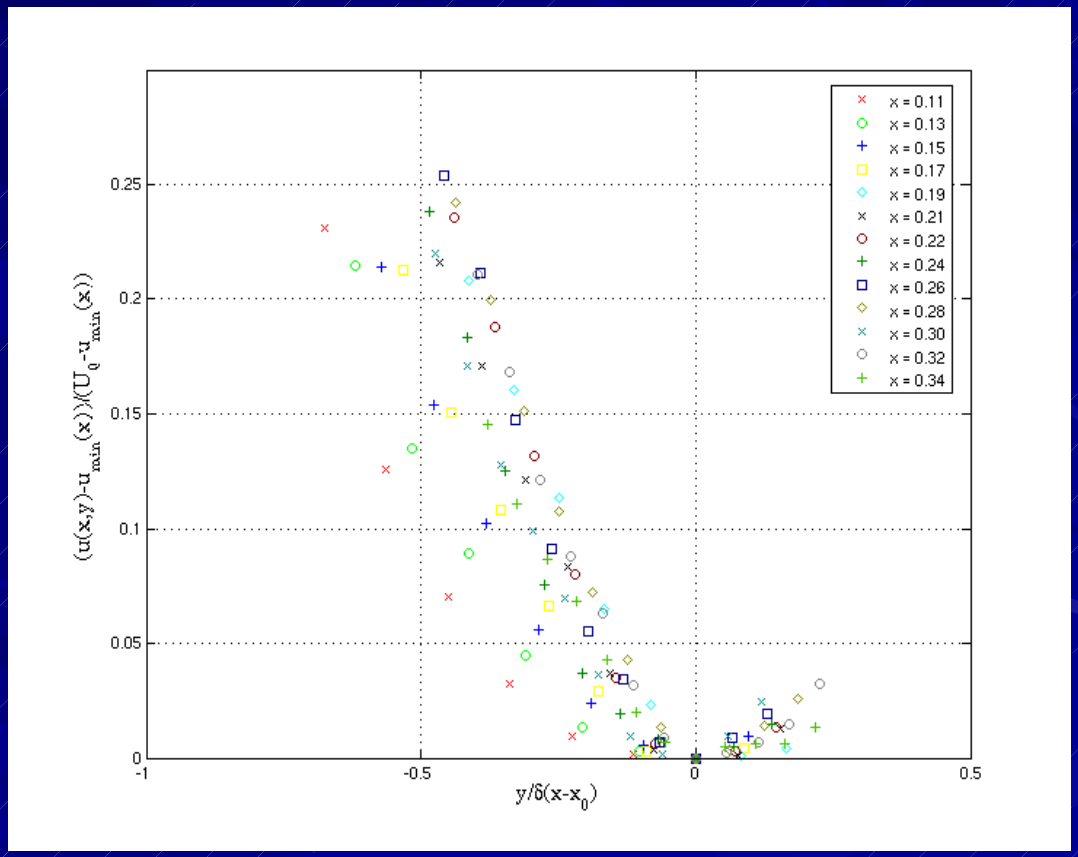

Air entrainment model: growth rate

Measurements of the mixing layer growth:

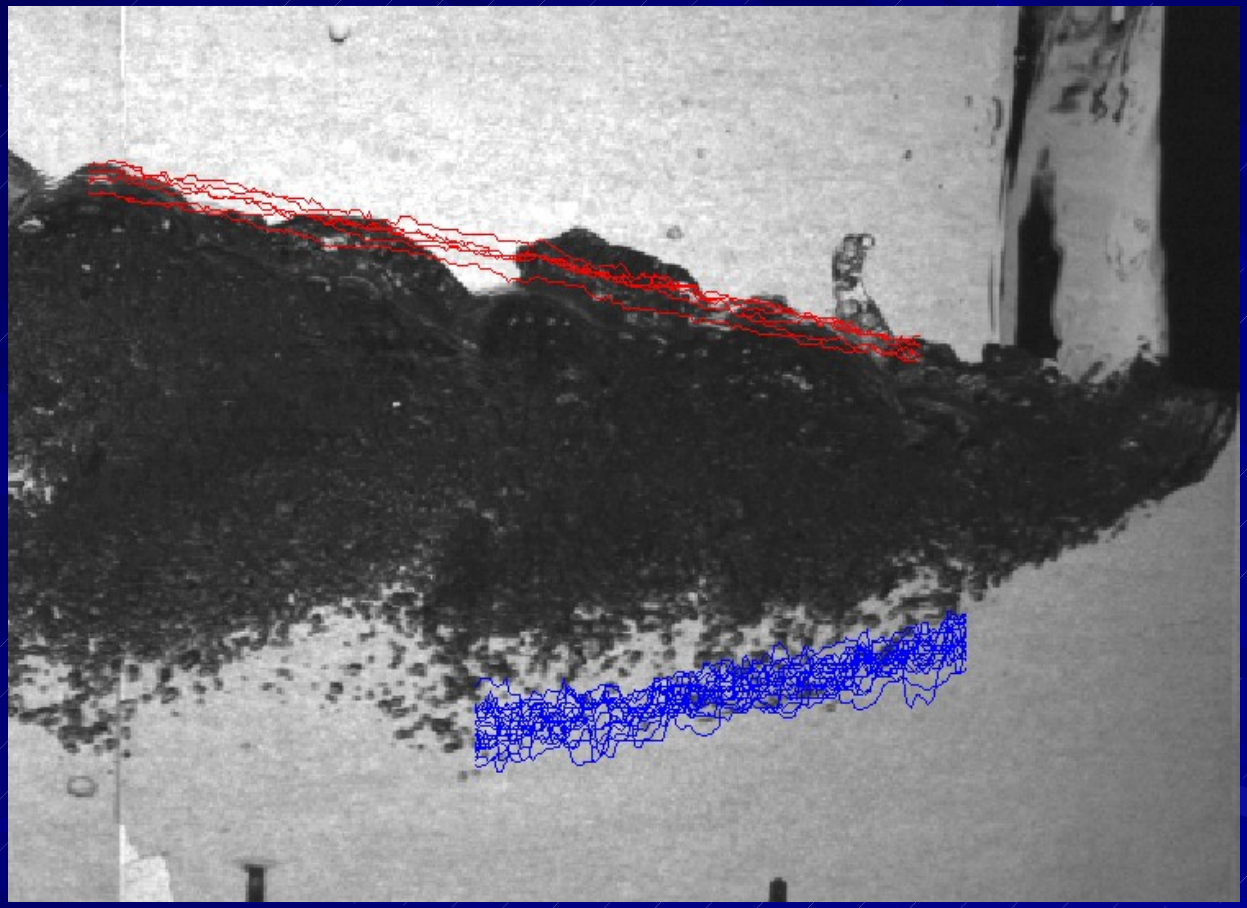

- From the measured profiles the relation $l = l(x)$ will be obtained for different flow conditions
- Work in progress for the later model

deep-water stern breaker

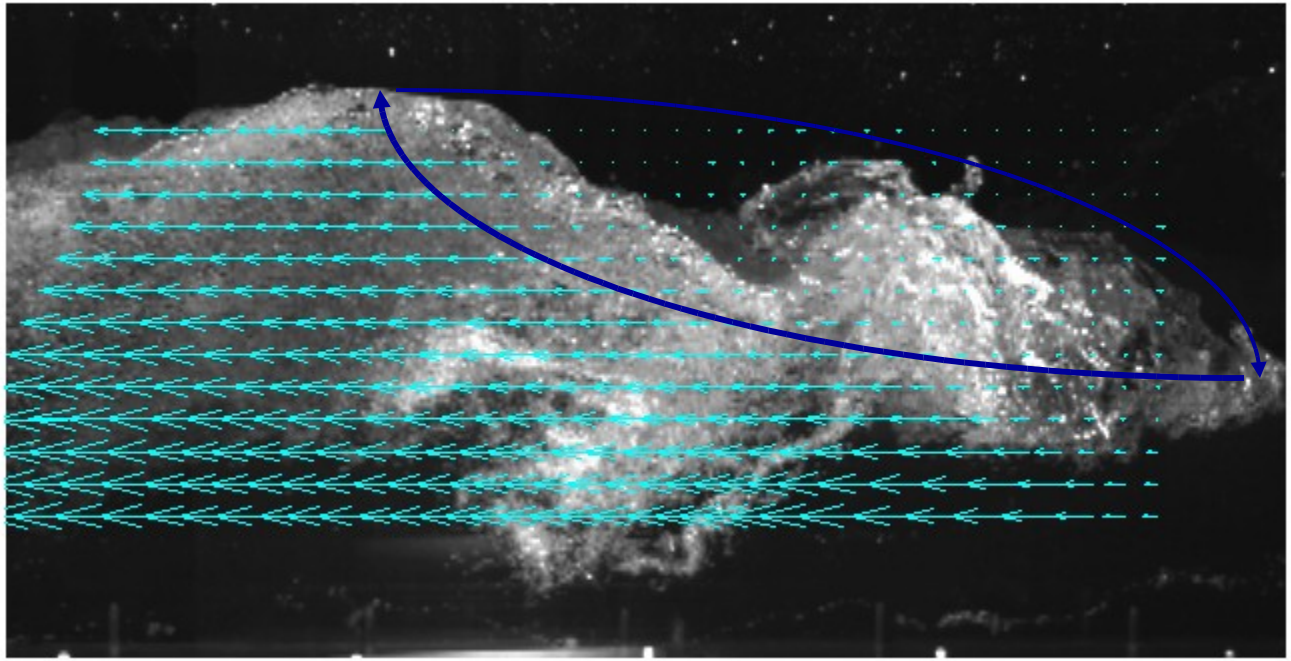

3-D deep-water stern breaker

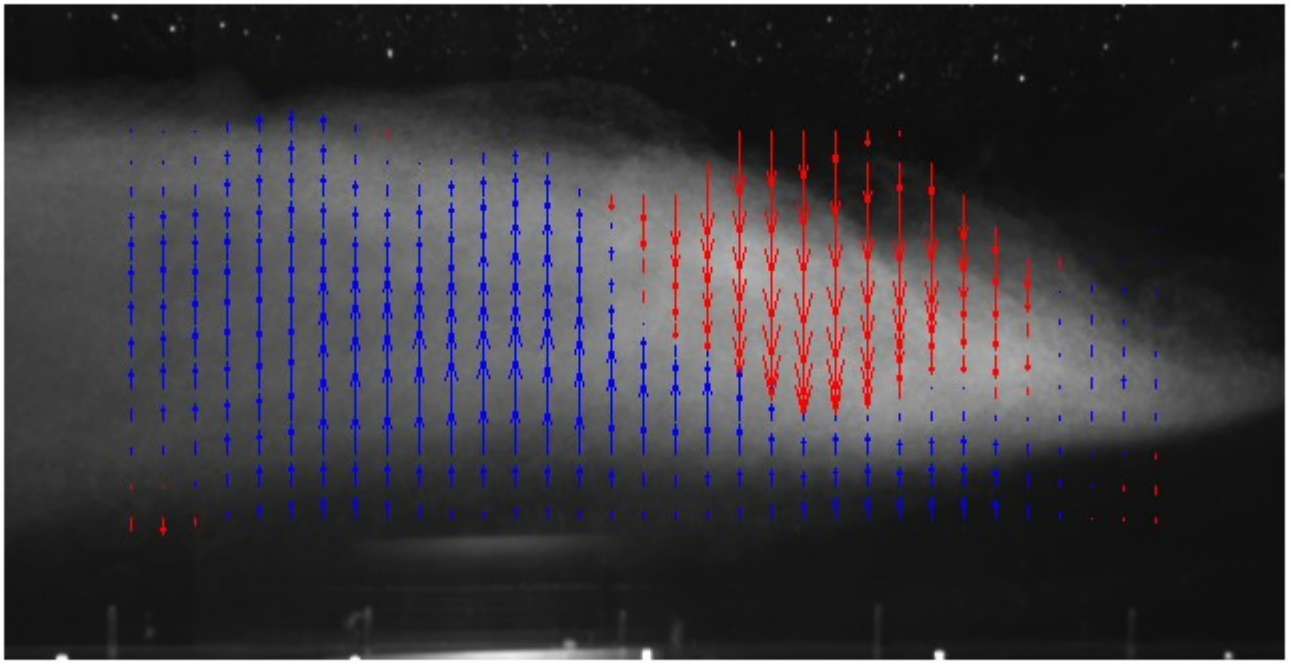

Mean Vertical Velocity

Upwards, Blue; Downwards, Red

Air entrainment model (I): Modeling of a single LS

Entrainment of a single large turbulent feature:

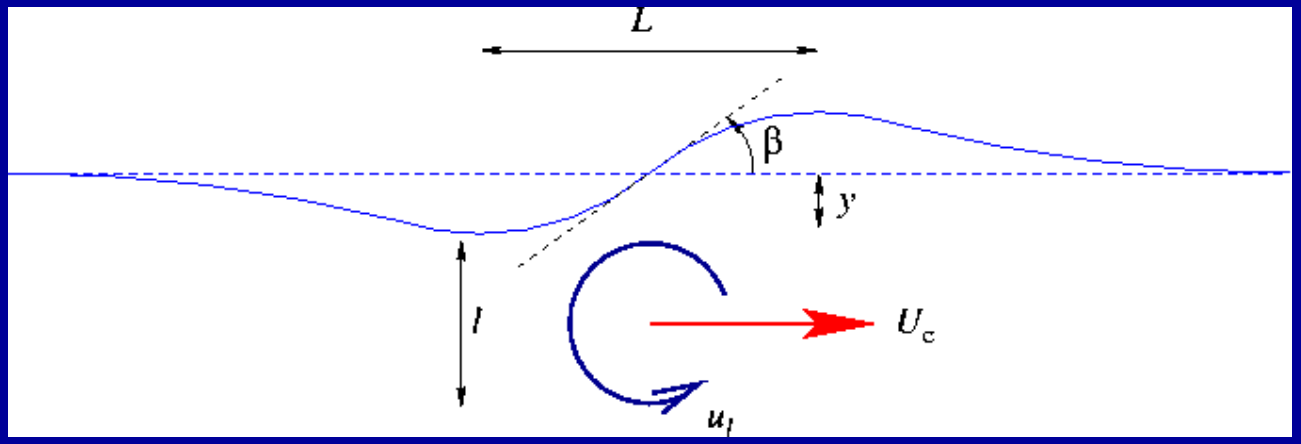

l	Characteristic size of the LS (assumed to be of the same order of its dept
$L \sim l$	Length of free surface perturbed by the LS
y	Characteristic surface deformation
U_c	Convective velocity of the LS
u_l	Turnover velocity of the LS
β	Maximum slope of the free surface

Air entrainment model (II): entrainment condition

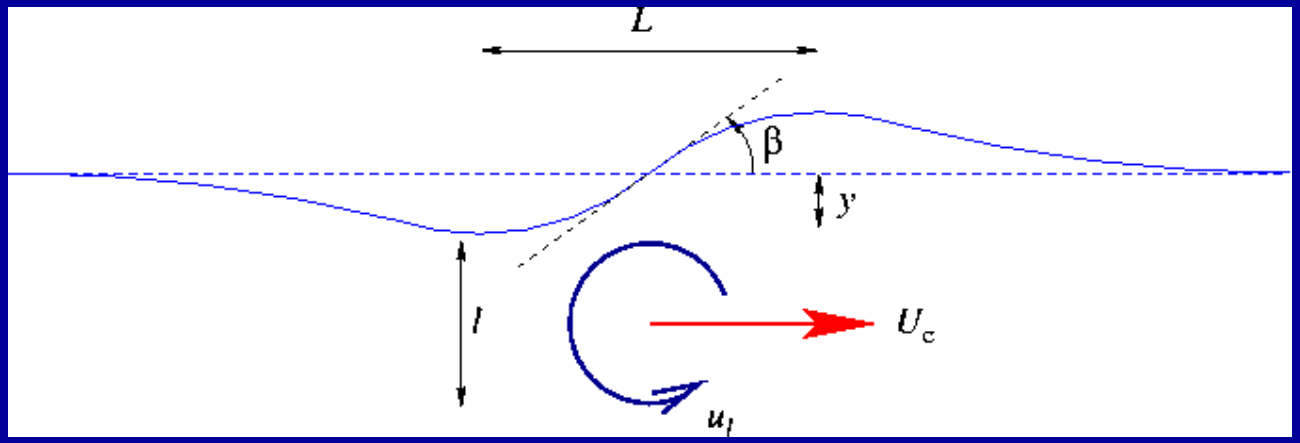

The surface deformation can be estimated from a pressure balance

$$\rho g y \gg \rho u_l^2 \Rightarrow y \gg \frac{u_l^2}{g}$$

Hypothesis: the entrainment occurs when the deformation of the surface, β, is greater than a critical value β_{crit}

$$\beta \gg \frac{y}{L} \mu \frac{y}{l} \gg \frac{u_l^2}{gl} > \beta_{crit}$$

or equivalently

$$Fr_l = \frac{u_l^2}{gl} > Fr_{crit}$$

Air entrainment model (III): quantification

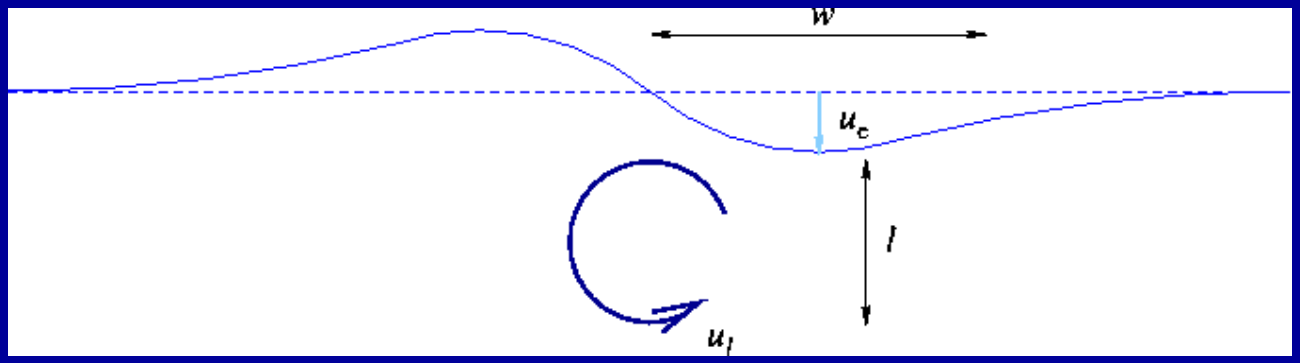

W=Entrainment length of the LS

u_e=Entrainment velocity

Assuming that ρu_e^2 is proportional to a characteristic pressure difference $\Delta p = \rho u_l^2 - Fr_{crit}\, \rho g l$, dimensional analysis yields:

$$u_e = \alpha \sqrt{gl}\sqrt{Fr_l - Fr_{crit}}$$

For the entrainment length:

$$\frac{W}{l} = W\left(Fr_l\right)$$

Thus the entrainment rate of a LS per unit span:

$$\dot{q}/\sqrt{gl^3} = \alpha W\left(Fr_l\right)\sqrt{Fr_l - Fr_{crit}}$$

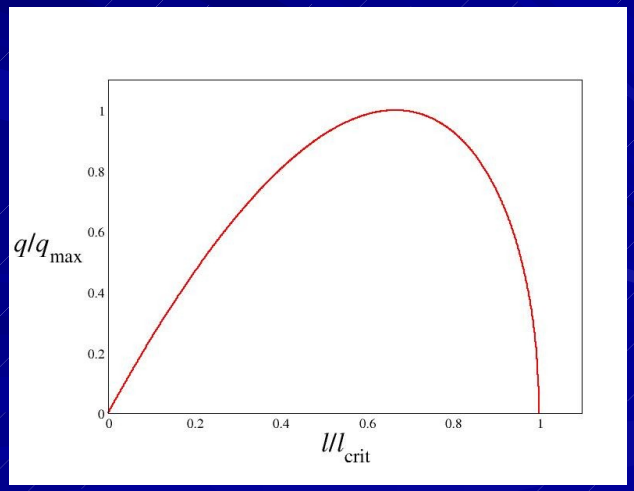

Model integration into a RANS code

A) Entrainment condition:

$$Fr_l = \frac{u_l^2}{gl} > Fr_{crit}$$

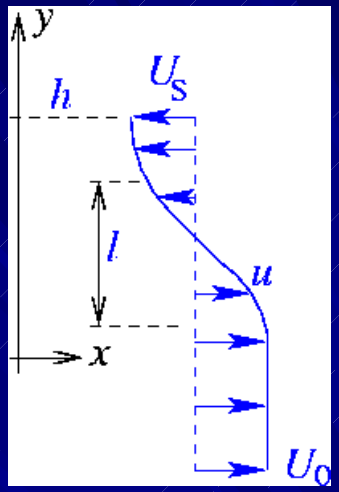

To compute the local Froude number, Fr_l, the following estimation of the parameters is proposed

$$u_l = \frac{U_0 + U_S}{2} \qquad l = \left(\frac{2}{U_0 + U_S}\right)^2 \int_{-¥}^{h} (U_S + u)(U_0 - u)\, \mathrm{d}y$$

B) Air entrainment per unit span:

$$\dot{q}\, l \sqrt{gl^3} = \alpha W(Fr_l) \sqrt{Fr_l - Fr_{crit}}$$

In order to implement the model, the following constants must be measured from experiments (work in progress):

$$Fr_{crit} \qquad \alpha W(Fr_l)$$

Wave generation mechanisms (I)

- Two mechanisms may explain the development of the wave:
  - Deep water analogous to the shallow water “roll waves” (Dressler 1949, Yu & Kevorkian 1992 and others)

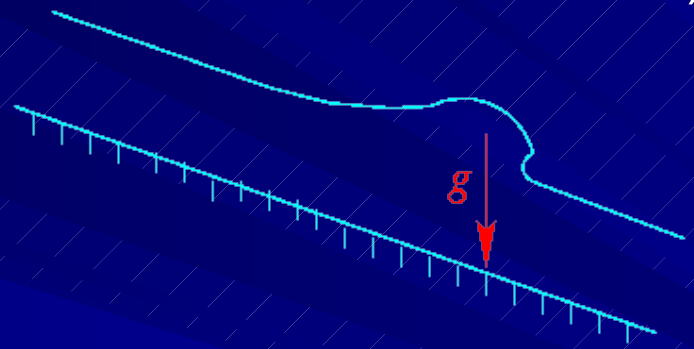

  - Shear between the lower high-speed stream and the upper spilling flow + vortex stretching effect due to small variations in u_x

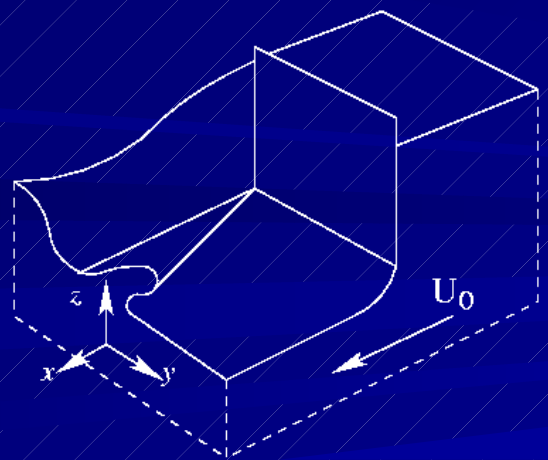

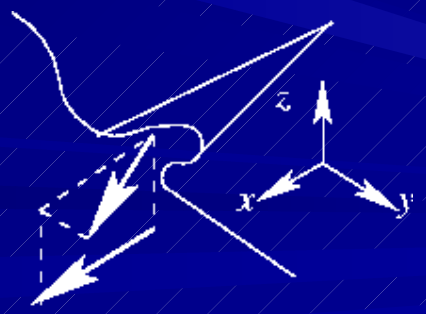

Transversal velocity/vorticity & free surface

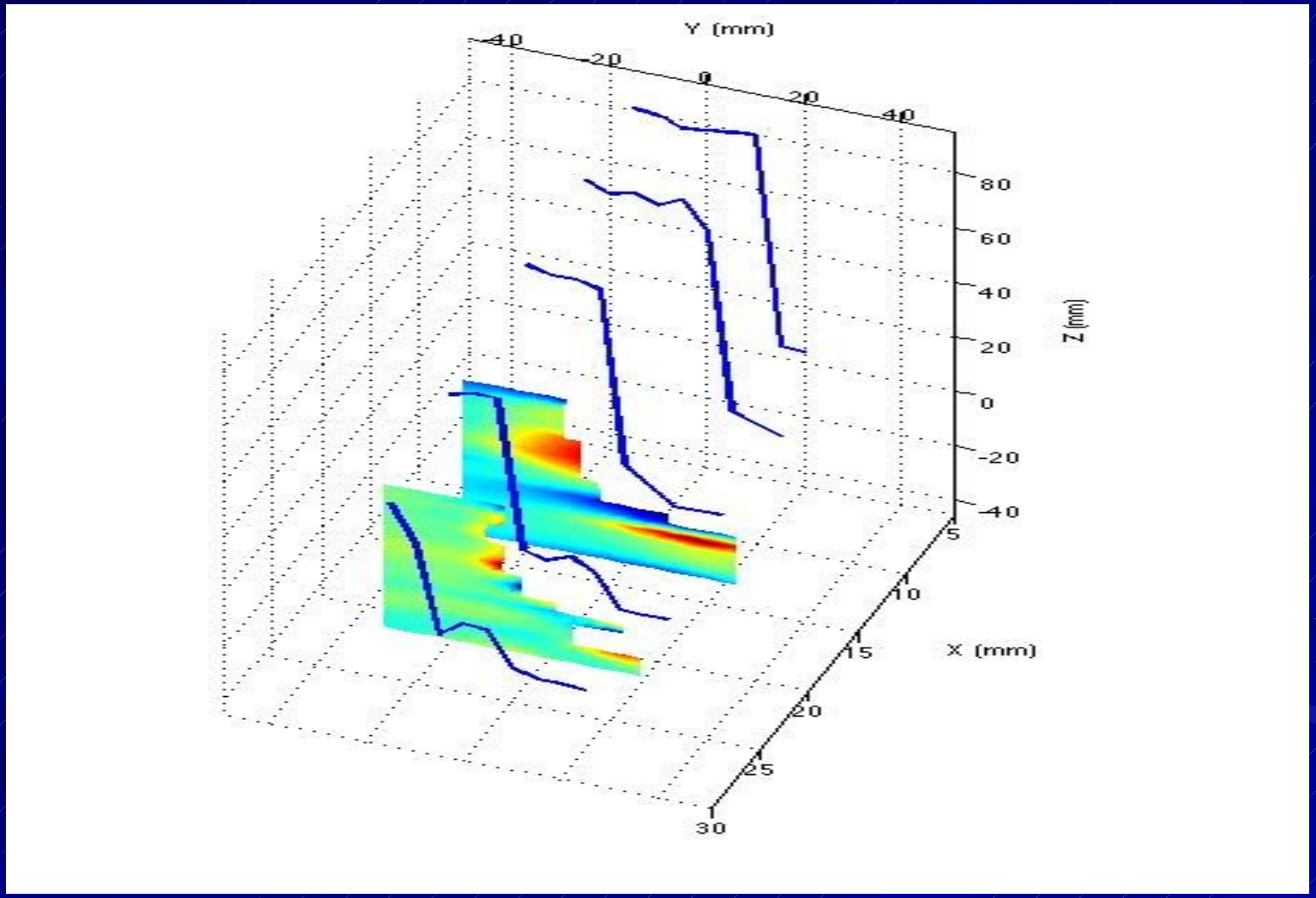

Which mechanism generates the wave?

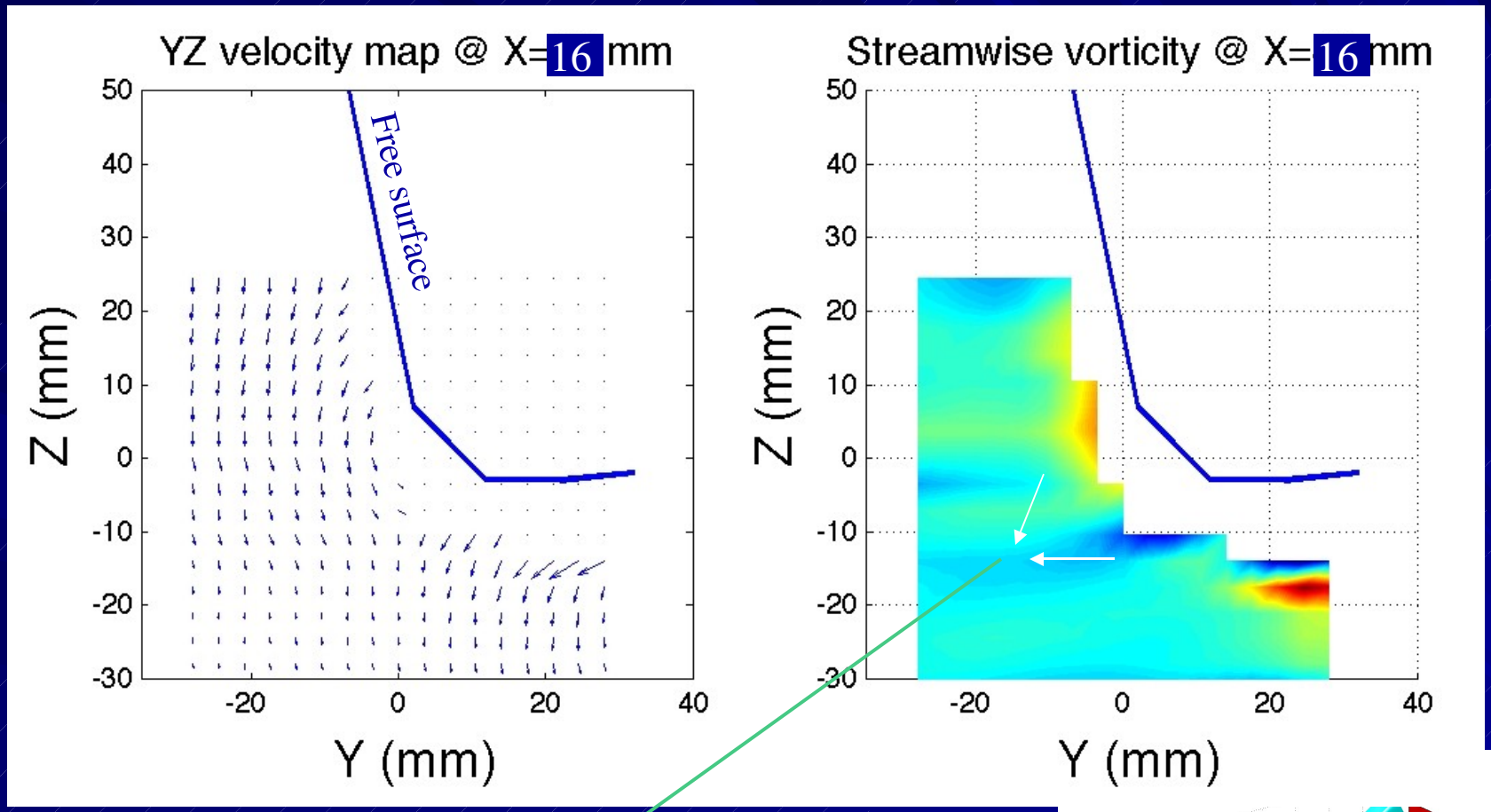

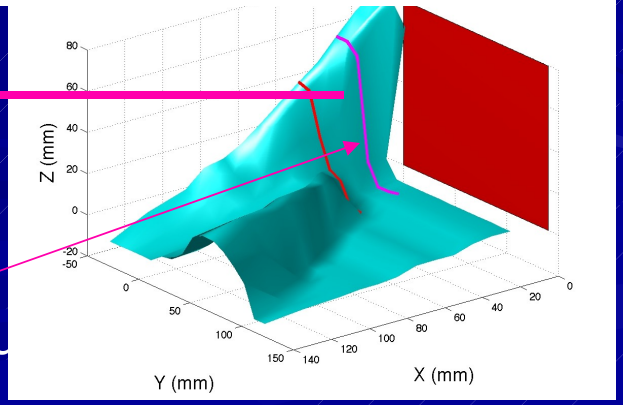

Vorticity of opposite sign
Is observed at the height of the plate.

This section is as close to the plate as we could measu


David Jeon. Caltech

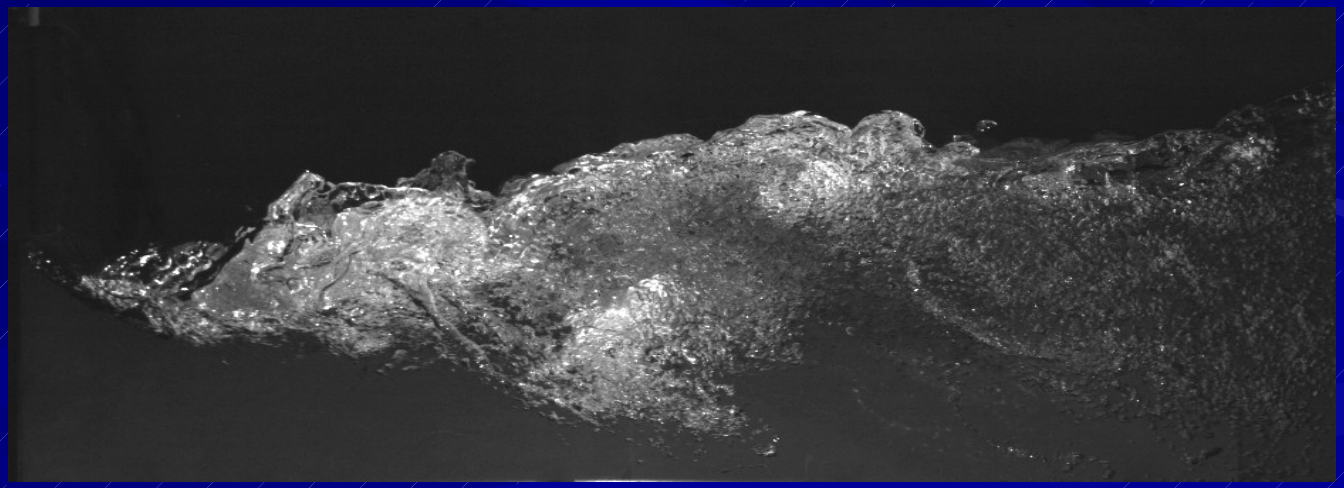

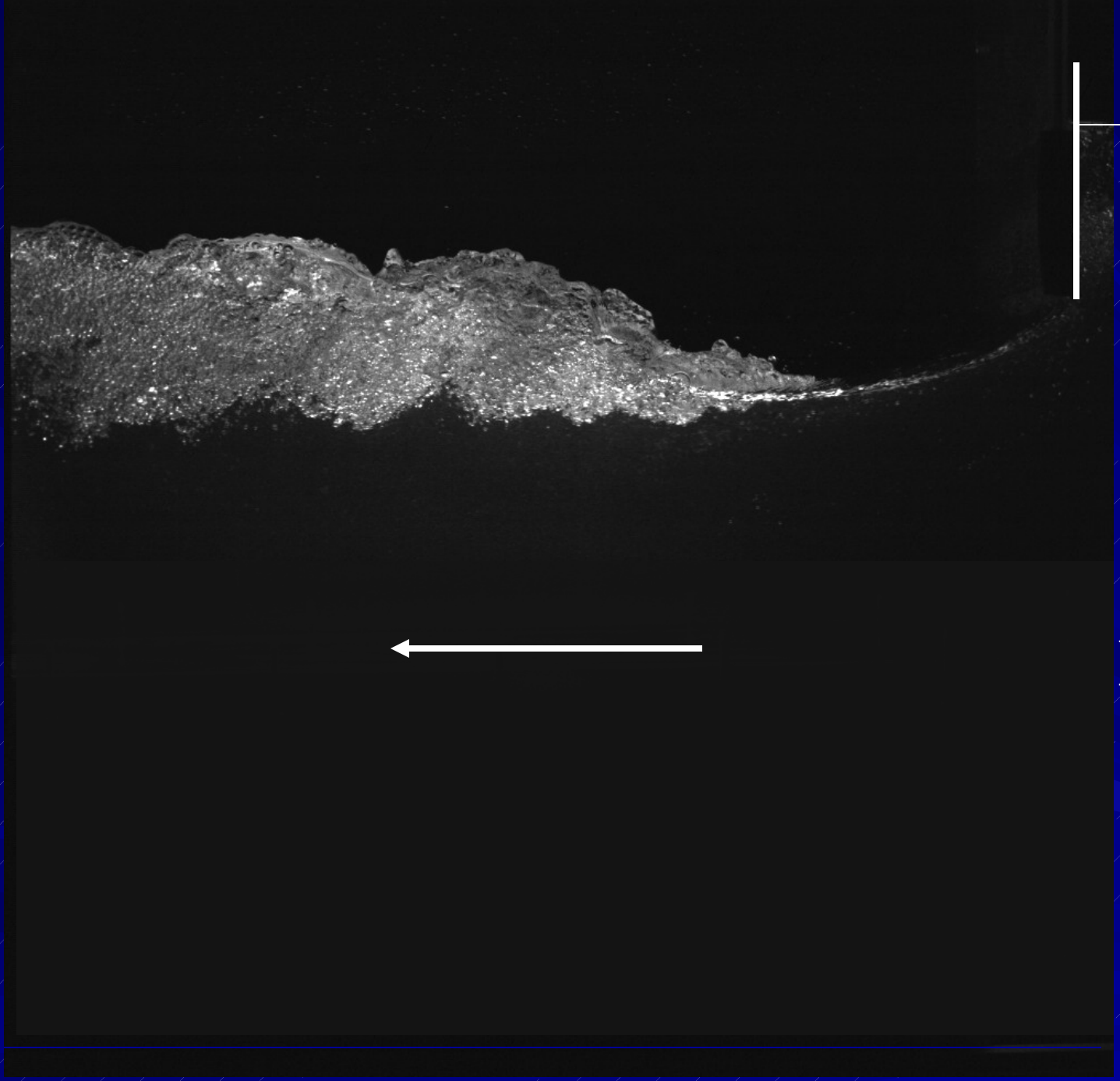

Side View

2-D Stern Breaker

Deep-Water

Air entrainment length
deep-water stern breaker

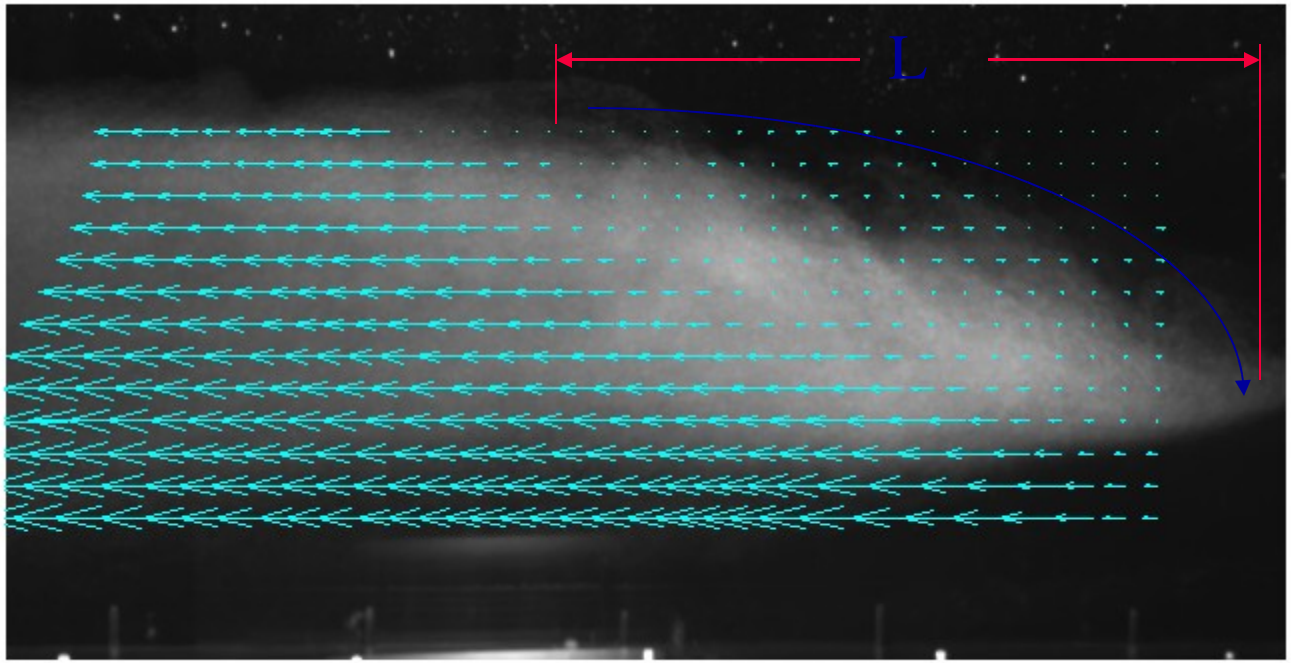

Mean Horizontal Velocity showing the so called “roller” reported in previous studies (LDV measurements)

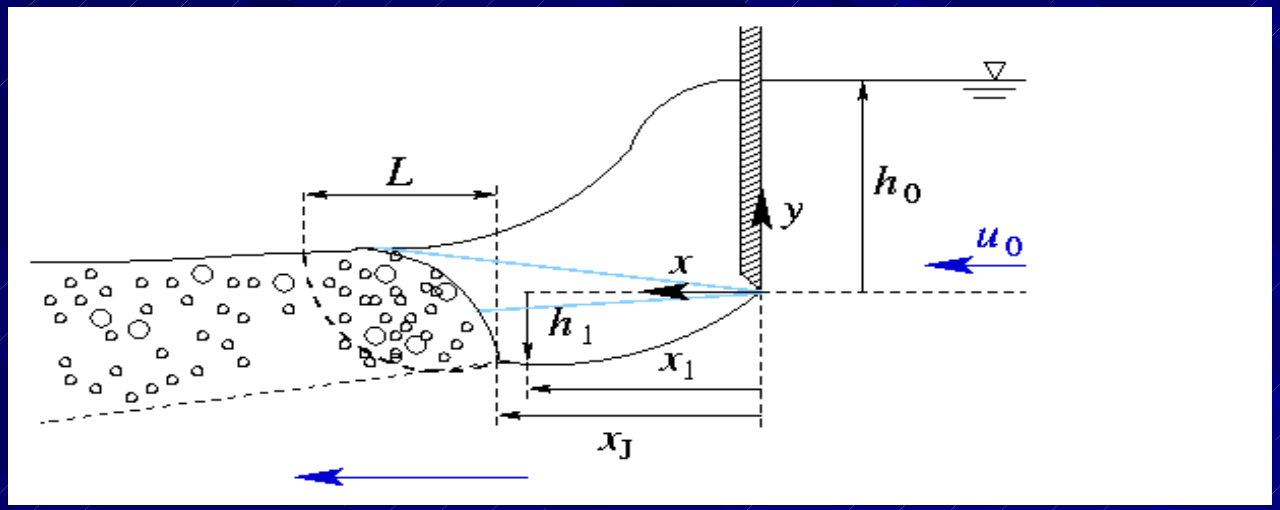

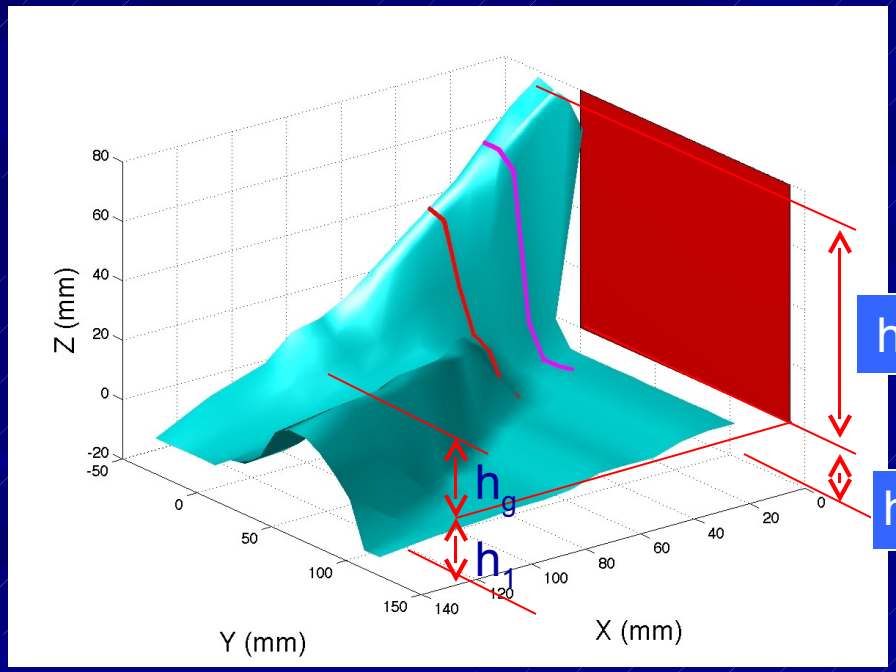

h_o-h_1

h_g-h_1

Impingement Velocity & Plunging-Spilling Transition

- The "range" of the ballistic trajectory depends on the ratio of the two dimensionless parameters that we used to determine the plunging/spilling criterion.

- The value found for the critical Froude number ($Fr_{g,\,crit} \approx 20$) agrees fairly well with the value of the ratio $Fr / (h_g-h_1)/(h_0-h_1) \approx 24$ measured at the transition condition.

- Transition should be: $Fr_g > Fr_{g,\,crit} \approx 20$.

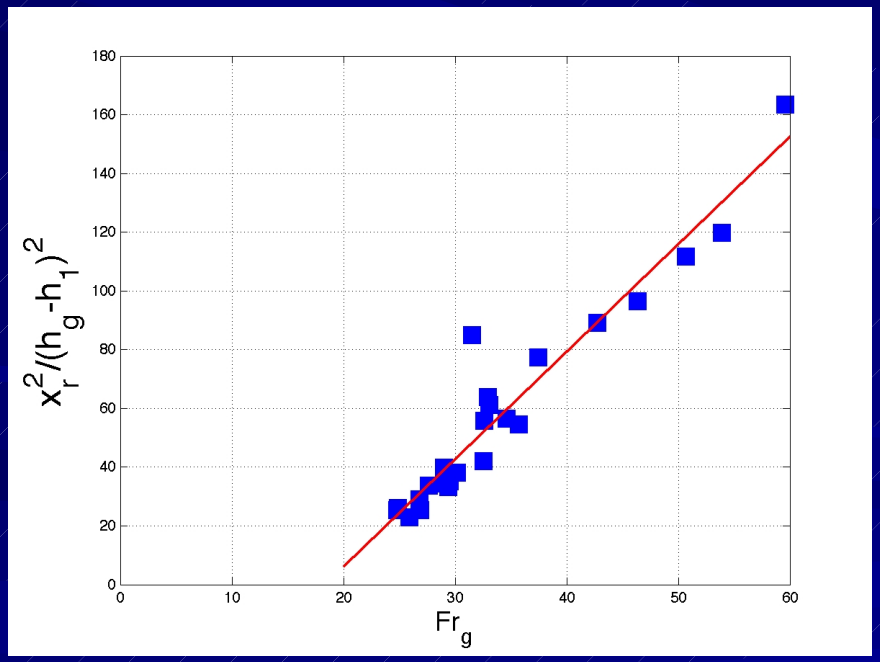

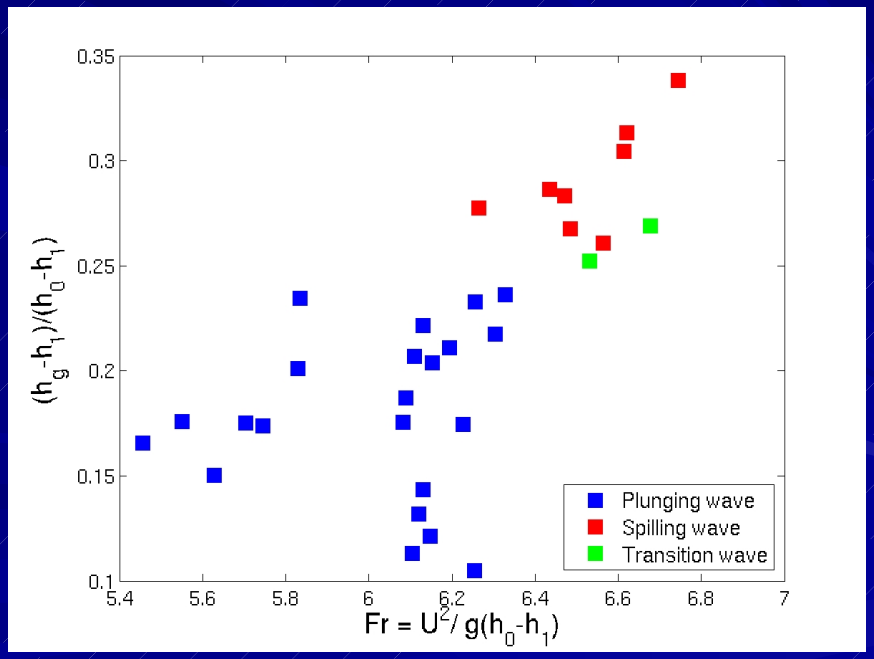

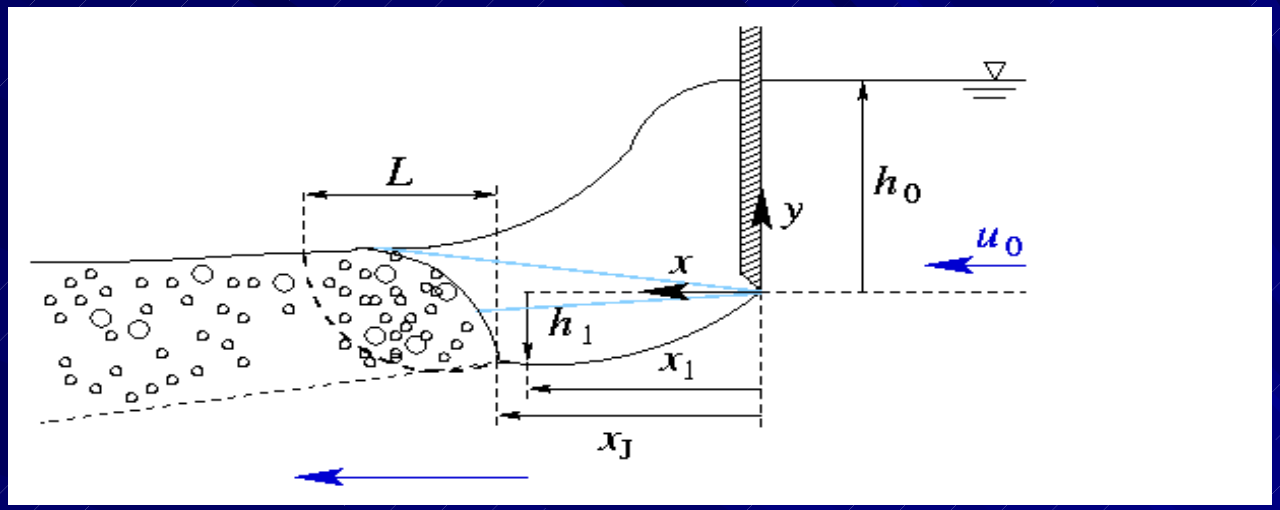

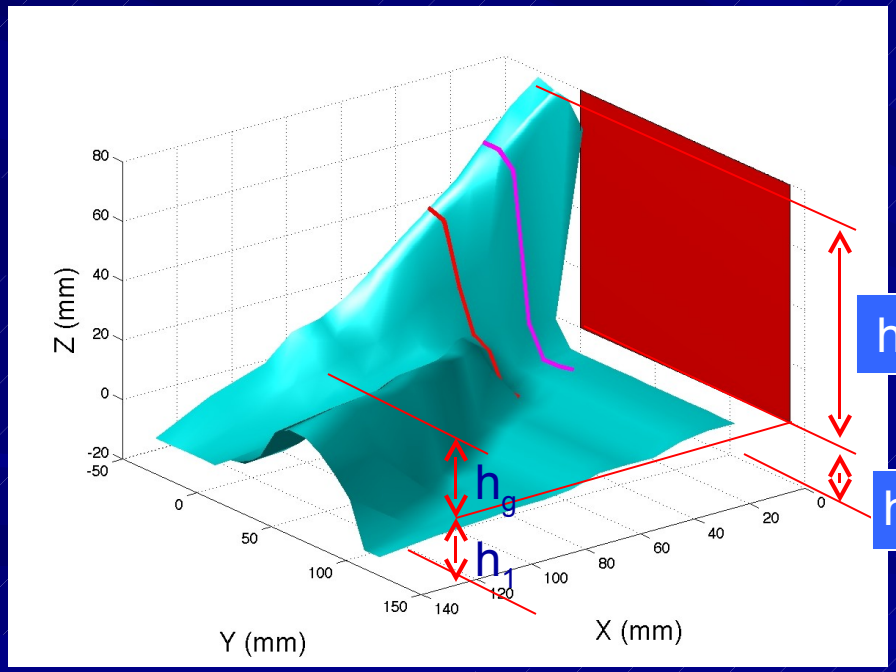

h_o-h_1

h_g-h_1

Experimental results

Wave breaking regime: Plunging

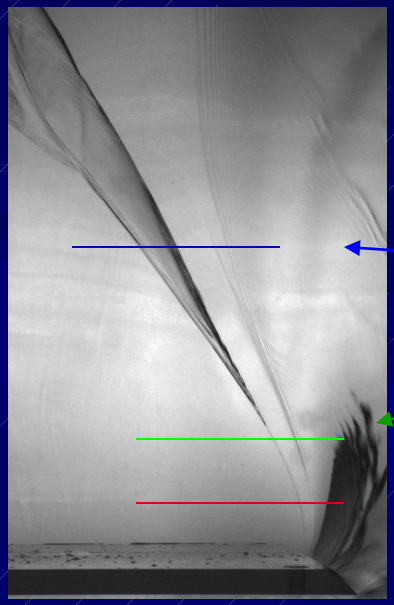

Plunging